2009

The biomechanics of reverse shoulder arthroplasty

Sergio Gutiérrez
University of South Florida

The Biomechanics of Reverse Shoulder Arthroplasty

by

Sergio Gutiérrez

A dissertation submitted in partial fulfillment
of the requirements for the degree of
Doctor of Philosophy
Department of Chemical & Biomedical Engineering
College of Engineering
University of South Florida

Major Professor: William E. Lee, III, Ph.D.
Mark A. Frankle, M.D.
John T. Wolan, Ph.D.
Mark Jaroszeski, Ph.D.
Charles Nofsinger, M.D.

Date of Approval:
July 1, 2009

Keywords: Rotator Cuff, Surgery, Reversed, Scapula, Implant

DEDICATION

I would like to dedicate this dissertation to my mom and dad for all their support over the years. Los quiero mucho!!!!

ACKNOWLEDGMENTS

I would like to thank Dr. Mark Frankle for all his help and mentoring over the years. I would also like to thank Dr. William Lee for his tireless help, not just on my behalf, but for every student in Biomedical Engineering.

Thank you to my girlfriend Suzanne Alameda, whose constant encouragement helped me find the strength to finish my dissertation.

TABLE OF CONTENTS

LIST OF TABLES

LIST OF FIGURES

THE BIOMECHANICS OF REVERSE SHOULDER ARTHROPLASTY

Sergio Gutiérrez

ABSTRACT

Rotator cuff deficiency with glenohumeral arthritis presents a unique challenge to the orthopaedic surgeon. Under these conditions, total shoulder replacement has yielded poor results as a result of eccentric loading of the glenoid leading to loosening and early failure. Multiple procedures have been recommended to resolve this problem including total shoulder arthroplasty, shoulder arthrodesis, and hemiarthroplasty. Hemiarthroplasty, the current standard of care for this condition, offers only limited goals for functional improvement and only a modest improvement in pain.

Recently, there has been renewed interest in reverse shoulder arthroplasty. The main concept behind the reverse shoulder implant is the stabilization of the joint by replacing the head of the arm with a socket and placing a ball on the shoulder side. This “reverse” configuration creates a fixed fulcrum through which the deltoid can act more efficiently at raising the arm and thus increasing range of

motion and returning the patient to a more normal level of function. This dissertation attempts to fill in some of the gaps in reverse basic science with six published studies. The important results found in these studies were:

(1) Implantation of the glenosphere with an inferior tilt reduces the incidence of mechanical failure of the baseplate.

(2) A positive linear correlation is present between abduction range of motion (ROM) and center of rotation offset (CORO).

(3) When comparing several factors affecting ROM and scapular impingement, CORO had the largest effect on ROM, followed by glenosphere position. Neck-shaft angle had the largest effect on inferior scapular impingement, followed by glenosphere position.

(4) Stability is determined primarily by increasing joint compressive forces and, to a lesser extent, by increasing humerosocket depth.

(5) There are three distinct classes of arc of motion relative to the articular constraint: I – arc of motion decreased with increased constraint, II – arc of motion with a complex relationship to constraint, and III – arc of motion increased with increased constraint.

The information presented in this dissertation may be useful to the orthopaedic surgeon when deciding on an appropriate reverse implant and improving surgical technique, as well as aiding engineers in improving reverse implant design.

CHAPTER 1 - INTRODUCTION

Shoulder Anatomy

The shoulder is a complex assembly of muscles, tendons, ligaments, cartilage and bones. For it to function in a normal and efficient manner, all of these structures have to be healthy and be able to work in conjunction with one another. If any one of these structures becomes injured or diseased, it can have a negative ripple effect on the other structures, i.e. one structure will affect the function of another structure which will affect another structure and so on and so forth. Because of this complexity, it is also the joint with the greatest range of motion in the body.

There are three main bones that constitute the shoulder: the humerus or upper arm, the scapula (sometimes called the shoulder blade) and the clavicle (also called the collarbone). (*For the purposes of simplicity and narrowing the focus of this dissertation, further discussion will be limited to the relevant structures of the scapula and the humerus*). The relevant structures of the humerus include: the humeral head, greater and lesser tuberosities and the shaft of the humerus. The relevant structures of the scapula include: the acromion, coracoid, glenoid and

the body of the scapula. The humeral head articulates with the scapula via the glenohumeral joint and specifically articulates on the glenoid.

The humerus is attached to the scapula through a fibrous capsule, ligaments and the following muscles: infraspinatus, supraspinatus, subscapularis, teres minor (together referred to as the rotator cuff) and deltoid (anterior, lateral and posterior bundles). The main function of the rotator cuff is to stabilize the humerus on the glenoid as the arm is being articulated. This stabilization allows the humeral head to rotate on the glenoid through a relatively fixed center of rotation. The main function of the deltoid is to abduct (raise) the arm (from a resting position at the side of the body).

Etiology of Rotator Cuff Disease

Rotator cuff disease encompasses the deterioration of one or more of the rotator cuff muscles or tendons. This deterioration can be due to normal aging or conditions such as arthritis, tendonitis or bursitis. It can also be due to a traumatic event such as a fall or an accident. The main function of the rotator cuff is to stabilize the head of the humerus on the glenoid. The concerted action of the rotator cuff directs the humeral head joint reactive force into the glenoid throughout arm motion. This directed force into the glenoid prevents the humeral head from traversing out of the glenoid in a superior direction due to the superiorly directed force of the deltoid during early stage abduction. As the

rotator cuff begins to fail, the humeral head tends to migrate superiorly instead of rotating at the glenoid. This superior migration is normally counteracted by the stabilizing effects of the infraspinatus and subscapularis, and the rotating effects of the supraspinatus.

Multiple procedures have been recommended to resolve this problem. These include semi-constrained and constrained total shoulder arthroplasty, shoulder arthrodesis (fusion of the shoulder joint), and hemiarthroplasty (replacing only the humeral head and leaving the glenoid untouched). Hemiarthroplasty, the current standard of care for this condition, offers only limited goals for functional improvement and only a modest improvement in pain. The reverse shoulder implant was developed due to the lack of a good solution for this problem.

History of Reverse Shoulder Arthroplasty

The fixed fulcrum shoulder implant was first developed in 1970 by Charles Neer with assistance from Robert Averill. Neer began his quest to develop a device that would aid in the stabilization of the shoulder joint when the rotator cuff muscles were deficient. The main concept he was striving for was the reconstruction and reattachment of the rotator cuff muscles to the remaining bony anatomy. He accomplished this through different iterations of the Mark prosthesis, culminating in the Mark III. This last prosthesis had a small glenosphere and a multi-axis humeral component that helped improve range of

motion. The small glenosphere allowed Neer to attempt to reconstruct the rotator cuff. Unfortunately, Neer abandoned this concept since he believed the constrained nature of the reverse did not preclude repairing the rotator cuff.

Several other attempts at developing a viable reverse shoulder implant were tried from the mid to late 1970's, with the same failed results. These failed reverses included the Reeves prosthesis, the Gerard and Lannelongue prosthesis, the Kolbel prosthesis, the Kessel prosthesis, the Bayley-Walker prosthesis, the Jefferson prosthesis of Fenlin, the Liverpool prosthesis of Beddow, the Buechel-Pappas-DePalma prosthesis and the trispherical prosthesis of Gristina. It wasn't until 1985 when Paul Grammont began development of his "Delta" (derived from "deltoid"…) series that the reverse implant came into its own. The main principles that Grammont championed were the medialization of the center of rotation by using a hemispherical glenosphere (also called metaglene) and the placement of the glenosphere more inferiorly on the glenoid. The main reason for these principles (as theorized by Grammont) was increasing the deltoid moment arm. The final version of the Grammont design, which is still in use today, is called the Delta III.

Today, there are a plethora of different reverse designs with different driving principles from companies such as Tornier, Zimmer, DJO Surgical (formerly Encore Medical), Exactech, Biomet and Lima LTO. Each one has its benefits

and drawbacks, but they all are based on the same driving principle of reversing normal anatomy.

Objectives of this Dissertation

Although many different designs of reverse are presently on the market (and many more are sure to be introduced), the biomechanical reasoning behind their design has been, unfortunately, lacking. The six articles presented in this dissertation help shed some light on this reasoning and include some of the first articles to describe basic biomechanical principles related to reverse shoulder arthroplasty. These principles include decreasing baseplate shear forces by inferiorly tilting the baseplate, increasing range of motion by lateralizing the center of rotation and increasing glenosphere/socket stability by increasing the joint compressive force. It was, therefore, the goal of this dissertation to:

(1) Help surgeons understand the biomechanics of reverse shoulder arthroplasty.
(2) Improve patient outcomes through improvements in surgical technique.
(3) Help engineers design new reverse implants as well as improve current designs.

Podium, Poster Presentations and Book Chapter

This work and others have been presented through posters, podium presentations and a book chapter. Please see Appendix A, B and C, for a list.

Dissertation Outline

The format of this dissertation includes the body of six peer reviewed journal articles. Although there is information that is redundant from chapter to chapter, it is, hopefully, the most efficient way to present the information which was originally presented in PDF format.

Chapter 2 investigated the effects of baseplate tilt on the forces underneath the baseplate, as well as the displacement of the baseplate as the arm is abducted through 60 degrees of motion.

Chapter 3 discussed how changes in center of rotation offset can affect both the amount of motion possible as well as alter where the implant or bone impinges on the scapula.

Chapter 4 evaluated range of motion and adduction deficit of theoretical reverse implants and alterations in surgical technique. It set up the notion of investigating

the concept behind the reverse shoulder implant instead of testing a specific manufacturer's implant.

Chapter 5 established a hierarchy of factors that affected stability in reverse shoulder arthroplasty.

Chapter 6 developed a hierarchy of surgical and implant related factors and their effects on range of motion and adduction deficit. This study began the use of validated virtual simulations to test concepts instead of conducting physical experiments.

Chapter 7 continued the use of virtual simulations to test how changes in component geometry, specifically socket depth, affected impingement-free arc of motion.

CHAPTER 2 - ARTICLE I: BIOMECHANICAL COMPARISON OF COMPONENT POSITION AND HARDWARE FAILURE IN THE REVERSE SHOULDER PROSTHESIS

Introduction

Rotator cuff deficiency with glenohumeral arthritis presents a unique challenge to the reconstructive surgeon. The complex motions of the shoulder joint require stability throughout an extended range of motion. When the rotator cuff is deficient or nonfunctional, total shoulder replacement has yielded poor results as a result of eccentric loading of the glenoid leading to loosening and early failure.[1] In the modern era, multiple procedures have been recommended to resolve this problem. These include semiconstrained [2-4] and constrained total shoulder arthroplasty,[5,6] shoulder arthrodesis,[7-10] and hemiarthroplasty.[10-14] Hemiarthroplasty, the current standard of care for this condition, offers only limited goals for functional improvement[15] and only a modest improvement in pain.[16,17]

Recently, there has been renewed interest in semiconstrained reverse shoulder arthroplasty. Currently, there are minimal basic science data available on which to base rational clinical decisions. Several authors have reported promising results in the short and medium term using a reversed or inverted shoulder

implant.[18-22] The most recent study involving the Delta III prosthesis (DePuy Orthopaedics, Warsaw, IN) in the treatment of glenohumeral osteoarthritis with massive cuff rupture, a multicenter study of 80 shoulders in 77 patients, reported significant improvements in all 4 areas of the Constant score. However, 49 cases (63.6%) were noted to have medial component encroachment and scapular notching without evidence of loosening.[21]

The Reverse Shoulder Prosthesis (RSP - Encore Medical, Austin, TX) attempts to address the issue of scapular notching by providing the option for a more lateral center of rotation. However, this lateral placement yields a greater moment arm and, hence, generates greater torque at the glenoid baseplate-bone interface, creating concerns regarding early loosening and failure. In an effort to address this concern, the RSP uses enhanced baseplate fixation by use of a fixed-angle central screw with 4 peripheral locking screws. This configuration has demonstrated stability to cyclic loading equivalent to that of the Delta III design in the laboratory.[23] To better understand the mechanical factors involved in these early failures, we examined the effect of baseplate orientation on the distribution of forces and micromotion at the bone-prosthesis interface. Three angles of implantation were examined: +15°, 0°, and -15° of scapular plane tilt.

Materials and Methods

An apparatus was developed to simulate movement of the humerus through 60° of abduction (Figure 1).

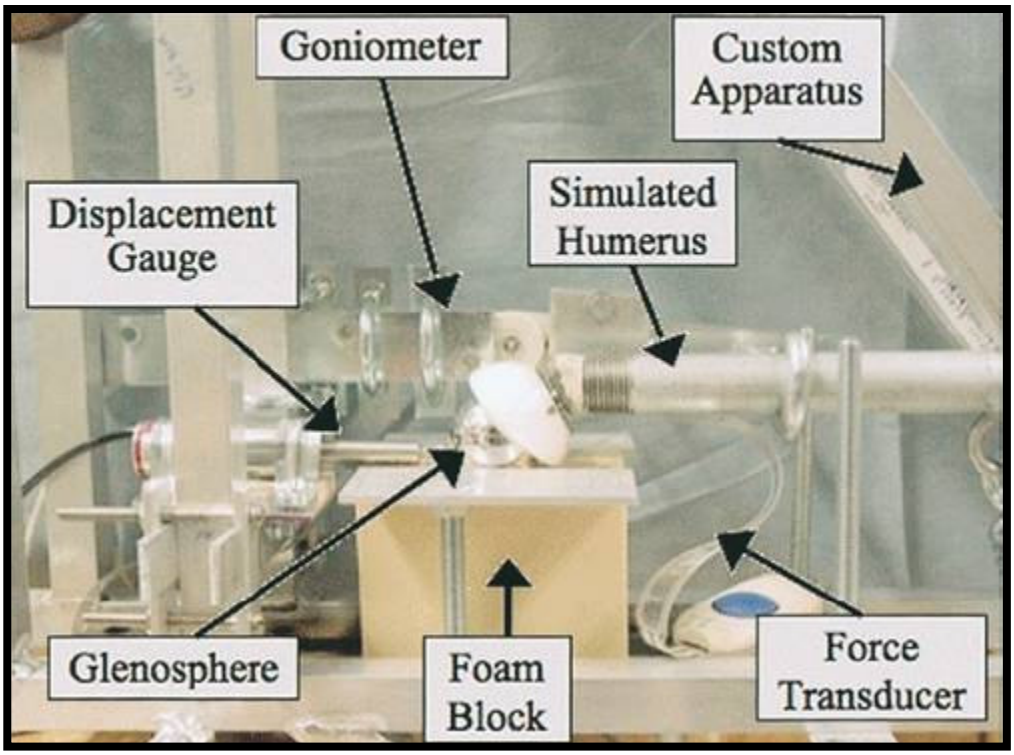

Figure 1. Experimental apparatus shown with its basic components.

A movable sled with a 500-lb load cell (model LCH-500; Omega Engineering, Stamford, CT) was connected via a cable through a series of pulleys to the distal portion of a steel pipe used to simulate the humerus. The angle of abduction (± 0.01°) was measured by use of an electronic goniometer (Greenleaf Medical, Palo Alto, CA) attached via a ring that moved with the steel pipe. At

approximately half the distance between the glenohumeral joint and the cable attachment, a spring was attached (spring constant (k) = 18.67 lbf/in) that gradually increased the forces at the glenoid, simulating the forces present at the glenohumeral joint during humeral abduction. Silicone spray was used in the joint to simulate synovial fluid. The reverse baseplate (standard 25-mm central screw baseplate; Encore Medical) was attached to a solid rigid polyurethane block (30 pounds per cubic foot (pcf); Pacific Research Laboratories, Vashon, WA) via a central attachment screw and peripheral captured screws. The baseplate was implanted with a custom-made torque screwdriver (Encore Medical) to approximately 60 lbf/in. The peripheral screws were all torqued to 20 lbf/in. FlexiForce© force transducers (Tekscan, Boston, MA) were attached to the underside of the baseplate with cyanoacrylate at the superior and inferior positions. A linear voltage displacement transducer (RDP Electrosense, Pottstown, PA) was placed with its tip at the base of the glenosphere and measured microdisplacement (± 0.003 mm) in the superior and inferior directions. Eight different blocks were used for each different baseplate angle (15° superior inclination, 15° inferior inclination, and 0° [or normal] inclination), and ten runs were performed per block. Data was collected by use of a custom-made LabVIEW graphic interface (National Instruments Corporation, Austin, TX), and the following information was gathered: superior and inferior forces between the baseplate and the foam, superior and inferior displacement of the glenosphere, angle of humeral abduction, and force at the origin of the cable. Data was exported into a Microsoft Excel spreadsheet (Microsoft, Redmond,

WA), and means and SDs were calculated. Statistical analysis was performed by use of a 1-way analysis of variance and a Student's t-test.

Results

Table 1 summarizes the biomechanical data. Both superior and inferior forces under the baseplate increased when going from an inferior inclination to a superior inclination (Figure 2). The type of force, though, changed when going from an inferior inclination to a superior inclination. The inferior transducer in the inferior inclination showed a progression from a lesser compressive force to a greater compressive force. The same held true for the normal inclination, although the magnitude of the compressive force was less when 60° was reached. Superior inclination had no compressive force present in the inferior force transducer. Forces under the superior force transducer, on the other hand, were compressive forces. The magnitude of this force increased when going from an inferior inclination to a superior inclination. The displacement data showed that the majority of movement was in the superior direction (Figure 3). It was not until 50° was reached in the inferior inclination and 60° in the normal inclination that movement in the inferior direction was noted. The magnitude of all displacement remained under 60 μm, well under the crucial displacement of 150 μm, when osteocytes cannot rebuild bone.[24]

Table 1. Results from baseplate inclination.

	Abduction angle (degrees)	Superior force mean (N)	Superior force StDev (N)	Inferior force mean (N)	Inferior force StDev (N)	Displacement mean (μm)	Displacement StDev (μm)
15° Inferior	10	13.82	10.55	−11.58	18.55	16.93	6.29
	20	29.40	19.15	−9.28	18.41	27.44	10.61
	30	39.72	24.96	−1.03	16.69	28.44	6.39
	40	43.36	26.96	18.73	15.31	17.26	7.86
	50	42.75	26.54	45.43	17.84	−4.14	10.39
	60	36.91	22.28	75.94	23.99	−32.59	14.23
0° Normal	10	35.47	17.52	−12.16	7.75	20.37	3.81
	20	65.65	31.30	−16.77	9.80	36.05	5.23
	30	86.88	39.65	−14.82	8.82	41.64	8.57
	40	98.49	45.68	−6.71	7.08	34.75	14.74
	50	102.51	49.88	11.27	10.93	17.04	22.63
	60	98.46	50.83	37.50	20.66	−8.95	28.34
15° Superior	10	46.45	29.75	−32.48	20.56	26.61	7.97
	20	78.04	28.30	−41.55	23.26	43.98	6.21
	30	108.43	35.96	−47.08	26.08	52.03	7.00
	40	126.03	41.67	−47.25	26.06	49.05	7.11
	50	136.26	43.80	−42.71	25.43	35.48	8.52
	60	137.59	44.19	−31.85	20.30	11.93	13.74

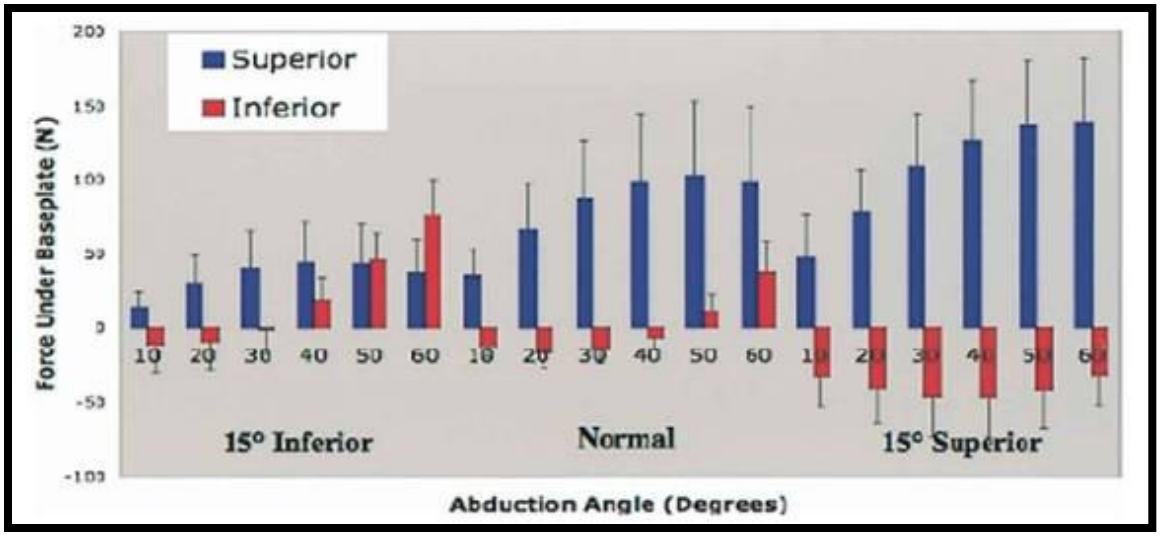

Figure 2. Difference in force between superior and inferior force transducers (bars below 0 N indicate a decrease in compressive force from initial pre-compression). The graph shows an increase in the magnitude of forces, as well as a decrease in compressive force, when going from an inferior inclination to a superior inclination.

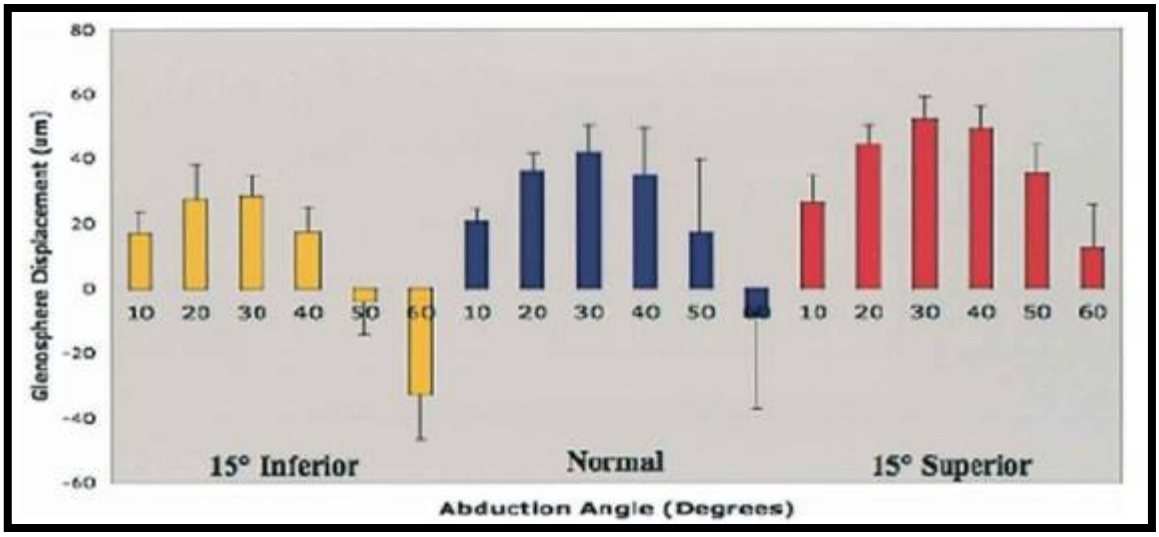

Figure 3. Difference in displacement between different inclination angles (bars below 0 µm show displacement in the inferior direction). The inferior inclination shows less superior displacement and more inferior displacement when compared with the other inclinations. The superior displacement is greater in magnitude and is always in a superior direction.

Discussion

Laboratory testing provides a biomechanical basis for rational clinical decision making. We can infer, by looking at results obtained by use of high-density polyethylene blocks, that glenoid component positioning may affect the stability of the baseplate-bone interface. Implants with 15° of inferior tilt had the most uniform compressive forces and the least micromotion when compared with the 0° and 15° superiorly tilted baseplate. These results indicate that an inferior tilt of approximately 15° will maximize implant stability and minimize mechanical failure for the glenosphere and baseplate component of the RSP. Stable fixation that minimizes resultant micromotion has been demonstrated to be a critical factor for

promoting durable implant fixation via bony ingrowth.[25,26] The baseplate used in this study has a porous titanium surface. In our biomechanical model, the magnitude of displacement remained under 60 μm. Whereas a maximum micromotion of 100 to 150μm has been reported to be a threshold value to allow bony ingrowth,[27] recent studies have suggested that the value may be as low as 20 to 40 μm.[28,29] Although the exact threshold value is unclear, what is certain is that a lack of stable fixation results in the formation of a fibrous membrane, predisposing shoulders to early loosening and poor clinical outcomes.[27,30,31] In addition, even distribution of compressive forces and minimization of sheer strain at the bone-prosthetic interface also promote ingrowth and may, likewise, play a critical role in the implant-bone microenvironment.[32] Reverse total shoulder arthroplasty has emerged as a promising surgical solution for patients with glenohumeral arthritis and rotator cuff deficiency.[12,33,34]

Early results have been encouraging, but failure at the glenoid baseplate–host bone interface remains a concern. The moment arm of the glenoid component produces torque at the bone-prosthetic interface. Alteration of the angle of this lever will alter the magnitude of force at the interface. Furthermore, the angle of the interface relative to the applied force (movement of the arm) will affect the types of stress occurring at the interface. In addition, the distribution of the types of stress (compression or shear) is likewise associated with the tilt of the component. The benefits of implanting a baseplate in an inferior inclination are: decreased overall magnitude of force, a decrease in the total micromotion over

the full range of abduction, and more even distribution of compressive forces beneath the baseplate.

Maximizing stability by closely approximating the ideal angle of implantation theoretically provides short- and long-term benefits. In the short term, the risk of mechanical failure is minimized while simultaneously promoting osseous ingrowth necessary for stable long-term implant incorporation. The percentage of osseous ingrowth necessary and the clinical significance of radiolucent lines under the baseplate have yet to be determined for this implant type.

No published studies have evaluated component positioning of the RSP. In a multicenter trial of the Delta III prosthesis, Sirveaux et al[21] mention that it is better to position the glenoid component with a slight tilt. However, there is no further discussion of this finding nor are any clinical or biomechanical data presented in support of this statement.

The limitations of our study were as follows. The first limitation was the Sawbones© polyurethane blocks have a mechanical stiffness, yield, and ultimate strength similar to those of the human glenoid, but conditions differ from cadaveric glenoids and, therefore, do not simulate a cadaveric study. The second limitation was the active muscle forces were not simulated, and no stabilizing forces from the ligaments and joint capsule were present—the

absolute magnitudes of measured forces and displacements cannot be correlated to those occurring in vivo.

In conclusion, our results indicate that an inferior tilt of approximately 15° will maximize implant stability and minimize early mechanical failure for the glenosphere and baseplate component of the RSP. The magnitude of displacement remained under 60 µm, which is well below the critical threshold of 100 to 150 µm necessary to promote bony ingrowth and implant incorporation. The relationship between the amount of osseous versus fibrous ingrowth and long-term implant survivorship remains to be determined by cadaveric retrieval studies.

CHAPTER 3 - ARTICLE II: CENTER OF ROTATION AFFECTS ABDUCTION RANGE OF MOTION OF REVERSE SHOULDER ARTHROPLASTY

Introduction

Interest in reverse shoulder arthroplasty has provided evidence of pain relief and functional improvement for patients with arthritis and rotator cuff deficiency.[21,35-37] An understanding of the pathologic features in the rotator cuff-deficient shoulder has guided improvement in surgical technique and implant selection which minimizes complications and enhances functional improvement.

Improving shoulder function and relieving pain in the patient with rotator cuff deficiency is the hallmark of the reverse shoulder implant. Substantial increases in shoulder elevation have been documented in clinical reports using the reverse shoulder implant.[21,35,37] Surgeons may choose from several reverse shoulder implant designs with various features, notably glenoid component (glenosphere) size and center of rotation offset. Differences in range of motion (ROM), stability, security of fixation, and motor function may vary among the different implant geometries, therefore, selecting the appropriate shoulder prosthesis requires a priori understanding of implant geometry.

Using dynamic radiographs, Seebauer et al [38,39] studied isolated glenohumeral elevation after reverse shoulder implant surgery in a cohort of 35 patients undergoing primary surgery and 22 patients undergoing revision surgery. Active glenohumeral elevation in the series[39] was a maximum of 53°. Using a cadaver model, Nyffeler et al[40] reported improvements in glenohumeral elevation (abduction range of motion) by shifting the glenosphere inferiorly on the glenoid. Maximizing ROM is a key element for functional gains achievable with reverse shoulder prosthetic designs. It is, thus, essential to understand the potential ROM achievable by the prosthetic design since ROM in the plane of abduction is limited by impingement of the prosthesis on various components of the shoulder and implant.

We ascertained the potential ROM of the reverse designs and identified points of impingement. We proposed that impingement points would vary depending on reverse implant design, that ROM would vary with reverse design, and that the center of rotation offset of the glenosphere would directly correlate with the potential glenohumeral ROM (abduction).

Materials and Methods

We designed an apparatus to determine differences in abduction range of motion for seven configurations of reverse shoulder implants. We used an electronic goniometer to measure abduction range of motion (ROM). Digital video analysis

was then used to determine impingement points that limited range of motion at the initiation of motion and at maximal abduction. Finally, a correlation analysis was performed to evaluate the relationship between ROM and the effect of changing the center of rotation of the glenosphere.

We evaluated abduction ROM with the Reverse Shoulder Prosthesis (RSP - Encore Medical, Austin, TX), which is available with a glenosphere center of rotation offset relative to the glenoid ranging from 0 to 10 mm. A RSP baseplate (25-mm long central screw) and humeral stem (size 10) were implanted by an orthopaedic surgeon (AS) into three surrogate bone models (Sawbones© shoulder model, large left scapula, model #1050-10, and large left proximal humerus, model #1051; Pacific Research Laboratories, Vashon, WA). The humeral components were implanted using a non-cemented, press-fit procedure. One baseplate was used throughout to implant the six available RSP glenospheres: the 32-mm Neutral and Minus 4, 36-mm Neutral and Minus 4, and 40-mm Neutral and Minus 4. In the 36-mm Minus 4, 40-mm Minus 4, and 40-mm Neutral, a portion of the inferior edge of the glenoid was removed to allow unhindered installation of the glenosphere because these head sizes have a lip on the inferior edge of the glenosphere encroaching medially on the glenoid. Each implant was placed into the same surrogate bone model, changing only the socket and glenosphere for each configuration. This was then repeated for the other two surrogate bone models. For comparison purposes, we also examined a Delta III reverse shoulder implant (DePuy Orthopaedics, Warsaw, IN). Using

an additional three surrogate bone models, a standard humeral component and baseplate for the Delta III was used in conjunction with a 36-mm diameter glenosphere. Three replicates of each implant were performed in an attempt to limit measurement error. We installed the RSP and Delta III devices according to the manufacturer's recommended surgical techniques using the appropriate surgical instruments. Silicone spray lubricant was used in the joint to simulate synovial fluid.

The center of rotation offset is defined as the distance of the geometric center of the glenosphere from the baseplate–glenoid interface (i.e. the distance of the theoretical center of rotation for the humeral component about the glenosphere from the baseplate–glenoid interface). Reverse Shoulder Prostheses are identified by glenosphere diameter and center of rotation offset (Table 2). For example, the Minus Four has a center of rotation 4 mm more medial than the Neutral version. The various implants are referred to as: 32 Neutral, 32 Minus 4, 36 Neutral, 36 Minus 4, 40 Neutral, 40 Minus 4, and the Delta III.

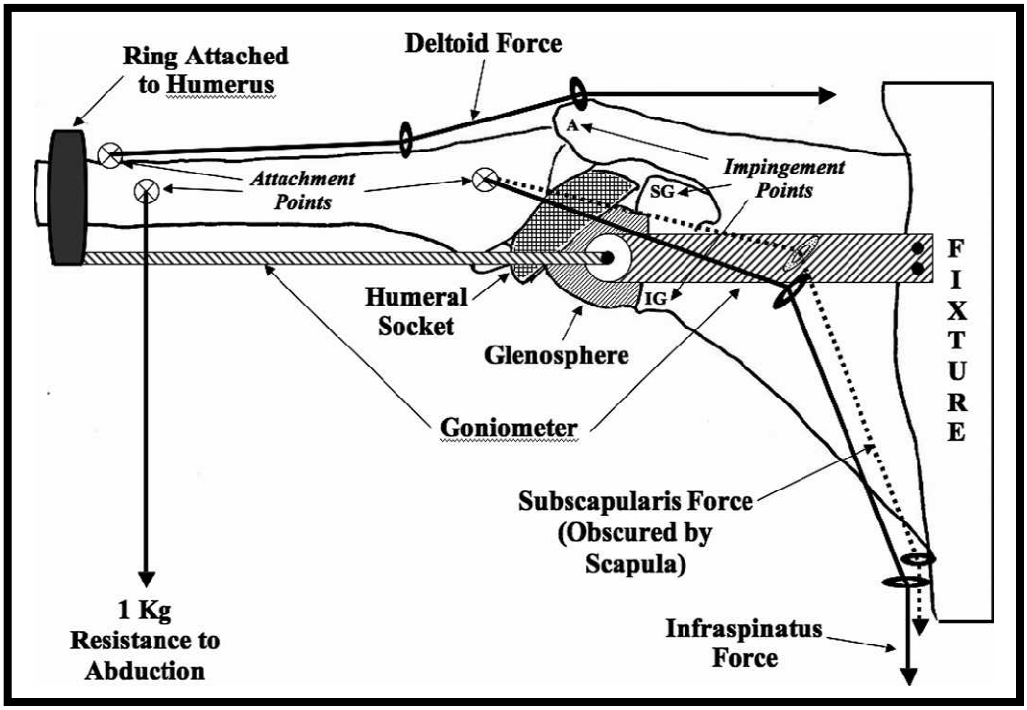

Figure 4. A diagram of the abduction-adduction apparatus shows the line of action for the deltoid, infraspinatus, and subscapularis (obscured by the scapula). The scapula is angled 30º anteriorly in the scapular plane. The humerus is shown in full abduction (parallel to the floor). This is in contrast to the humerus in full adduction in which the arm is perpendicular to the floor (not shown). Impingement point: A = acromion; SG = superior glenoid; IG = inferior glenoid.

Table 2. Tested devices and their respective center of rotation offset.

Glenosphere	Radius (mm)	Center of Rotation Offset (mm)
RSP* 32 Minus 4	16	6.1 ± 0.1
RSP* 32 Neutral	16	10 ± 0.4
RSP* 36 Minus 4	18	2.1 ± 0.1
RSP* 36 Neutral	18	6.0 ± 0.1
RSP* 40 Minus 4	20	0.6 ± 0.1
RSP* 40 Neutral	20	4.2 ± 0.2
Delta III†	18	0.5 ± 0.1

*Reverse Shoulder Prosthesis; Encore Medical, Austin, TX; †DePuy Orthopaedics, Warsaw, IN

We developed an apparatus to simulate abduction of the humerus in the scapular plane (Figure 4). A surrogate bone scapula was rigidly clamped to a custom-made fixture with two lag bolts going through the scapula and fixture and oriented so the humerus began abduction perpendicular to the floor (analogous to the arm being at the side of the body). The scapula was oriented (with the coracoid process rotated anteriorly along the frontal plane) to simulate the 30º angle of the scapular plane. This orientation was deemed closest to physiologic because this is how the scapula is oriented in relation to the rib cage. A goniometer (Eval System; Green Leaf Medical, Palo Alto, CA) was attached to the humerus using a metal ring restricting abduction of the humerus to the scapular plane. A movable sled was connected by a cable through a series of pulleys to the distal portion of the surrogate bone humerus (attached to the insertion point of the medial head of the deltoid). Nylon cables were attached to the insertion point on the humerus of the infraspinatus and subscapularis. The nylon cables were then fed through eyelet screws attached to the point on the scapula identified as the center for the origin of the muscle bundle. One-kilogram weights were then attached to the end of each of the cables to provide tension to the system and allowed movement in the scapular plane. A 1-kg weight was also attached to the distal end of the humerus to provide resistance to abduction.

A digital video camera (Canon Elura 50; Canon, Lake Success, NY) captured the range of motion of the humerus. The video was then imported using video processing software (ImageJ, Rasband, WA; National Institutes of Health,

Bethesda, MD) and calibrated using the same standard reference point available in all videos. ImageJ was also used to determine the center of rotation offset, which was measured as the distance from the glenoid to the center of a sphere placed over the glenosphere of each device. Angle and distance were measured to ± 0.3º and ± 0.5 mm of precision by taking 10 repeated measures and analyzing their standard deviation and ± 0.1º and ± 0.1 mm of accuracy based on the image pixel resolution.

The abduction ROM was measured from 0º (or the inferior-most point of impingement between the polyethylene socket and the scapula; minimal abduction) to the superior-most impingement point (either the greater tuberosity on the acromion or the polyethylene socket on the superior edge of the glenoid; maximal abduction). Because of inferior impingement with the glenoid, the Delta III began abduction at an angle not perpendicular to the floor. Minimal abduction and maximal abduction were measured for all three surrogate bone scapulas. Each measurement was repeated three times to limit measurement error. The means and standard deviations of these values were then calculated.

Comparisons of ROM for each pair (all devices against each other) using Student's t-test were performed in addition to an analysis of variance (ANOVA), and a linear regression was performed to determine best-fit prediction of ROM (dependent variable) and center of rotation offset (independent variable). The data met the assumptions of a parametric test including: normality, equal

variance, and independence. The assumption of normality was met by performing a Shapiro-Wilk's W test (p=0.3751) with a W = 0.9522. The assumption of equal variances was met by performing the O'Brien, Brown-Forsythe, Levene's, and Bartlett's tests for equal variances. All these tests had p values greater than 0.05 (0.1605, 0.3604, 0.2846, and 0.4957, respectively). Significance was set at $p<0.05$. Statistical analyses were performed using the JMP statistical software package (SAS; SAS Institute, Cary, NC).

Results

The glenosphere with the most lateral center of rotation offset (32 Neutral) had the greatest ($p<0.001$) abduction ROM (97º, standard deviation, 0.9º), whereas the least ($p<0.001$) abduction ROM (67º, standard deviation, 1.8º) occurred with the glenosphere with the most medial center of rotation offset (40 Minus 4) (Table 3). With the exception of the Delta III, all reverse shoulder implants showed minimum adductions approaching 0°.

Table 3. Mean values (± standard deviation) for all measurements.

Glenosphere	Minimum Abduction Range of Motion (°)	Maximum Abduction Range of Motion (°)	Total Abduction Range of Motion (°)	Center of Rotation Offset (mm)
RSP 32 Minus 4	2.47 ± 0.1‡	84.7 ± 0.3†	82 ± 0.4	6.1 ± 0.1
RSP 32 Neutral	0.34 ± 0.4	97.1 ± 0.5†	97 ± 0.9	10 ± 0.4
RSP 36 Minus 4	0.59 ± 0.2‡	70.1 ± 0.6§	70 ± 0.8	2.1 ± 0.1
RSP 36 Neutral	2.04 ± 0.4‡	81.2 ± 0.4†	79 ± 0.8	6.0 ± 0.1
RSP 40 Minus 4	0.73 ± 0.7‡	67.2 ± 1.1§	67 ± 1.8	0.6 ± 0.1
RSP 40 Neutral	0.42 ± 0.2‡	76.2 ± 0.1†	76 ± 0.3	4.2 ± 0.2
Delta III	32.3 ± 1.0‡	86.7 ± 0.8†	54 ± 1.8	0.5 ± 0.1
Analysis of variance	p < 0.0001	p < 0.0001	p < 0.0001	

*Analysis of variance shows significant differences among RSP devices; †Superior impingement on the acromion; ‡Impingement on the inferior edge of glenoid/scapula; §Impingement on the superior edge of the glenoid; RSP = Reverse Shoulder Prosthesis; Encore Medical, Austin, TX

Motion was always limited by impingement on a portion of the scapula. Minimum adduction was always limited by impingement on the inferior aspect of the lateral border of the scapula. Maximal abduction was limited by impingement on the acromion for the 32 Neutral, 32 Minus 4, 36 Neutral, 40 Neutral, and Delta III. Maximal abduction was limited by impingement on the superior edge of the glenoid for the 36 Minus 4 and 40 Minus 4.

There was a positive linear correlation (r^2 = 0.96, $p<0.001$) between increasing abduction ROM and reverse shoulder implant center of rotation offset (Figure 5).

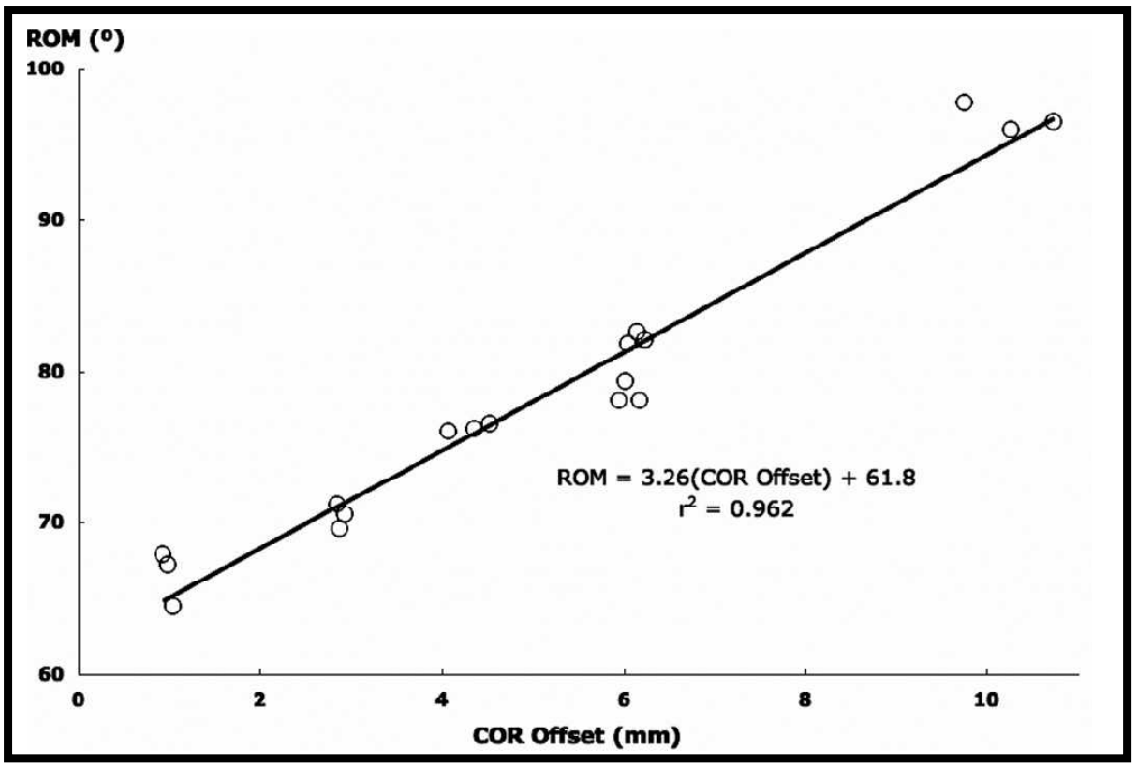

Figure 5. A linear regression scatter plot shows the linear relationship between ROM and center of rotation (COR) offset. Glenospheres with greater center of rotation offset had greater ROM.

Discussion

As the use of the reverse shoulder implant increases, efforts to maximize functional outcomes become more important. To achieve maximal functional improvement, it is necessary to obtain a more complete understanding of the potential benefits and limitations of the available implants. Because ROM is a key element in achieving functional improvement, it is imperative to define the factors affecting glenohumeral motion. The intent of this study was to clarify the potential motion achievable by different reverse shoulder designs, identify the impingement points that limit motion, and determine if a more lateral center of rotation correlates with greater abduction ROM.

Limitations of our study design mostly relate to implantation of the device. To limit variability among the specimens, each device was implanted according to the manufacturer's recommended surgical techniques by an orthopaedic surgeon familiar with the use of reverse shoulder implants. Thus, we did not examine the role of superior and inferior positioning of the glenosphere on the glenoid. Any improvement in motion achievable by translating the position of the glenosphere would likely be true for each of the seven specimens. Further research into the effect of superior and inferior translation is needed. We used a surrogate bone model to mechanically evaluate glenohumeral-ROM response of seven commonly used reverse prostheses. The major advantage of using a surrogate bone model was being able to test inherent differences in ROM related to the

geometry of the devices independent of cadaveric anatomic differences. Our ability to precisely define the center of rotation offset of each implant relative to the glenoid ensured variations in abduction ROM were related to geometric and not anatomic differences. However, the surrogate bone model is not physiologic from the standpoint of material properties or muscle and arm loading. These issues were not deemed a concern, because our aim was to characterize kinematic rather than load-bearing behavior.

Improvements in shoulder elevation have been documented in some clinical reports using reverse shoulder arthroplasty.[21,35,37] The only clinical attempt to isolate improvement in glenohumeral elevation after reverse shoulder arthroplasty was reported by Seebauer et al.[39] Using image intensification, maximal active glenohumeral abduction in the scapular plane using the Delta III prosthesis was 53°.[38,39] Using a cadaver model, Nyffeler et al evaluated abduction ROM of the Delta III with a 36-mm glenosphere.[40] When implanted based on the manufacturer's surgical technique, the mean abduction arc in the scapular plane ranged from 25° to 67° with an average total abduction arc of 42°.[40] In our study, the Delta III was positioned according to the manufacturer's surgical technique. Glenohumeral abduction in the scapular plane ranged from 23.3° to 86.7° with an average total abduction arc of 54.4°. This correlated well with previous clinical and kinematic studies using the Delta III and validated our approaches.

Improvements in ROM correlated with increased distances from the glenoid to the center of rotation of the glenosphere. If the center of rotation was farther away from the scapula, the proximal humerus and humeral socket had more clearance before impinging on the acromion or superior glenoid, thus maximizing glenohumeral abduction (Figure 6).

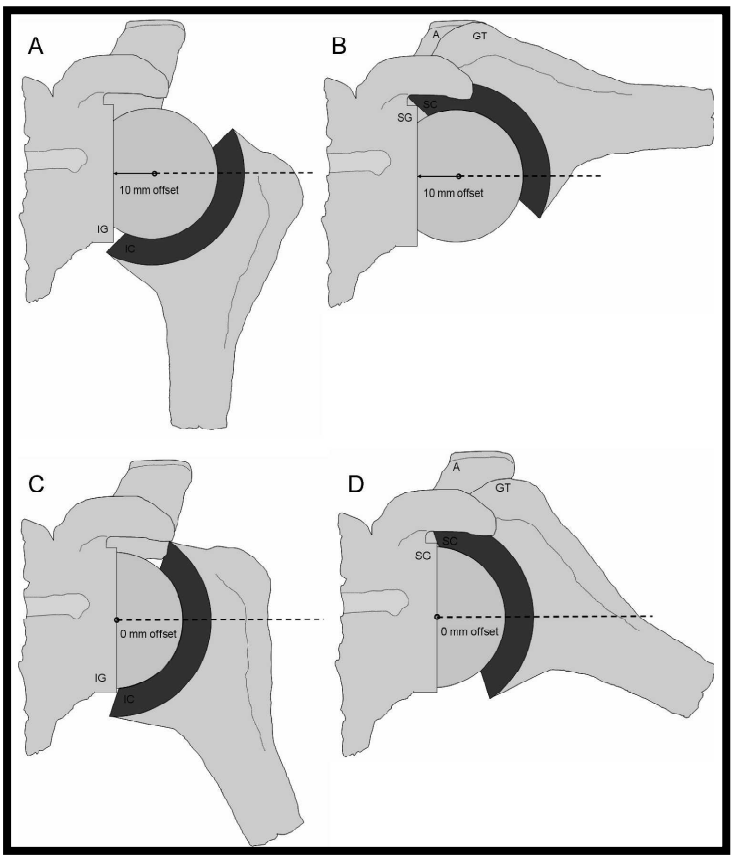

Figure 6. The schematic illustrations show the concept of limitations to isolated glenohumeral motion because of impingement. Changes in (A) adduction ROM, (B) abduction ROM, (C) adduction ROM, and (D) abduction ROM are affected by changes in glenosphere center of rotation offset (+ 10 mm for A and B and no offset for C and D). A = acromion; GT = greater tuberosity; SG = superior glenoid; IG = inferior glenoid; SC = superior cup; IC = inferior cup. Range of motion in the illustration does not include scapular motion. For abduction, impingement may occur on SG (shown) or A.

In adduction, a more lateral center of rotation ensured the medial neck of the prosthesis did not impinge on the inferior aspect of the scapula. This decreased the risk of inferior scapular erosion and improved overall abduction ROM. Because altered glenohumeral geometry affects shoulder muscle forces during abduction,[41] additional study is needed to determine how changes in the center of rotation offset relative to the glenoid may influence shoulder muscle function.

When selecting the appropriate implant for a patient with rotator cuff deficiency, several important factors must be considered: glenosphere baseplate fixation, instability, muscular weakness or deficiency, and the degree of bone loss. In cases which optimal baseplate fixation can be achieved and risk of instability is minimal, maximization of function may be considered. In these patients, surgeons may want to select an implant allowing for the largest ROM possible. Glenospheres with centers of rotation farther away from the glenoid provided greater potential ROM. However, in cases which glenosphere baseplate fixation may be compromised or risk of instability is high, maximizing ROM may not be the highest priority. In these patients, a glenosphere with a more medial center of rotation and a larger radius may maximize stability and baseplate fixation.[23] A complete understanding of the role glenosphere center of rotation offset has on baseplate fixation, implant stability and muscle strength is necessary to optimize implant selection in the patient with rotator cuff deficiency. Abduction and adduction ROM are important variables when selecting an appropriate shoulder

implant. Improvements in total ROM correlated with glenospheres having greater distances from the glenoid to the center of rotation.

CHAPTER 4 - ARTICLE III: EVALUATION OF ABDUCTION RANGE OF MOTION AND AVOIDANCE OF INFERIOR SCAPULAR IMPINGEMENT IN A REVERSE SHOULDER MODEL

Introduction

Reverse shoulder arthroplasty is a successful surgical procedure to treat pain and provide functional improvements in patients with glenohumeral arthritis and rotator cuff deficiency.[21,35-37] However, careful examination of the functional outcomes seen with the reverse shoulder implant reveals variable improvements in range of motion. Valenti et al [42] and Boulahia et al [43] showed active elevation ranging from 30º to 100º and external rotation ranging from 20º to 50º. Frankle et al [36] showed active elevation ranging from 30º to 180º and external rotation ranging from 10º to 65º. This variability is likely due to multiple factors including severity of disease, variable degrees of muscle loss, surgical technique and prosthetic design.

Inferior impingement of the reverse shoulder implant on the inferior scapular neck has been noted as the mechanism for the development of scapular notching.[35,43] Typically, this impingement occurs when the arm is in a resting position, and biomechanically has been referred to as an adduction deficit.[40] Reduction of the adduction deficit is of particular interest, because progressive scapular notching

has been observed to a variable degree radiographically, including 56% by Valenti et al,[42] 63% by Boulahia et al,[43] 65% by Sirveaux et al,[21] 74% by Boileau et al,[35] and 96% by Werner et al[37] and has even been implicated as the cause of failure in several patients.[44] A previous study by Nyffeler et al[40] demonstrated adduction deficit was decreased by placing the base plate flush with the inferior edge of the glenoid, with the glenosphere extending below the inferior border of the scapula. This result suggested that surgical technique could help to reduce adduction deficit.

Looking specifically at prosthetic design, there are currently several different reverse shoulder implants available, and many others likely in development. Each of these implants differs in several basic design parameters, including: center of rotation (COR) offset, glenosphere diameter, and humeral neck-shaft angle relative to the horizontal plane. COR offsets can vary from 0 to 10 mm lateral to the glenoid fossa. The diameter of available glenospheres also varies from 32 to 42 mm, and humeral neck-shaft angles range from 135º to 155º. The implication of these different design factors on shoulder kinematics is poorly understood and may have a dramatic influence on outcomes following surgical reconstruction. To date, no biomechanical study has systematically evaluated the effect of reverse shoulder prosthesis design and implant positioning on glenohumeral motion.

The purpose of this study was not to create a surgical technique, but to determine how different parameters contribute to the total glenohumeral abduction ROM and adduction deficit in a reverse shoulder model. Our hypothesis was that glenosphere position, COR offset, glenosphere diameter and humeral neck-shaft angle had different effects on abduction ROM and adduction deficit.

Materials and Methods

Reverse shoulder implant components consisted of a ball that was attached to the glenoid (glenosphere) and a humerosocket that was attached to a wooden dowel. These components were manufactured using Delrin®, which is a wear resistant and low friction plastic. The glenospheres were manufactured with three diameters (30, 36, and 42 mm) and three COR offsets (0 mm or hemispherical, +5 mm and +10 mm offset from the glenoid) (Table 4). The glenoid components were rigidly attached to the glenoid surface of a Sawbones© shoulder model (Large left scapula, model #1050-10, Pacific Research Laboratories, Vashon WA).

Table 4. Glenosphere and humerosocket component geometry.

Glenosphere		Humerosocket	
Diameter (mm)	**COR offset (mm)**	**Humeral angle (°)**	**Depth (mm)**
30	0	130	8.4
30	5	150	8.4
30	10	170	8.4
36	0	130	10.1
36	5	150	10.1
36	10	170	10.1
42	0	130	11.8
42	5	150	11.8
42	10	170	11.8

COR, center of rotation.

In order to implant the glenospheres in a consistent manner, we used the block on the medial side of the Sawbones© scapula as a reference for measurement. The glenoid on each Sawbones© scapula was reamed flat so that the plane of the glenoid was parallel to the plane medial border of the block of the scapula.

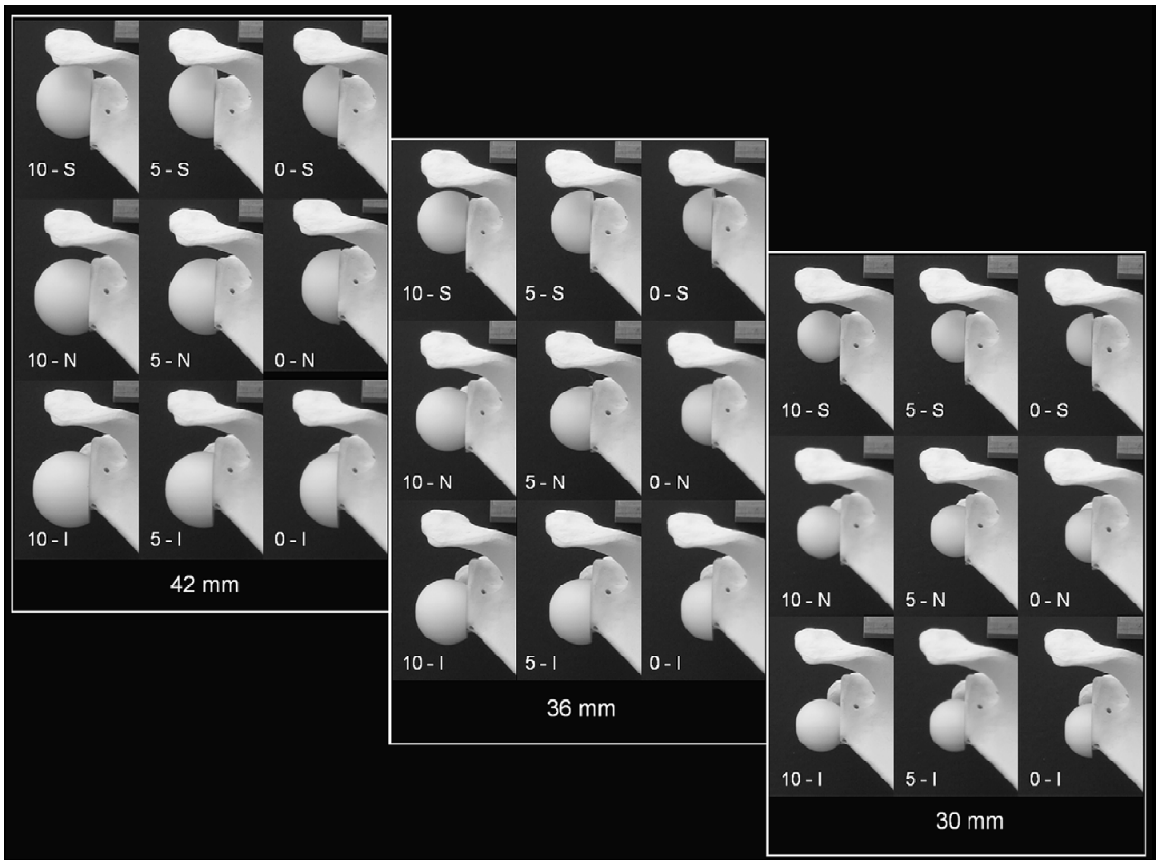

Figure 7. Photograph sequence illustrates the 9 glenoid component arrangements, consisting of the 3 center of rotation offsets of 0, +5 and +10 mm and the 3 glenosphere positions of superior (S), neutral (N), and inferior (I), for each of the 3 different diameter glenospheres (10, 36 and 42 mm).

Three different positions on the glenoid were studied (superior, neutral and inferior) (Figure 7). The neutral position was centered in the glenoid, while the superior and inferior positions were halfway between the center and the superior and inferior edges of the glenoid, respectively. Variations in glenosphere component geometry and placement on the glenoid were consistent with clinical practice with the exception of the superiorly placed glenospheres.[19,21,23,35,36,38,40] Although rarely used in the senior author's practice, the superior position was

included in this analysis to understand its effect on ROM and inferior scapular impingement.

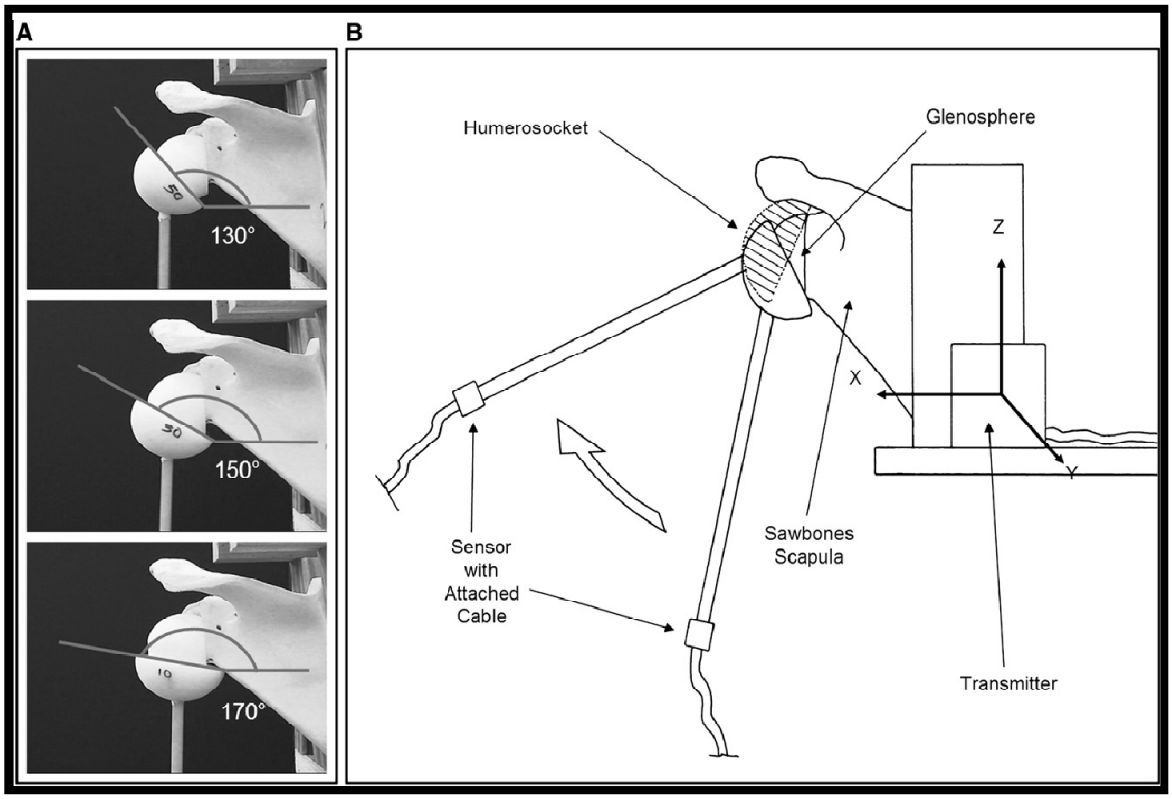

Figure 8. A, photographs show the 3 different humeral neck-shaft angles. The 170º humeral neck-shaft angle is not currently available in clinical practice. B, Schematic illustration shows the experimental setup used for adduction-abduction range of motion measurements.

Humeral components were manufactured for each glenosphere with three humeral neck-shaft angles: 130º, 150º and 170º. The inside diameter of the humeral socket matched the glenosphere diameter, and the socket depth was designed with a constant depth to radius ratio (d/r) of 0.56. This d/R ratio was chosen as the mean of the commercial reverse implants (0.46 to 0.67). A hole

was machined in the humerosocket component to orient the sockets at each of the three neck-shaft angles (Figure 8-A). Machining tolerances were approximately ± 0.05 mm, and machined component geometries were measured using a digital caliper (± 0.025 mm precision). The humerosocket outer diameters for this study were held constant throughout all devices (50 mm), which is a typical diameter for the normal humeral head. Table 4 summarizes the humeral component depth for each of the three socket diameters and three humeral angles. A wooden dowel was inserted into the hole to simulate the humeral shaft. The dowel was 33 cm long which is the approximate length of the average humerus.[19]

The Sawbones© scapula model was used in conjunction with a three-dimensional coordinate measurement system to measure total glenohumeral abduction ROM of the humerosocket component in the scapular plane (Figure 8-B). The scapula was rigidly fixed and oriented to simulate the 30º angle of the scapular plane and tilted 23° anteriorly to the sagittal plane. The scapula was held in neutral abduction with the glenoid face perpendicular to the floor. A six-degree of freedom, electromagnetic goniometer (Flock of Birds, Ascension Technology Corporation, Burlington, VT) with an accuracy of ± 0.05 mm and ± 0.15º was rigidly attached to the distal end of the wooden dowel.

With the scapula-glenoid component fixed, each of the nine glenospheres was evaluated using the three different humeral neck-shaft angled components.

Glenohumeral abduction ROM was limited superiorly by impingement of the socket on either the superior edge of the glenoid or the acromion, whereas glenohumeral adduction was limited by impingement on the inferior glenoid or scapula (adduction deficit) or 0º (neutral position of the humeral shaft), whichever occurred first. The humeral component (dowel) was manually manipulated from minimum adduction to maximum abduction. X, Y, and Z-coordinates were recorded at minimum adduction and at maximum abduction, wherein the X, Z-coordinates corresponded to the abduction plane. The adduction deficit was determined by the resting position in maximal adduction. If adduction was 0°, no adduction deficit (NAD) was present. Total glenohumeral abduction ROM was determined from the difference between maximal adduction and maximum abduction.

Statistical analyses were conducted using the JMP statistical-software package (SAS, SAS Institute, Cary, NC). Four independent factors (diameter, COR offset, glenoid placement and humeral neck-shaft angle) were compared to the dependent factors (abduction ROM and adduction deficit angle). Descriptive statistics were performed using a standard least squares regression and a multivariate analysis of variance (MANOVA). The MANOVA analyzed the effect of each factor on the dependent variables. A balanced factorial design with the same number of observations for each factor was used. The significance level was set at $p<0.05$ for all statistics.

Results

Total Abduction ROM

The greatest total abduction ROM was 117.5º (42 mm, +10 mm COR, Inferior, 170º), whereas the least maximum total abduction ROM was 40.2º (30 mm, 0 mm COR, Neutral, 170º and 30 mm, 0 mm COR, Neutral, 150°) (Table 5).

Table 5. Glenohumeral abduction range of motion measurements (mean ± standard deviation) for the 4 different design factors studied.

Glenosphere position	COR offset	Humeral component	Abduction range of motion (°)		
			30 mm	36 mm	42 mm
Superior	0 mm	130°	48.2 ± 5.8	45.2 ± 4.8	43.2 ± 3.3
		150°	47.9 ± 5.8	43.9 ± 3.8	43.4 ± 4.5
		170°	48.6 ± 5.3	45.2 ± 3.6	43.7 ± 3.7
	+5 mm	130°	58.8 ± 5.4	55.0 ± 5.2	54.4 ± 5.3
		150°	58.1 ± 4.9	55.4 ± 5.2	53.8 ± 4.8
		170°	58.9 ± 4.5	55.8 ± 4.6	53.9 ± 4.2
	+10 mm	130°	70.5 ± 6.5	67.6 ± 5.0	64.8 ± 3.5
		150°	69.4 ± 6.3	66.8 ± 5.3	66.1 ± 5.1
		170°	69.7 ± 6.0	67.9 ± 5.7	66.3 ± 5.2
Neutral	0 mm	130°	41.8 ± 1.1	50.0 ± 1.8	59.2 ± 2.3
		150°	40.2 ± 0.8	49.9 ± 0.9	57.6 ± 1.2
		170°	40.2 ± 2.0	50.6 ± 0.5	58.2 ± 1.3
	+5 mm	130°	68.1 ± 2.3	75.5 ± 1.2	83.1 ± 2.0
		150°	67.4 ± 0.7	74.7 ± 1.3	83.1 ± 1.4
		170°	67.6 ± 1.0	75.4 ± 1.2	83.6 ± 0.7
	+10 mm	130°	90.1 ± 1.3	92.3 ± 0.9	94.5 ± 1.0
		150°	89.1 ± 0.5	95.9 ± 1.0	102.7 ± 1.1
		170°	89.3 ± 0.7	96.2 ± 0.4	102.9 ± 0.6
Inferior	0 mm	130°	62.3 ± 0.7	65.7 ± 0.9	67.8 ±2.4
		150°	65.3 ± 0.9	73.7 ± 1.4	79.5 ± 0.8
		170°	65.5 ± 1.2	73.0 ± 1.1	79.1 ± 0.7
	+5 mm	130°	73.3 ± 1.1	76.5 ± 1.3	77.0 ± 1.5
		150°	86.4 ± 1.1	92.2 ± 1.3	96.2 ± 1.0
		170°	86.2 ± 0.7	92.5 ± 1.4	98.4 ± 0.6
	+10 mm	130°	84.3 ± 1.1	87.1 ± 2.1	89.2 ± 2.7
		150°	102.2 ± 0.7	105.1 ± 1.2	106.6 ± 0.7
		170°	106.0 ± 0.9	112.1 ± 0.9	117.5 ± 0.8

COR, center of rotation.

Maximal abduction was limited by impingement on either the acromion or the superior edge of the glenoid. Significant effects on total glenohumeral abduction ROM were found for all the factors studied ($p<0.0001$). The factor with the greatest effect on total abduction ROM was glenosphere COR offset ($p < 0.0001$, $F = 2,118$), followed by glenoid position ($p<0.0001$, $F = 1,740$), glenosphere diameter ($p<0.0001$, $F = 79$) and humeral angle ($p<0.0001$, $F = 77$). Glenospheres with positive COR offset improved the total abduction ROM for all glenoid positions examined. Glenospheres with a COR offset of +10 mm were associated with up to a 91% increase (neutral glenoid position) in total abduction ROM, compared to glenospheres with no COR offset (0 mm) (Figure 9).

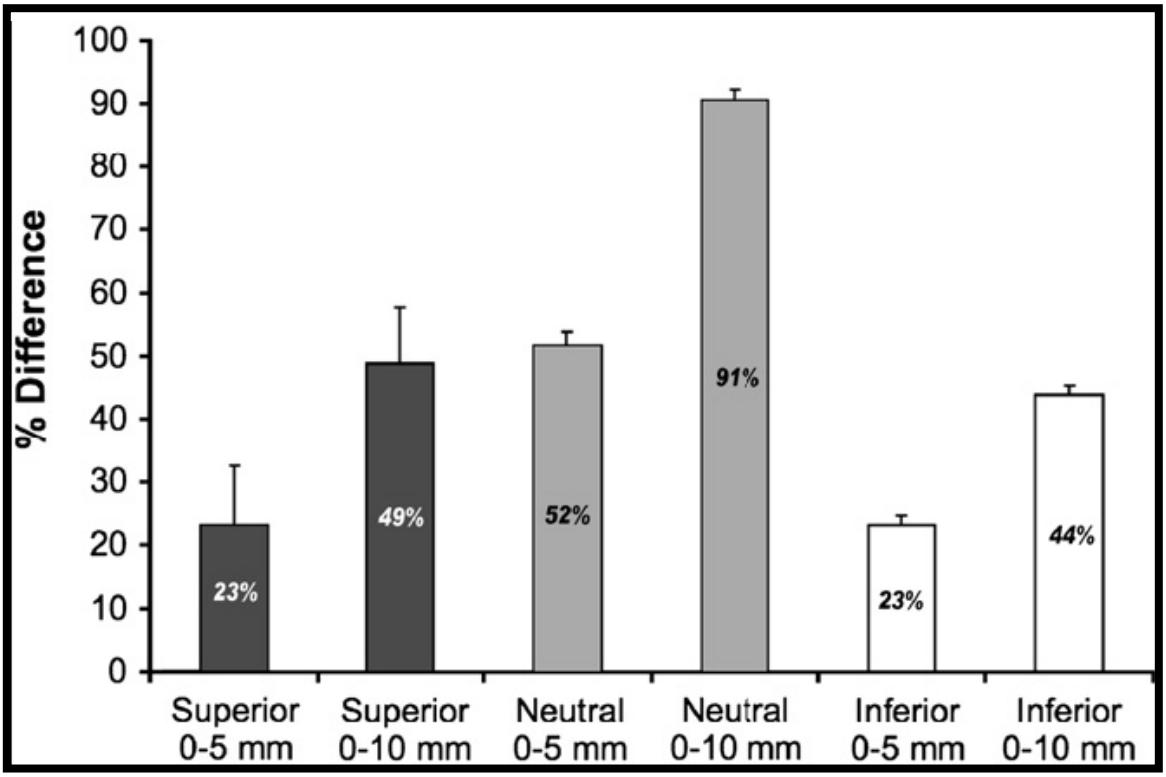

Figure 9. Graph shows the percentage difference in abduction range of motion (ROM) between components with +5 and +10 mm center of rotation (COR) offset (arranged according to glenosphere position). The mean combined ROM and COR offset data (n = 45) is presented with the standard deviation (error bars).

Adduction Deficit

The largest adduction deficit was 64.4º (30 mm, 0 mm COR, Superior, 170º), whereas the minimum adduction deficit was 0º or NAD (Table 6). Significant effects on adduction deficit were found for all the factors studied ($p<0.0001$). The factor with the greatest effect on decreasing adduction deficit was humeral neck-shaft angle ($p<0.0001$, $F = 3,264$), followed by glenosphere position ($p<0.0001$, $F = 2,054$), glenosphere COR offset ($p<0.0001$, $F = 1,212$) and glenosphere diameter ($p<0.0001$, $F = 116$). The three specific factors that had the greatest effect on adduction deficit were the 130º humeral neck-shaft angle, inferior position and +10 mm COR offset ($p<0.0001$) (Figure 9).

Table 6. Adduction deficit measurements (mean ± standard deviation for the 4 different design factors studied).

Glenosphere position	COR offset	Humeral component	Abduction deficit angle (°)		
			30 mm	36 mm	42 mm
		130°	27.9 ± 1.2	24.6 ± 1.0	21.5 + 1.6
	0 mm	150°	46.4 ± 1.7	44.2 ± 0.7	39.9 ± 1.7
		170°	64.4 ± 1.5	61.4 ± 0.7	58.4 ± 1.6
		130°	15.6 ± 1.1	13.4 ± 0.9	9.9 ± 2.0
Superior	+5 mm	150°	34.2 ± 1.7	32.1 ± 0.5	29.5 ± 1.5
		170°	52.6 ± 1.2	50.2 ± 0.4	47.2 ± 1.9
		130°	3.7 ± 0.4	1.9 ± 0.7	2.0 ± 0.6
	+10 mm	150°	21.9 ± 1.3	19.9 ± 0.8	17.4 ± 1.6
		170°	40.3 ± 1.4	37.4 ± 2.1	35.4 ± 1.2
		130°	24.0 ± 1.4	21.2 ± 1.6	16.0 ± 1.9
	0 mm	150°	43.7 ± 1.3	39.8 ± 1.0	34.8 ± 1.6
		170°	62.6 ± 2.1	57.1 ± 0.9	53.1 ± 1.3
		130°	11.5 ± 3.0	7.7 ± 1.5	2.8 ± 2.1
Neutral	+5 mm	150°	29.6 ± 0.8	27.0 ± 1.5	21.5 ± 2.1
		170°	47.8 ± 0.9	44.2 ± 1.3	39.9 ± 1.4
		130°	1.1 ± 0.5	0°*	0°*
	+10 mm	150°	18.4 ± 0.6	14.7 ± 1.7	10.5 ± 1.5
		170°	36.5 ± 0.8	33.4 ± 0.9	29.2 ± 1.3
		130°	0°*	0°*	0°*
	0 mm	150°	15.1 ± 1.4	10.4 + 1.8	6.0 ± 0.9
		170°	32.9 ± 1.3	28.7 ± 1.5	25.0 ± 1.4
Inferior		130°	0°*	0°*	0°*
	+5 mm	150°	5.4 ± 1.2	3.4 ± 1.9	0°*
		170°	23.4 ± 1.0	20.1 ± 2.3	16.1 ± 1.4
		130°	0°*	0°*	0°*
	+10 mm	150°	0°*	0°*	0°*
		170°	15.0 ± 0.8	11.5 ± 1.1	7.9 ± 1.0

COR, center of rotation.
*No adduction deficit.

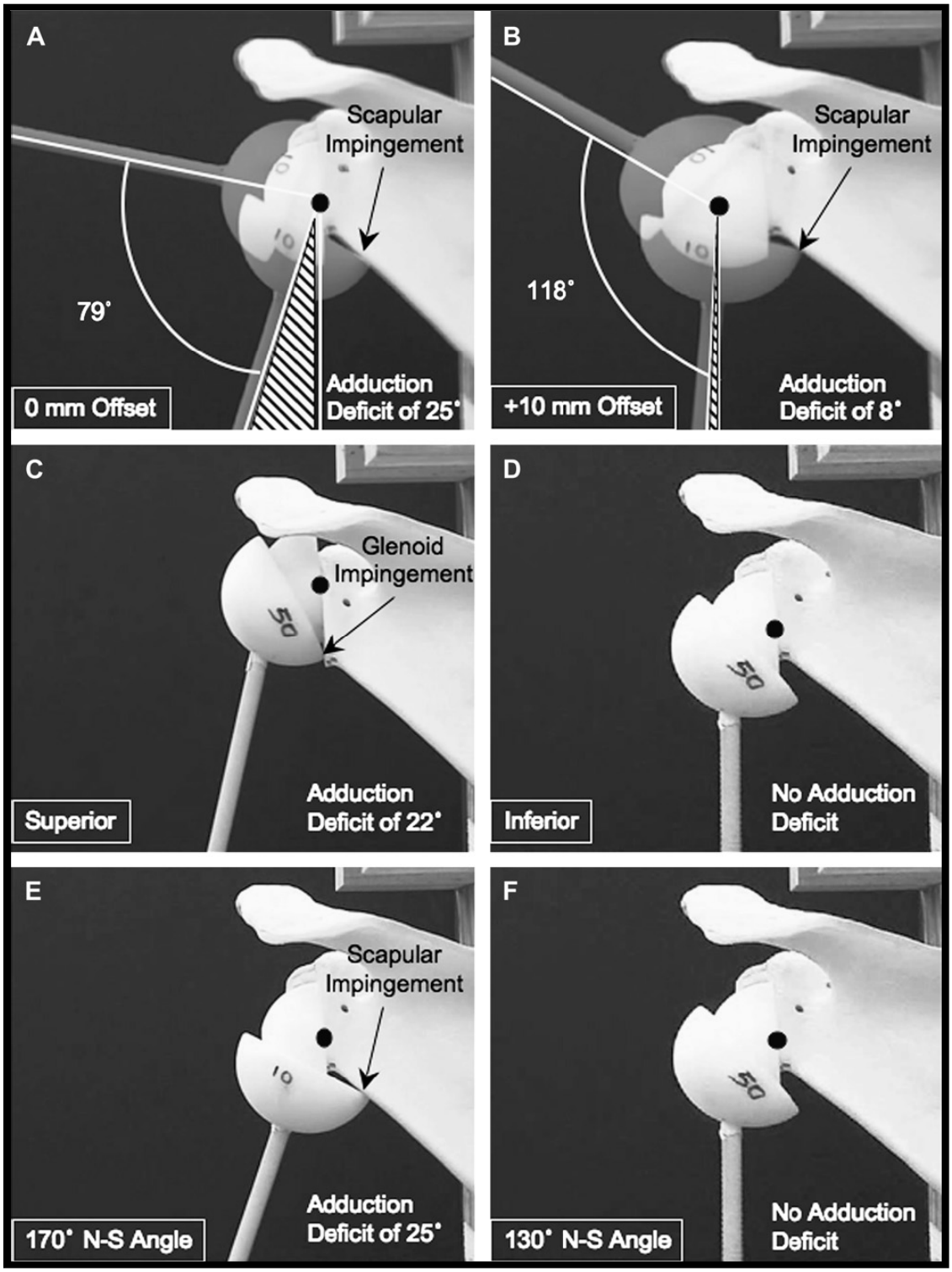

Figure 10. Photographs show the differences in adduction deficit. A and B, Center of rotation (COR) offset of 0 mm vs. a COR offset of +10 mm. C and D, Superior placement on the glenoid vs. inferior placement on the glenoid. E and F, A 170º neck-shaft (N-S) angle vs. a 130º N-S angle.

Discussion

A careful analysis of the outcomes following reverse shoulder replacement reveals variable improvements in shoulder elevation.[36,42,43] In order to further accurately judge these improvements, isolated glenohumeral motion must be evaluated. However, up to now, this information is largely lacking. Seebauer et al [38,39] conducted the only clinical study to isolate the improvement in glenohumeral elevation after a reverse shoulder implant. Based on dynamic fluoroscopic radiographs, they reported that the maximum active glenohumeral abduction ROM in the scapular plane using the Delta III prosthesis was 53°. A similar amount of glenohumeral motion was seen in a cadaver model using the same prosthesis.[40] Nyffeler et al [40] evaluated the abduction ROM of the Delta III with a 36 mm glenosphere. When implanted using the manufacturer's recommended surgical technique, the mean abduction ROM in the scapular plane ranged from 25° to 67° (total abduction ROM of 42°). When implanted in an inferior position on the glenoid, the average abduction ROM ranged from 1º to 81º (total abduction ROM of 80°).[40] Thus, modification of surgical technique not only improved the overall motion, but helped to limit the adduction deficit from 25°, for the manufacturer's recommended placement, to 1º for an inferior placement on the glenoid.

In the current study, evaluation of abduction ROM noted statistically significant differences for different implant designs and changes in implant position on the

glenoid. The variable that resulted in the greatest improvement in ROM was COR offset ($p<0.0001$, $F = 2,118$). The larger the COR offset, the greater the abduction motion. Additionally, placement of the glenosphere inferiorly on the glenoid resulted in improved motion ($p<0.0001$, $F = 1,740$). Moving the center of rotation further away from the scapula, or placing the glenosphere more inferiorly, gives the humerosocket more clearance before impinging on the acromion or superior glenoid, thereby maximizing glenohumeral abduction ROM. While glenosphere diameter and humeral angle resulted in improvements in motion, these improvements were small when compared to COR offset and glenosphere position. This can be exemplified by comparing differences in ROM between different diameters vs. different COR offsets and comparisons between different glenosphere positions vs. different neck-shaft angles (Table 6). For example, changes in diameter netted a ROM improvement of only 5.5º (30 mm to 42 mm, 0 mm offset, inferior placement, 130º neck-shaft angle), while changes in COR offset netted a larger change of 22º (0 mm to +10 mm offset, 30 mm, inferior placement, 130º neck-shaft angle). Changes in neck-shaft angle showed a small change of 3.2º (130º to 170º neck-shaft angle, 0 mm offset, 30 mm, inferior placement) in comparison to 20.5º for a change in glenosphere position (neutral to inferior placement, 0 mm offset, 30 mm, 130º neck-shaft angle). Thus, maximizing abduction range of motion is best achieved with larger COR offset and inferior translation of the glenosphere placement.

Examination of the adduction deficit noted significant differences depending on the design examined and the position of implantation. In general, adduction deficit was primarily dependent on humeral component angle ($p<0.0001$, $F = 3,264$), followed by glenosphere position ($p<0.0001$, $F = 2,054$), and glenosphere COR offset ($p<0.0001$, $F = 1,212$). Larger glenosphere diameters were able to limit adduction deficit only minimally ($p<0.0001$, $F = 116$). Several of the constructs displayed no adduction deficit (NAD), and were therefore able to be adducted to at least 0º. Thus, modifications in both surgical technique (inferior translation), and prosthetic design (more varus neck-shaft angle and larger COR offset) resulted in a reduction of the adduction deficit.

A Sawbones© scapula model was used to biomechanically evaluate the effects of changing the center of rotation (COR) offset, glenosphere position, glenosphere diameter and humeral neck-shaft angle on glenohumeral abduction ROM and adduction deficit in reverse shoulder implants. The major advantage of using a Sawbones© scapula model was the ability to test inherent differences in ROM related to the geometry of the devices, independent of anatomical differences present when using cadaver models.[45,46] Using a cadaver model, Nyffeler et al noted that motion was always limited by impingement on areas of the scapula.[40] Thus, the Sawbones© model was able to best replicate a consistent model of the scapular anatomy in an effort to study how motion is limited by scapular impingement.

Limitations of this study include omission of the proximal humeral anatomy, lack of variation in glenosphere tilt, changes relating to human scapular morphology (including inclination of the inferior glenoid neck and its intersection with the lateral body of the scapula), no scapulothoracic motion, notching in locations other than inferior to the glenoid component and truncation of the glenoid vault (which can occur during reaming).[40] In the anatomic shoulder, ROM is limited by mechanical impingement and also by soft tissue tension. Presumably, similar impingement points are present in reverse shoulder arthroplasty, but actual impingement can vary greatly depending on the placement of the humeral component in the humeral shaft and glenosphere orientation. Given the relatively large number of design factors considered in this study, we elected to omit considerations of glenosphere tilt and proximal humeral geometry and focus on the effects of humeral and glenoid component geometry on abduction ROM and inferior scapular impingement. One other limitation of this study was the lack of soft tissue tension (muscle and tendon forces) in the mechanical model. Readers should be cautioned that the findings of this study may have involved prosthetic combinations and positions that are clinically unfeasible due to the excessive soft tissue tension they would generate that could lead to limited motion and stiffness (i.e. overstuffing the joint), or due to the lack of soft tissue tension that could lead to instability. It should be stated that this study did not determine the safe limits of any of the parameters tested and that component size and position must be individualized for each clinical situation.

Ultimately, when selecting a reverse shoulder implant, several important design and surgical factors must be considered. These include, but are not limited to: baseplate-host bone fixation, stability (resistance to subluxation and dislocation), muscular weakness or deficiency, the degree of bone loss and soft tissue tension. In cases where optimal baseplate fixation can be achieved and risk of instability is minimal, maximization of function may be considered. In these cases, surgeons may wish to select an implant that allows for the largest ROM and the least amount of adduction deficit. Based on the results of this study, glenospheres with a greater distance from the glenoid to the center of rotation and an inferior placement on the glenoid provide for greater potential ROM. Adduction deficit can best be improved by selecting prosthesis with a varus neck-shaft angle, and inferior placement of the glenosphere on the glenoid.

In summary, glenosphere geometry and position on the glenoid are important variables to consider in selecting a reverse shoulder implant. Indeed, as pointed out previously by Hasan and associates,[47] greater attention to achieving proper component position and postoperative motion may lead to increased patient satisfaction after shoulder arthroplasty. Our results show that increasing glenosphere center of rotation offset and inferior placement of the glenosphere on the glenoid provided the greatest improvements in total glenohumeral abduction ROM in a biomechanical Sawbones© model. It should be noted that in-vivo clinical situations may be more complex than what we have tested here. Other factors, such as soft tissue tension and bone quality as well as

glenosphere geometry and position on the glenoid must be considered when the surgeon needs to find a compromise between range of motion and stability when performing reverse shoulder arthroplasty. Adduction deficit can be best reduced by a varus neck-shaft angle and inferior placement on the glenoid.

CHAPTER 5 - ARTICLE IV: HIERARCHY OF STABILITY FACTORS IN REVERSE SHOULDER ARTHROPLASTY

Introduction

Management of patients who have an irreparable rotator cuff tear in the presence of glenohumeral arthritis and instability historically has been a challenge. Treatment options continue to evolve, and one of the newest is reverse shoulder arthroplasty (RSA).[35,36] The uniqueness of RSA is its conversion of the humerus into a socket (humerosocket) and the glenoid into a ball (glenosphere) with more stable congruent articulation for compensation of the dysfunctional rotator cuff. Recent clinical studies have provided evidence of pain relief and functional improvements after RSA. [33,35-37,42,43,48,49]

Although improving glenohumeral stability is the ultimate aim of RSA, subluxation and dislocation of RSA devices still occur. Dislocation rates have been shown in the range of: 2.4%, 6.3%, 8.6%, 16.7% and 31%.[37,50-53] In one study, dislocation rate (7.5%) was found to be the most common complication.[54] Joint stability, extensively studied in total shoulder arthroplasty (TSA),[55,56] has been associated with joint contact characteristics, such as prosthetic surface geometry and the coefficient of friction present at the interface. Preservation of the joint

compressive force is also a key factor in stability. Based on this biomechanical information in TSA and clinical observations, it is believed that these factors may also be critical to joint stability in RSA. However, their importance in relation to the stability of the implant has not been defined. As a result, selection by the surgeon of current prosthetic designs is largely empirical, which inevitably increases the probability of undesirable outcomes in RSA.

In order to elucidate the concept of stability in reverse shoulder implants, we addressed two questions. First, what is the hierarchy of importance of joint compressive force, prosthetic socket depth, and glenosphere size in relation to stability? Second, is this hierarchy defined by underlying joint contact characteristics, including surface geometry and coefficient of friction, which are theoretically predictable?

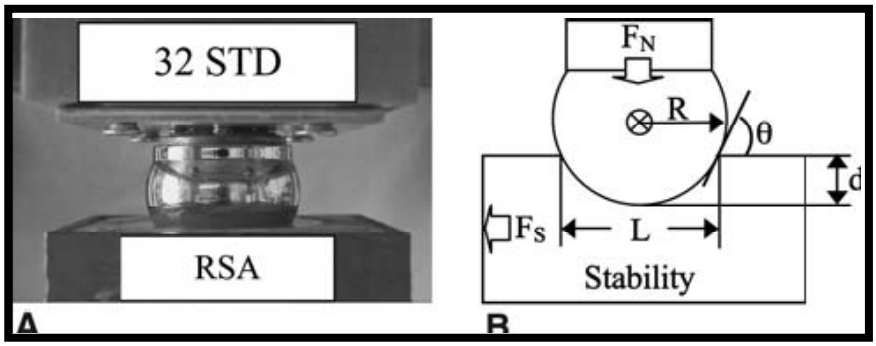

Figure 11. A, photograph shows how the glenosphere (32 mm) lays on top of the standard humerosocket liner. B, The diagram illustrates the stability model and its variables. F_N = compressive force applied to the glenosphere; F_S = force required to dislocate glenosphere; R = radius of glenosphere; d = depth of humerosocket; L = chord length of humerosocket; θ = incident angle between the glenosphere and the humerosocket edge.

Materials and Methods

Examination of RSA stability was addressed in both experimental and theoretical models. In the experimental model, the dependent variable, dislocation force F_S, was examined through three independent variables: the compressive force F_N, the humerosocket depth d and the glenosphere radius R (Figure 11). The results were analyzed statistically by either two-sample or multi-sample inference. A theoretical simulation was performed using a rigid body joint contact model.

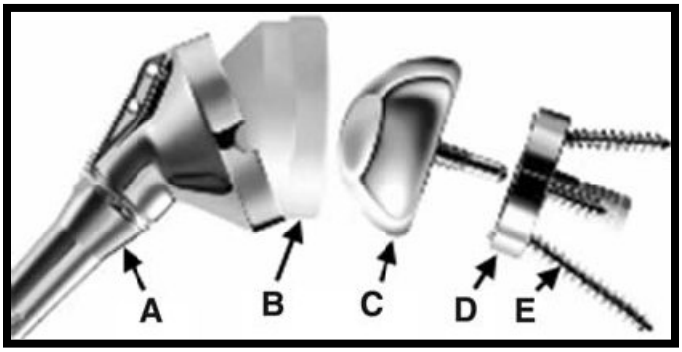

Figure 12. A representation of a typical reverse shoulder implant and all of its parts is shown. A = humerosocket; B = UHMWPE humerosocket liner; C = glenosphere; D = baseplate; E = peripheral screws (Delta III 36-mm glenosphere and standard polyethylene humerosocket).

We used eight currently available RSA devices, six Encore (Encore Medical Corp, Austin, TX) and two Delta III (DePuy Orthopaedics, Warsaw, IN), in the study. The devices consisted of congruent ball and socket components with cobalt-chrome glenospheres and ultrahigh-molecular-weight polyethylene (UHMWPE) sockets (Figure 12). We used three component sizes defined by the

diameter of the glenosphere as 32 mm, 36 mm, and 40 mm. Each humerosocket had a known depth and socket radius (Figure 12). For a given component size, socket depth was evaluated in terms of the ratio of socket depth d to socket radius R (d/R). The RSA UHMWPE socket inserts were either of standard (STD) depth or of a semi-constrained (SC) depth, in which the SC socket is deeper than the STD socket. The typical 36 Encore SC, 36 Encore STD, 36 Delta SC, and 36 Delta STD had d/R ratios of 0.56, 0.48, 0.68, and 0.46, respectively.

Three additional congruent glenospheres and humerosockets were machined from Delrin® for evaluation of the mathematical model. In these specimens, the glenosphere radius varied, and the d/R ratio (chosen to be in the midrange of the studied RSA devices) was held constant at 0.56.

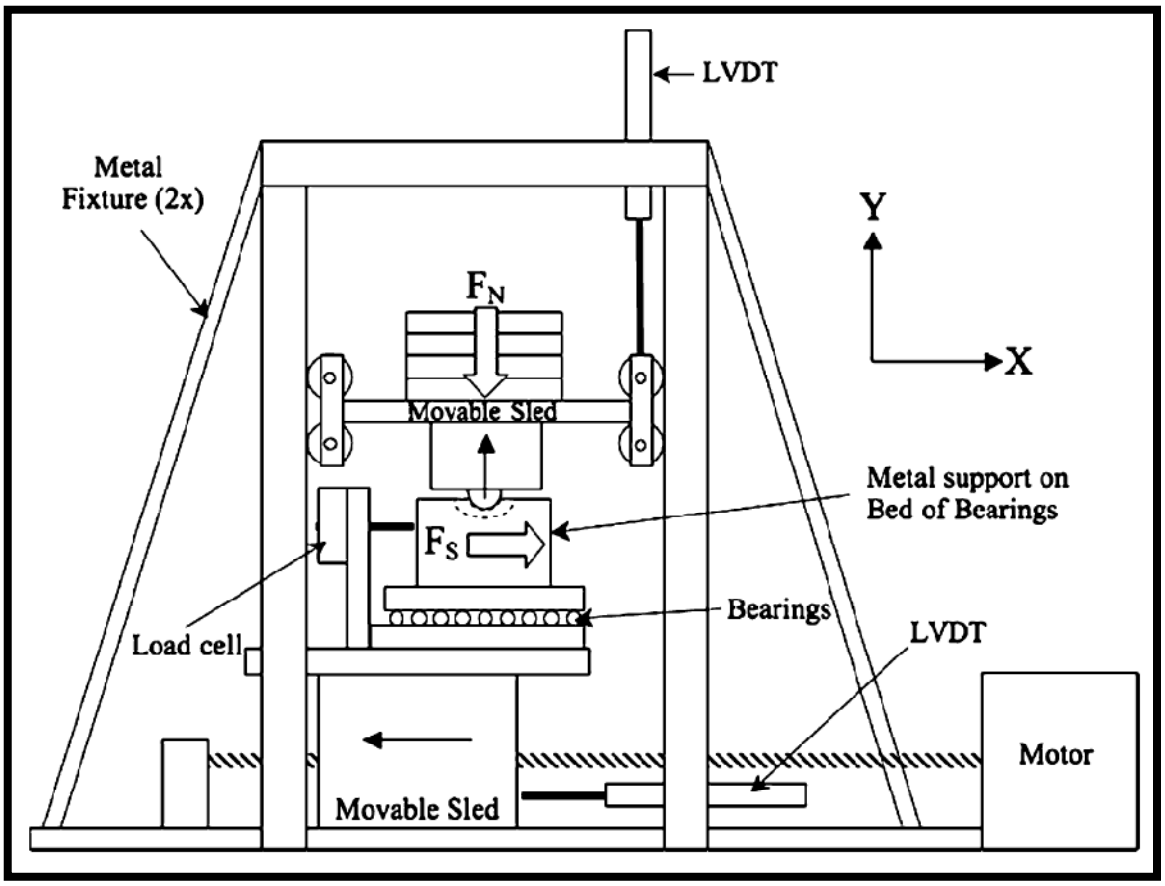

Figure 13. A schematic illustration shows the custom, biaxial testing apparatus used to measure RSA stability. A compressive force (F_N: 66 N, 110 N, 155 N, or 200 N) is applied in the Y direction to the glenosphere, which is attached to the bottom of the movable sled. The amount of force it takes to dislocate the glenosphere from the humerosocket F_S is measured by a load cell attached to a metal fixture resting on a bed of bearings. The load cell, metal fixture, and bearings all rest on a movable sled that moves in the X direction at a constant 5 cm/minute. LVDT = linear voltage displacement transducer used to measure movement of the sleds.

We performed mechanical testing of RSA stability on a custom biaxial loading fixture (Figure 13) that was based on several total shoulder arthroplasty (TSA) stability studies.[55,56] The humerosocket was attached to a horizontal sled that could translate freely only in the X-axis, whereas the glenosphere was attached to a vertical sled that could translate freely only in the Y-axis. We used weights,

placed on the vertical sled, to apply compressive forces F_N (up to 200 N) to each RSA device. The F_N corresponded to the range of unresisted physiological shoulder joint forces.[56-58] A motor translated the horizontal sled at a constant speed of 5 cm/min,[55,59] and a 2,200 N load cell (Omega Engineering Inc, Stamford, CT) was used to measure the dislocation force F_S. We performed five conditioning runs and then five recorded runs for each RSA configuration at each force level. Custom Labview software (National Instruments, Austin, TX) and a 12-bit data acquisition system (National Instruments) were used to collect data (100 samples/second). We used silicone spray lubricant to simulate synovial fluid. [60-63]

The mathematical model of RSA stability was modified from a previous model for studying conventional TSA.[55] For dislocation to occur in a ball and socket joint (Figure 11), the resultant force must be directed outside of the socket surface.[64] If both ball and socket components are assumed to be rigid bodies, the dislocation force F_S is determined by the ball-socket incident angle (constraint angle) and friction and is given by:

$$F_S = F_N \times \frac{TAN(\theta)+\mu}{1-\mu \times TAN(\theta)} \quad (1)$$

with

$$\theta = ATAN\left(\frac{L/2}{R-d}\right) \quad (2)$$

where μ is the coefficient of friction between the glenosphere and humerosocket, L is the chord length of the humerosocket, and θ is the incident angle between the glenosphere and the humerosocket edge.

For RSA, the congruency of ball and socket components determines the chord length and is given as L = 2[d(2R-d)]1/2; the expression for θ can then be rewritten as:

$$\theta = \mathrm{ATAN}\left(\frac{\sqrt{2\frac{d}{R}-\left(\frac{d}{R}\right)^2}}{\left(1-\frac{d}{R}\right)}\right) \quad (3)$$

In the experiment, we examined three factors and implants were grouped into three subsets accordingly:

(1) The compressive force F_N: We applied four compressive forces (66 N, 110 N, 155 N, and 200 N) corresponding to the range of unresisted physiological shoulder joint forces [57,58] to the implants with the 36 ball and socket size: 36 SC, 36 STD, 36 Delta SC, and 36 Delta STD.

(2) The socket depth (quantified by d/R ratios): We used four pairs of implants of the same size but with different socket depths: 32 SC and 32 STD, 36 SC and 36 STD, 40 SC and 40 STD, and 36 Delta SC and 36 Delta STD. The test was performed under a 155 N compressive force. This force

corresponded to a typical value of unresisted physiological shoulder joint force.[57,58]

(3) The RSA size: We grouped implants of different sizes defined by the radius R with the same d/R ratio as follows: group I – 32 SC, 36 SC and 40 SC, and group II – 32 STD, 36 STD, and 40 STD. The test was also performed under 155 N compressive force.

In the model computation, we calculated analytical values of F_S from equation (1). Friction coefficients were chosen to be 0.07 for the DePuy and Encore cobalt-chrome glenospheres and UHMWPE humerosockets based on that reported in the literature.[65] For the additional Delrin® component, μ was 0.27. This was estimated from equations (1) and (3) using the Delrin®-Delrin® ball and socket d/R ratio and the experimentally measured F_N and F_S.

We used a Student's t-test in detection of differences in each pair (32 SC and 32 STD, 36 SC and 36 STD, 40 SC and 40 STD, and 36 Delta SC and 36 Delta STD) to examine d/R ratio effect on RSA stability. A one-way analysis of variance (ANOVA) was used to detect differences in dislocation force among multiple groups of prostheses for determination of ball and socket size factor and compressive force factor. When we found significant differences, Tukey's honestly significant difference test was applied for post hoc comparison.[66]

Results

We found a hierarchy of stability factors in RSA. Implant stability was most affected by the compressive force with differences among the four compressive force conditions (Figure 14).

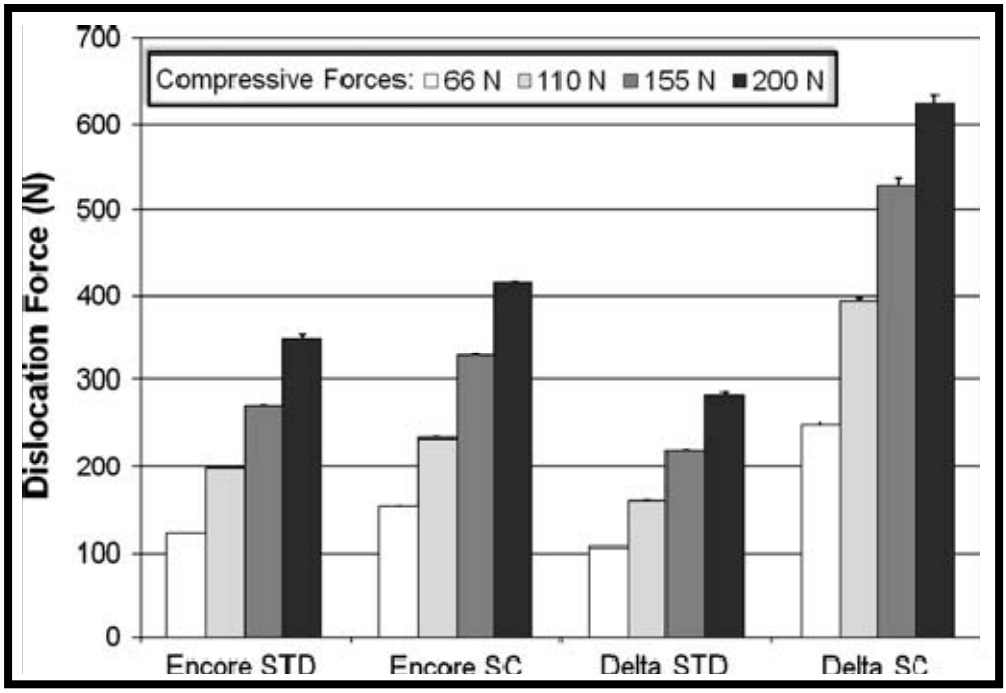

Figure 14. The graph shows how successively larger forces are required to dislocate the 36 mm glenospheres from the humerosocket when larger and larger compressive forces are applied to the glenosphere. It can also be seen how increasing the depth of the humerosocket (going from a STD depth to a SC depth) increases the force required to dislocate the glenosphere.

In the 36 STD, the dislocation force increased 186.1% ($p<0.0001$) and the difference was seen between every force level. In the 36 SC, the same force increased 168.3% ($p<0.0001$) with the difference seen between every level of force. Similarly, the dislocation force increased 165.4% in 36 Delta STD

($p<0.0001$) and 150.8% in 36 Delta SC ($p<0.0001$), respectively. The differences were also seen between every force level in each case. The d/R ratio had an effect on the stability of RSA's but to a lesser extent than the compressive force (Figure 15).

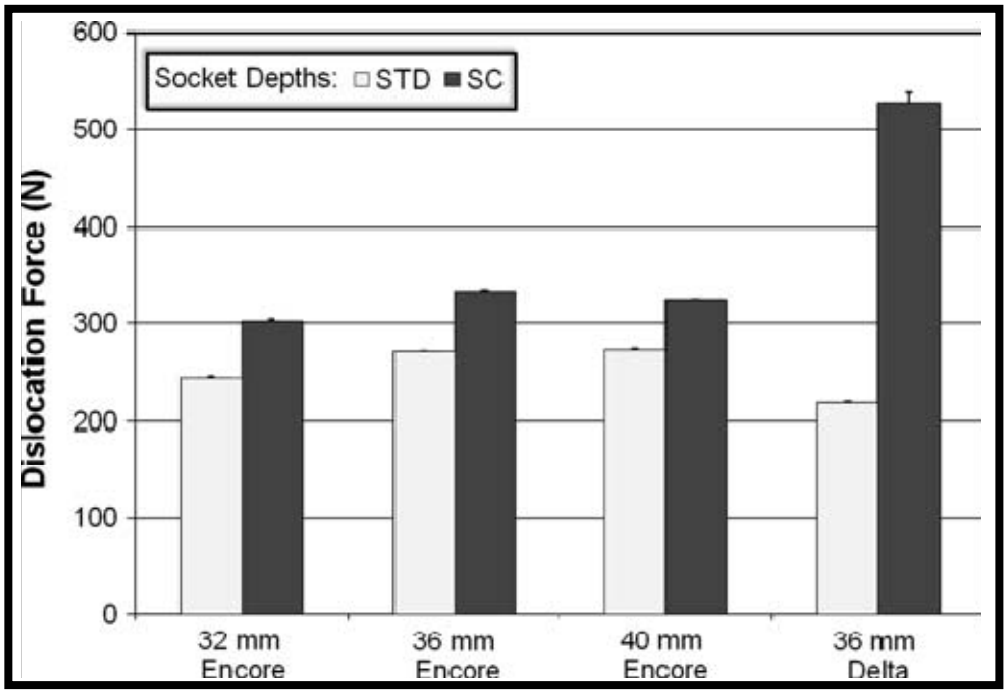

Figure 15. The graph shows how increasing the depth of the humerosocket (going from a STD depth to a SC depth) increases the force required to dislocate the glenosphere. The 36 mm Delta SC humerosocket has 2.4 times the stability when compared with the 36 mm Delta STD humerosocket.

The force F_S required to dislocate the ball and socket components was higher in semiconstrained devices (those with a deeper socket) than in standard ones for each pair compared. We observed an increase of 23.3% ($p<0.0001$) from 32 STD to 32 SC; 22.6% ($p<0.0001$) from 36 STD to 36 SC; 19.1% ($p<0.0001$) from 40 STD to 40 SC; and 140.6% ($p<0.0001$) from 36 Delta STD to 36 Delta SC. Overall, the 36 Delta SC with the highest d/R ratio of 0.68 demonstrated the

highest stability with a dislocation force of 527.7 N. The ball and socket size had much less of an effect on RSA stability (Figure 16).

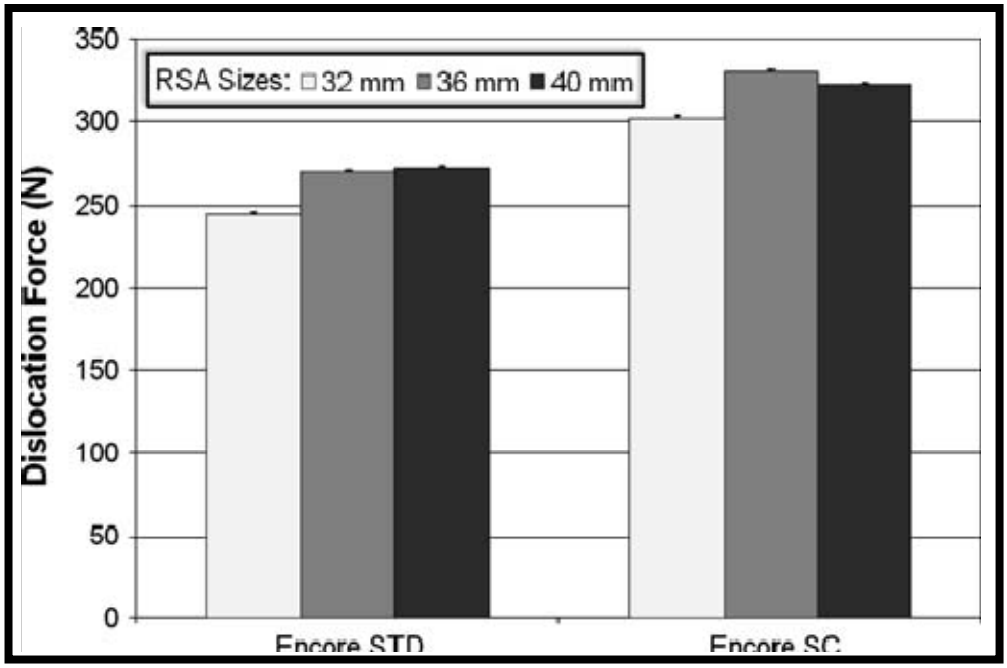

Figure 16. The graph shows minimum differences in dislocation forces for different implant sizes (32 mm, 36 mm, and 40 mm).

Only the smallest glenosphere (32) had a smaller dislocation force than the other two sizes (36 and 40) in both STD ($p<0.0001$) and SC ($p<0.0001$) (the difference ranging from 22.2 N to 29.2 N), which was approximately 10% of the dislocation force. The dislocation force had no difference between sizes 36 STD and 40 STD. The dislocation force also decreased from 36 SC to 40 SC ($p<0.0001$), but the decrease was only 7 N or approximately 2% of the dislocation force.

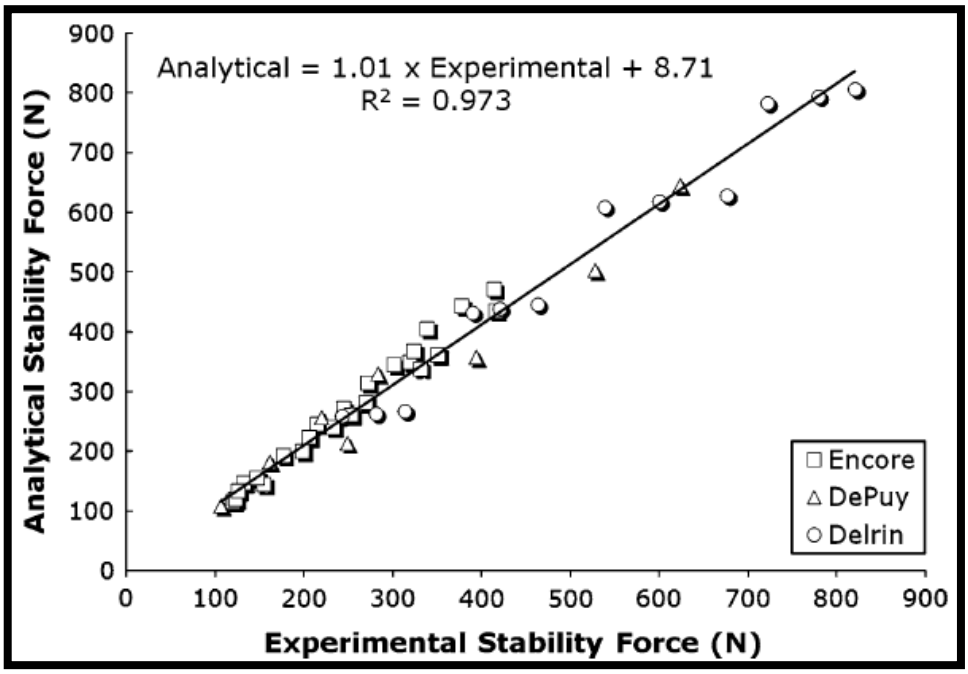

Figure 17. The graph shows a linear correlation between analytical and experimental data of stability force F_S with all RSA components studied.

The theoretical rigid body model accurately predicted the hierarchy of these factors associated with RSA stability (Figure 17). Considering all of the RSA and Delrin® devices tested, a considerable positive linear correlation (R^2 = 0.973, absolute average error of 7.98%) between the analytical and experimentally measured F_S was obtained:

$$\text{Analytical } F_S = 1.01 \times \text{Experimental } F_S + 8.71 \quad (4)$$

When simulating the compressive force from 0 to 200 N, the dislocation force changed linearly from 0 to 492.5 N (Figure 18-A). The d/R ratio affected the dislocation force in a less dramatic fashion. For the d/R ratio from 0.46 to 0.68,

the dislocation force increased from 283.4 to 592.6 N (Figure 18-B). The rigid body model also predicted that for a given d/R ratio, the change of ball and socket size would not cause any alteration in the dislocation force (Figure 18-C).

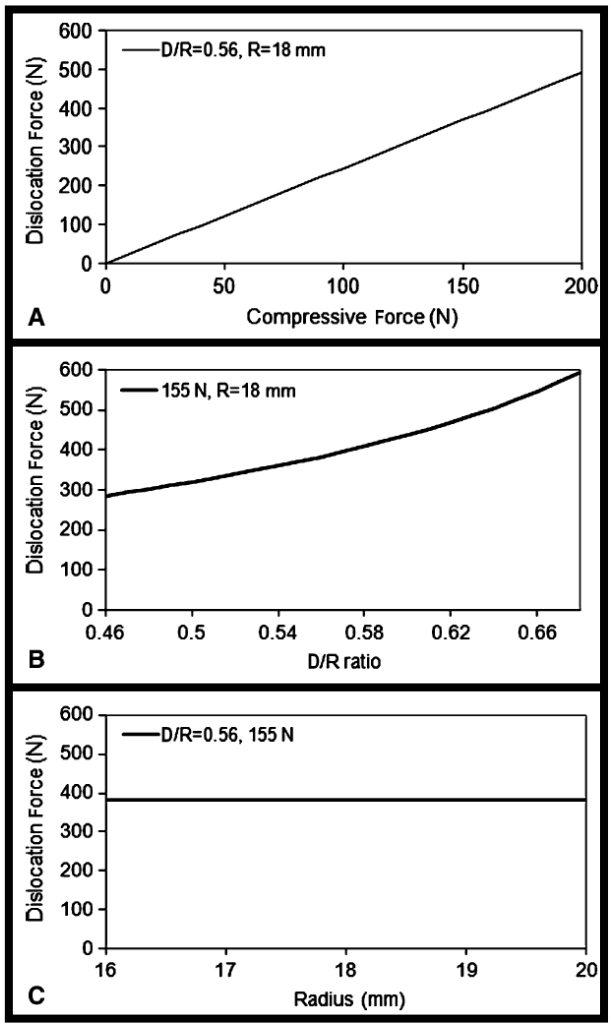

Figure 18. The graphs show the trends present when the analytical model for RSA stability is used to calculate dislocation force. A, this graph shows how the force it takes to dislocate the glenosphere from the humerosocket increases linearly as a function of increasing the compressive force applied. B, this graph shows how the force it takes to dislocate the glenosphere from the humerosocket increases exponentially as a function of increasing the depth of the humerosocket, represented by the d/R ratio. C, this graph shows how the force it takes to dislocate the glenosphere from the humerosocket remains constant as a function of increasing the radius of the glenosphere.

Discussion

As the use of RSA increases, efforts to maximize functional outcomes and limit complications become more important. Understanding how to prevent and manage prosthetic instability is, therefore, of paramount importance. Our intent was to clarify two critical concerns associated with RSA stability: the hierarchy of factors associated with the inherent stability of RSA devices and the predictability of the hierarchy by a simple theoretical rigid body model.

There are inherent assumptions and limitations associated with the study design. The glenosphere was limited to one joint motion component; translation relative to the humerosocket. This constraint was used to verify mathematical model predictions. Future studies will be needed to examine the validity of the hierarchy by including a rotational component and a full six-degree motion configuration. The second limitation was on the loading applied to the implant. A static compressive force was applied to simulate joint compression followed by a quasi-static transverse force to dislocate the ball-socket joint. We carefully selected the loading range corresponding to the range of unresisted physiological shoulder joint forces.[57,58] Such a loading condition had been used in mechanical studies for shoulder arthroplasty.[56,67] Compared with this idealized experiment, the manner in which RSA components are loaded in vivo may differ appreciably, namely the normal and surgically repaired shoulder experience complex forces that vary in magnitude, direction, and loading rate. At the present time, however,

the magnitudes and the directions of resultant forces that cause dislocation of the ball-socket articulation are not well understood. Also, resistance afforded by ligaments, joint capsule, and muscles was represented as a net compressive load, and the effects of asymmetric loading were not considered. Additional work may be needed to determine the role, if any, of active and passive tissue in RSA stability, and studies using cadavers are warranted. Finally, stability is not the only factor that should be considered in selecting a RSA design and selection, several others are also critical. The effect of prosthetic design on range of motion (ROM) of the device, impingement, scapular notching, glenosphere-baseplate fixation, muscular weakness or deficiency, and ability to manage bone deficiencies should also be considered.[36,68,69]

Measurement of joint resistance to dislocation provides quantitative support to the general concept that RSA devices are much more stable than the normal glenohumeral joint and TSA devices. The normal glenohumeral joint has a stability force ratio (maximum allowable subluxation force/joint compression force) of approximately 0.5,[70] while TSA exhibits less than 1.[55,71] In contrast, RSA has a stability force ratio greater than 2. Additionally, stability was altered only slightly by glenosphere size in the laboratory experiment, but this was not seen in the theoretical simulation, indicating that the size effect was associated with the non-rigidity of the actual system. The possible explanation was temporary distortion of the local congruency at the surface contact due to non-rigidity, leading to reduced stability as in the case of incongruent ball-socket

systems.[55] This size effect could be observed more clearly in the smaller size implants because of the increase in surface stress concentration.

The data suggests the most effective approach to increase RSA stability is through joint compressive force. Clinically, the compressive force is largely generated by active and passive structures of soft tissue together with the negative pressure within the glenohumeral joint. To date, techniques described to enhance RSA stability through soft tissue tension have focused on tensioning of the deltoid. This may be accomplished by lowering the humerus relative to the glenoid,[33] by lengthening the humerus by inserting a thicker polyethylene humeral component and retaining as much proximal humerus as possible, or by lateralizing the humerus.[36] In the case of lateralizing the humerus, the center of rotation (COR) of the glenosphere-humerosocket joint becomes closer to that of the anatomic COR of the humerus. The normal tension range of the soft tissues, including the deltoid and the residual rotator cuff muscles, may be preserved after surgery, prohibiting long-term adverse adaptability of soft tissues due to either undertensioning or overtensioning. The anatomically preserved soft tissues, in turn, may provide sufficient compressive force similar to that present in the normal glenohumeral joint as well as in anatomic TSA [72,73] (e.g., 200 N compressive force at 50° abduction [74]) to keep the glenosphere-humerosocket joint stable.

Another approach to improve RSA stability is with the use of a deeper socket. In this case, a potential tradeoff is a decrease in ROM. Clinically, however, this tradeoff may be diminished by placing the glenosphere more inferiorly relative to the glenoid or by increasing the glenosphere COR offset relative to the glenoid (selecting a glenosphere with a more lateral COR). Inferior placement of the glenosphere has been shown to provide glenohumeral abduction ROM of 81° compared to 68° for a glenosphere placed flush with the glenoid rim,[40] and a glenosphere with a 10 mm COR offset lateral to the glenoid surface has been shown to provide glenohumeral abduction of 97° compared to 54° for a glenosphere with a COR at the glenoid.[75]

Glenosphere-humerosocket stability is an important variable in selecting an appropriate RSA and is closely correlated to compressive force, socket depth, and to a lesser extent on implant size. The theoretical simulation further suggests this hierarchy of mechanical factors is primarily defined by rigid body contact characteristics. Greater understanding of the key components to stability of the RSA will help the surgeon prevent and manage complications related to prosthetic instability. Further research is needed to more fully understand the interrelationship between factors that affect stability and long-term clinical outcomes.

CHAPTER 6 - ARTICLE V: HIERARCHY OF SURGICAL AND IMPLANT DESIGN-RELATED FACTORS IN RANGE OF IMPINGEMENT-FREE ABDUCTION MOTION AND ADDUCTION DEFICIT OF REVERSE SHOULDER ARTHROPLASTY

Introduction

The management of patients who have an irreparable rotator cuff tear and severe glenohumeral arthritis has been a challenge historically. One of the few options is reverse shoulder arthroplasty (RSA).[33,35-37,42,43,48,49] The uniqueness of RSA is its conversion of the humerus into a socket (humerosocket) and the glenoid into a ball (glenosphere) with congruency that provides a more stable articulation to compensate for a dysfunctional rotator cuff. Recent RSA clinical studies have provided evidence of this, showing increased functional improvements as well as decreasing pain.[36,37,43]

A primary concern in RSA is the variability in functional outcomes after implanting this non-anatomic prosthesis. Range of motion (ROM) after RSA has been shown to vary from 30º to 180º in active elevation and from 10º to 65º in external rotation.[42,43] This variation in outcomes may be related to modifications in surgical technique, the amount of residual rotator cuff available in each patient and the underlying etiology for which the reverse prosthesis was initially selected.

Additionally, these differences in ROM may be the result of varying primary arcs of motion and the inherent impingement related to differences in implant design. One location where impingement may produce adverse clinical consequences in RSA is between the medial edge of the humerosocket and the lateral edge of the scapula. Impingement of the implant on the inferior scapular neck has been described as the mechanism for the development of scapular notching.[21,35] Typically, this impingement, referred to as an adduction deficit, occurs when the arm is in a resting position. The prevalence of progressive scapular notching has been reported radiographically in varying amounts (56% Valenti et al.[42], 63% Boulahia et al.[43], 65% Sirveaux et al.[21], 74% Boileau et al.[35] and 96% Werner et al[37]). It has been shown to correlate with poorer clinical outcomes,[76] and has even been implicated as the cause of failure in several patients.[40]

There are additional concerns regarding impingement in RSA. Impingement may also result in the introduction of prosthetic wear particles creating additional long term concerns.[77] Retrieval studies from total hip arthroplasty have offered evidence linking impingement to accelerated wear and levering-out dislocation.[78,79] Additional clinical concerns in total hip arthroplasty have suggested that prosthetic impingement may be a source of unexplained pain. These outcomes may correlate with the potential failure of RSA due to impingement. Recent work by Guery et al. has shown a dramatic decrease in patients pain relief as a function of time between 5 to 7 years in RSA shoulders.[80] Thus, for long-term clinical success of RSA, it is not only necessary, but critical to

have a better understanding of the underlying mechanism associated with the maximum impingement-free arc of motion.

There are a number of surgical and implant design-related factors which may play important roles in ROM and any associated impingement. Two methods have been proposed to avoid inferior scapular humeral impingement. One method involves alteration of the surgical technique by modifying the placement of the glenosphere on the face of the glenoid, either by placing it in a more inferior position,[40,77] or placing it with an inferior angular tilt.[21] The other method is alteration of prosthetic selection by choosing a glenosphere with a center of rotation lateral to the glenoid surface (and closer to the anatomical center of rotation) or changing the angulation of the humeral component.[36] No study to date, however, has evaluated and compared the effectiveness of these factors to maximize the abduction impingement-free ROM and to limit inferior scapular humeral impingement.

The purpose of this study was to systematically examine the abduction impingement-free ROM and adduction deficit under the regulation of five surgical and implant design-related factors (implant size, center of rotation offset, humeral neck-shaft angle, glenosphere location on the glenoid, and glenosphere tilt angle on the glenoid). A virtual computer model was developed to simulate abduction/adduction motion and its dependence on these five factors. The two questions to be addressed were: what was the hierarchy of these factors

associated with abduction impingement-free ROM and adduction deficit, and what were the factor combinations which offered sufficient abduction impingement-free ROM without adduction deficit?

Materials and Methods

Simulated Model

A computer aided design program, SolidWorks© (SolidWorks Corporation, Concord, MA), was used to model RSA and to simulate humeral abduction/adduction in relation to the glenoid in the scapular plane. The simulated model consisted of a scapula, a mounting block for the scapula, the glenosphere, the humerosocket, and a humeral shaft fixed in the humerus. The scapula and humerus were imported from CT scan images of a left large Sawbones© shoulder model (Pacific Research Laboratories, Vashon, WA). The images were converted into a stereolithography file by the program Mimics (Materialize, Leuven; Belgium).

Abduction impingement-free ROM was measured in the scapular plane by total degrees of abduction from inferior to superior impingement on the scapula or acromion in relation to the glenoid. Inferior impingement was defined by an adduction angle that kept the humerus from resting in a vertical position, i.e. the arm coming to rest at the side of the body.[81] Any adduction past this point, or

less than zero degrees, was noted as 0° or no adduction deficit since it was not anatomically possible. The model was validated both anatomically and mechanically prior to the virtual simulation.

Anatomical Validation

The model was validated by comparing the geometry of the scapula and humerus to 11 randomly selected RSA patients who had CT scans performed preoperatively (8 rotator cuff deficiency with glenohumeral arthritis and 3 rotator cuff deficiency with glenohumeral arthritis after previous rotator cuff surgeries. Average age = 79.9; Min: 56, Max: 85). Seven parameters previously defined in literature were used: glenoid height, glenoid width, glenoid depth, glenoid retroversion, glenoid inclination, distance from coracoid base to articular surface, and humeral head radius.[82,83]

Mechanical Validation

This was performed by comparing the abduction impingement-free ROM in the virtual simulations to an identically constructed experimental model[39] for 27 combinations including 3 center of rotation lateral offsets (0, +5 and +10 mm), 3 ball/socket diameters (30, 36 and 42 mm), and 3 humeral neck-shaft angles (130°, 150° and 170°) with glenosphere placed on the central glenoid without tilting.

Virtual Simulation

The virtual simulation was then performed with a total of 243 (3×3×3×3×3) different combinations from three conditions in each of the five factors: ball/socket diameters (30, 36 and 42 mm), humeral neck-shaft angle (130°, 150° and 170°), center of rotation lateral offsets (0, +5 and +10 mm), glenosphere locations on the glenoid (superior/+13 mm, neutral/0 mm and inferior/-13 mm), and glenosphere tilting angles (superior/+15°, neutral/0° and inferior/-15°).

Data Analysis

In the anatomic model validation, the patient CT measurement was represented by a 95% confidence interval. The sample size of 11 was used according to a power analysis, which detected any difference greater than 0.75 standard deviation for a two-sided test with 80% power ($\beta=0.2$) if $\alpha=0.05$. The measurements were made by one observer on two different occasions. Intraobserver reliability was evaluated by calculating the intraclass correlation coefficient between the two measurements.[84]

Mechanically, the abduction impingement-free ROM was compared between the virtual model prediction and experimental measurement for each of the 27 combinations. Linear regression was used to determine their correlation.

In the virtual simulation, factor hierarchy in the abduction impingement-free ROM was ranked by two measures from 15 testing conditions (3 conditions × 5 factors):

(1) The increase (decrease) of the averaged ROM over remaining 81 (3×3×3×3) combinations when one of the factors changed from condition 1 to condition 3. For example, in the factor of glenosphere location on the glenoid, the ROM was averaged over the ROM's from 81 combinations consisting of 3 implant sizes, 3 center of rotation offsets, 3 humeral neck-shaft angles, and 3 glenosphere tilt angles on the glenoid with the glenosphere on the inferior glenoid. The same procedure was repeated to determine the averaged ROM for superiorly located glenosphere. The ROM difference between these two positions was then determined.

(2) The number of combinations which had increased ROM from condition 1 to condition 3 was directly counted. For example, in the factor of glenosphere location on the glenoid, the number of combinations which had increased ROM when the glenosphere was moved from superior to inferior was determined.

Similarly, the factor hierarchy in the adduction deficit was quantified by two measures. First, the increase (decrease) of the averaged adduction deficit over 81 combinations when one of the factors changed from condition 1 to condition 3.

Second, the number of combinations which had no adduction deficit in each condition was directly counted.

In order to determine the combinations which offered abduction impingement-free ROM without adduction deficit, the combinations without adduction deficit were selected and ranked by the abduction impingement-free ROM.

Results

Anatomic Validation

The glenoid model was 37.8 mm in height, 25.0 mm in width, 2.8 mm in depth, 7.6° in retroversion, 11.3° in inclination, and 4.0 mm from coracoid base to articular surface. The humeral head radius was 24.2 mm. Each value had no significant difference from its counterpart of the RSA patient data determined by 95% confidence intervals ($p<0.05$) (Table 7).

Table 7. Comparison of the computer model with anatomic measurements.

Anatomic Measurement	Computer Model	95% Confidence Interval in Population of Patients with Reverse Shoulder Arthroplasty
Glenoid height *(mm)*	37.8	33.0-38.2
Glenoid width *(mm)*	25	24.2-29.4
Glenoid depth *(mm)*	2.8	2.4-4.4
Glenoid retroversion *(deg)*	7.6	6.1-13.3
Glenoid inclination *(deg)*	11.3	2.5-11.5
Distance from coracoid base to articular surface *(mm)*	4.0	2.6-4.8
Humeral head radius *(mm)*	24.2	20.9-24.7

*The computer model was validated anatomically by comparing seven parameters of scapular and humeral anatomy in that model with the same parameters in eleven randomly selected patients who had undergone a reverse shoulder arthroplasty[17,18]. The parameters in the model agreed with those in the patient population, as each was within the 95% confidence interval of the value for the patient population.

Mechanical Validation

The virtual simulation of abduction impingement-free ROM duplicated what was found in the mechanical experiment. A very strong positive correlation existed between measurement and simulation with R^2=0.994 and p<0.0001.

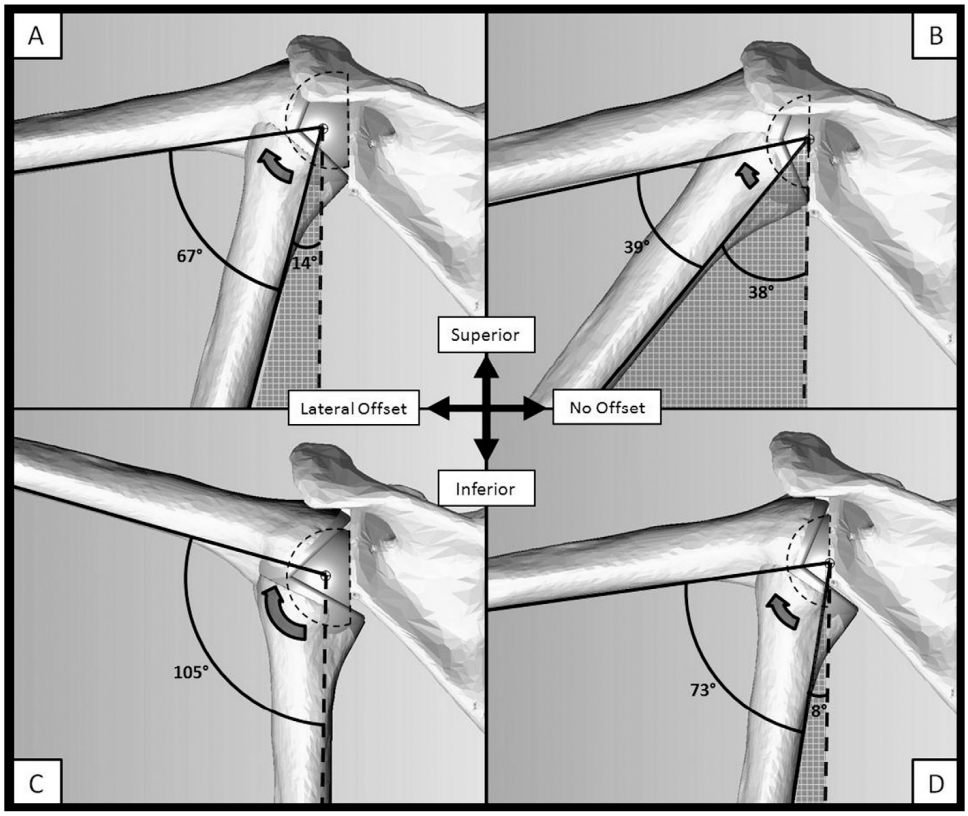

Figure 19. Illustration of the effects of center of rotation lateral offset and glenosphere location on the impingement-free abduction ROM and adduction deficit with 36 mm glenosphere diameter, 150° humeral neck-shaft angle and no glenosphere tilting. A, a superiorly positioned, 10 mm laterally offset glenosphere. B, a superiorly positioned, no offset glenosphere. C, an inferiorly positioned, 10 mm laterally offset glenosphere. D, an inferiorly positioned, no offset glenosphere. The shaded region represents adduction deficit. ROM, shown by the arrow, is from inferior impingement to superior impingement. The effect of center of rotation lateral offect can be seen from A to B, or from C to D. The effect of glenosphere location can be visualized from A to C, or from B to D.

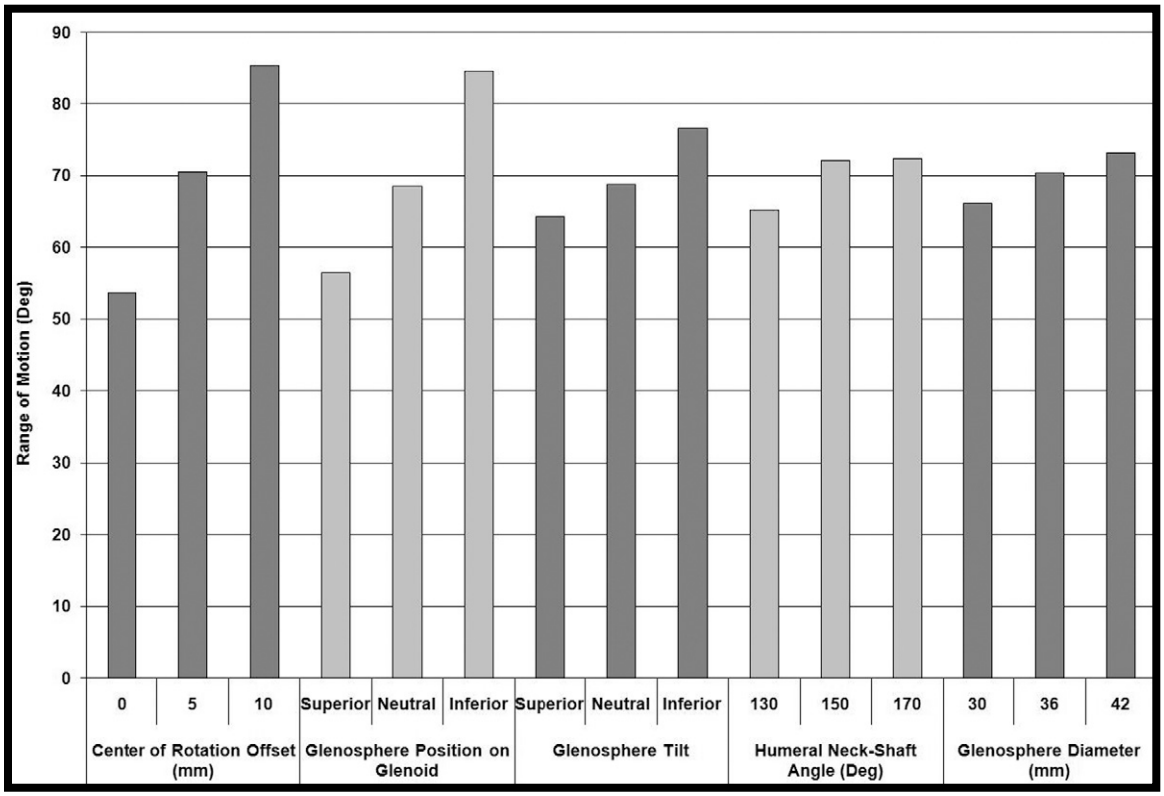

Figure 20. The range of impingement-free abduction motion averaged over 81 combinations under each of the 15 testing conditions.

Range of Impingement-Free Abduction Motion

The largest effect on impingement-free ROM was from center of rotation lateral offset (Figures 19 & 20). At the 0 mm position, the averaged ROM (over the remaining 81 combinations) was 53.6° (Min: 29.6°, Max: 86.0°). When the glenosphere was moved to the 10 mm position, the averaged ROM increased to 85.5° (Min: 38.6°, Max: 121.4°). 80/81 (99%) combinations increased their ROM while the glenosphere was moved from 0 to 10 mm position. The glenosphere location on the glenoid had the second largest effect with 28.1° increase from the

averaged 56.5° (Min: 29.6°, Max: 99.7°) ROM at the superior position to the averaged 84.6° (Min: 53.9°, Max: 118.4°) ROM at the inferior position (Figure 20). 71/81 (88%) combinations increased their ROM while the glenosphere was translated from superior to inferior. The next two factors were ranked as: glenosphere tilt, ∆12.5° increase from the averaged 64.2° (Min: 29.6°, Max: 118.4°) for the superior tilting to the averaged 76.7° (Min: 46.2°, Max: 113.8°) for the inferior tilting, an increase in 53/81 (65%) combinations; and neck-shaft angle, ∆7.1° increase from the averaged 65.2° (Min: 28.9°, Max: 97.4°) at 130° angle to the averaged 72.3° (Min: 29.6°, Max: 118.4°) at 170° angle, and increase in 49/81 (60%) combinations. The least sensitive one was prosthetic size, ∆6.9° increase from the averaged 66.2° (Min: 33.7°, Max: 106.9°) for the 30 mm to the averaged 73.1° (Min: 29.6°, Max: 118.4°) for the 42 mm, and increase in 61/81 (75%) combinations.

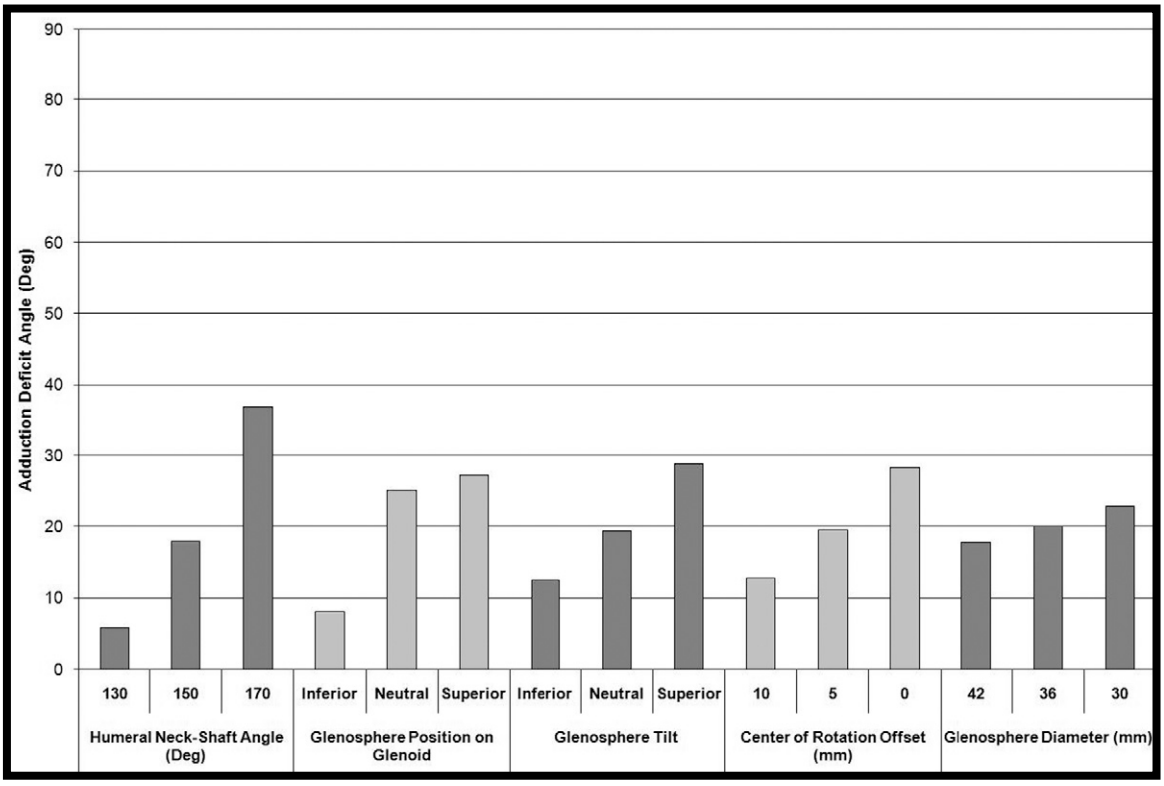

Figure 21. The adduction deficit averaged over 81 combinations under each of the 15 testing conditions.

Adduction Deficit

The primary factor affecting adduction deficit was humeral neck-shaft angle (Figure 21). When a 130° angle was used, the averaged adduction deficit (over the remaining 81 combinations) was 5.8° (Min: 0.0°, Max: 35.5°). When a 170° angle was used, the averaged adduction deficit increased 31.1° to 36.9° (Min: 6.2°, Max: 75.0°). The 130° neck-shaft angle had the highest factor combinations (49/81, 61%) which gave no inferior impingement (Table 8).

Table 8. Number of factor combinations with no adduction deficit under the fifteen tested conditions.*

Study Factor and Condition	No. (%) with No Adduction Deficit
Humeral neck-shaft angle	
130°	49 (60)
150°	17 (21)
170°	0
Glenosphere location	
Inferior	41 (51)
Neutral	13 (16)
Superior	12 (15)
Glenosphere tilt	
Inferior	30 (37)
Neutral	23 (28)
Superior	13 (16)
Center-of-rotation lateral offset	
10 mm	32 (40)
5 mm	22 (27)
0 mm	12 (15)
Glenosphere diameter	
42 mm	28 (35)
36 mm	21 (26)
30 mm	17 (21)

*A total of eighty-one combinations was tested for each condition.

The 170° neck-shaft angle was the worst factor with no combination having 0 adduction deficit. Glenosphere location had the next largest effect, Δ19.1° increase from the averaged 8.2° (Min: 0.0°, Max: 32.7°) adduction deficit at the inferior position to the averaged 27.3° (Min: 0.0°, Max: 75.0°) at the superior position (Figure 19). Glenosphere inferior location had the second largest combination for no adduction deficit (41/81, 51%). Glenosphere tilt had an increase of Δ16.4° from the averaged 12.4° (Min: 0.0°, Max: 46.9°) for the inferior tilt to the averaged 28.8° (Min: 0.0°, Max: 75.0°) for the superior tilt (Figure 22).

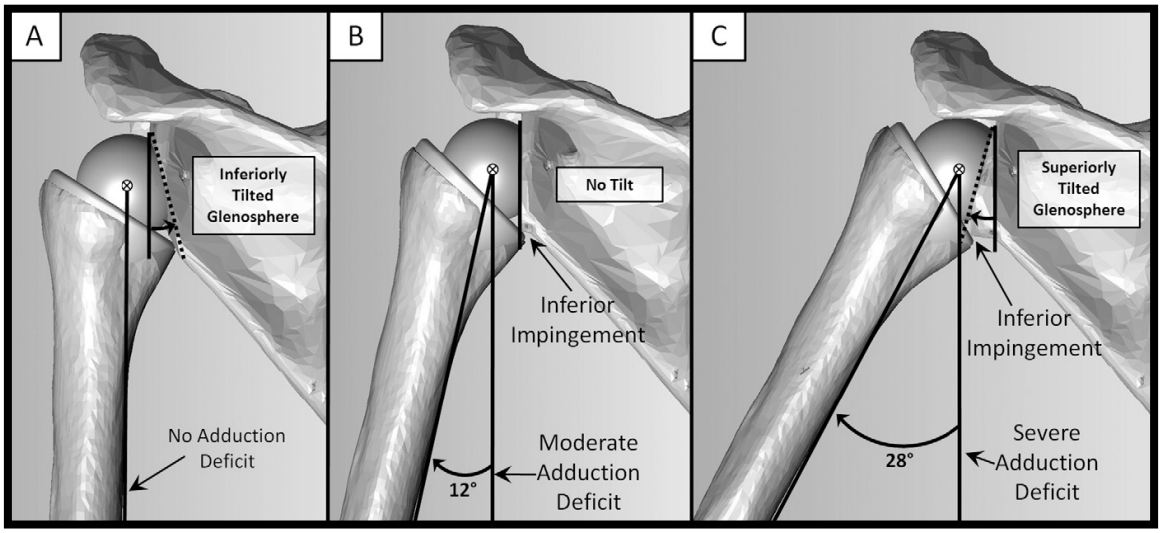

Figure 22. Illustration of adduction deficit caused by glenosphere tilting with central glenosphere location on the glenoid, 36 mm glenosphere diameter, 10 mm center of rotation lateral offset and 150° humeral neck-shaft angle. A, inferior glenosphere tilting which results in no adduction deficit. B, no glenosphere tilting which causes inferior impingement and moderate adduction deficit. C, superior glenosphere tilting which also results in inferior impingement and severe adduction deficit.

Inferior tilting avoided inferior impingement in 30 out of 81 combinations (37%). Center of rotation offset resulted in ∆15.5° increase from the averaged 12.8° (Min: 0.0°, Max: 50.8°) for the 10 mm offset to the averaged 28.3° (Min: 0.0°, Max: 75.0°) for the 0 mm offset (Figure 19). The 10 mm center of rotation offset had 32 out of 81 combinations (40%) without adduction deficit. Glenosphere diameter led to ∆5.0° increase from the averaged 17.8° (Min: 0.0°, Max: 68.7°) for the 42 mm to the averaged 22.8° (Min: 0.0°, Max: 75.0°) for the 30 mm. The 42 mm diameter had 28 out of 81 combinations (35%) without adduction deficit.

Maximum Range of Motion without Adduction Deficit

There were 18 combinations which could provide abduction ROM greater than 90° without inferior impingement. All but one of these had a center of rotation offset lateral to the glenoid (+5 or +10 mm) and all but three (all 130°) had a 150° neck-shaft angle. 15 out of 18 had an inferior position on the glenoid. 10 had 42 mm diameter and 5 had 36 mm diameter. Glenosphere tilt was distributed as 7 inferiorly, 4 neutrally and 7 superiorly.

Discussion

RSA design has been increasingly used in the treatment of rotator cuff deficient shoulders with concomitant osteoarthritis. Initially, the recommended glenosphere placement was centrally on the glenoid. Over the last few years, however, various recommendations have been made to modify the surgical technique in an effort to avoid potential complications. Inferior placement of the glenosphere has been stressed in an effort to decrease inferior scapular impingement,[21] and improve overall range of motion.[49] Additionally, placement of the glenosphere with an inferior tilt has been recommended to improve the biomechanical environment between the glenosphere and glenoid bone.[81]

In spite of these modifications, progressive scapular notching has been reported with a rather high frequency radiographically from 56% - 96%.[43,49,79,81,85]

Scapular notching has been clinically shown to have an adverse effect on the long-term outcomes of RSA,[76] and the impingement might further induce prosthetic wear and osteolysis.[77] Additionally, variations in ROM outcomes after RSA continued to be observed.[33,43,49] To our knowledge, we are the first to investigate the factors involved in maximization of impingement-free abduction after reverse shoulder arthroplasty.

Range of motion following RSA has been studied in a limited scope. In a clinical study using dynamic fluoroscopic radiographs, maximum active abduction ROM of 53° in the scapular plane for the Delta III prosthesis was measured.[39] A biomechanical study quantified abduction ROM and adduction deficit of the Delta III with a 36 mm glenosphere. When implanted using the manufacturer's recommended surgical technique,[40] the mean abduction ROM in the scapular plane was 42° and adduction deficit was 25°. When implanted in an inferior position on the glenoid, the average abduction ROM increased to 66º with the adduction deficit decreasing to 9°.[40] Thus, modification of surgical technique not only improved the overall motion, but helped to limit inferior impingement. The study, however, was limited to only two glenosphere locations on the glenoid, and other surgical and implant-related factors were not examined.

The present study is the continuation of an effort to better understand the mechanics behind RSA. The goal of this effort is to assist the surgeon in implant selection and modification of surgical technique in order to maximize

impingement-free abduction ROM, to avoid adduction deficit, and to eliminate scapular notching. Five surgical and implant design-related factors were systematically tested for their hierarchy in relation to abduction ROM and adduction deficit. The primary factors found to gain maximum abduction ROM without adduction deficit were +5 or +10 mm center of rotation lateral offset, 150° neck-shaft angle and inferior position of glenosphere on the glenoid. If the system, for example, utilizes a glenosphere with a center of rotation at the glenoid, maximum motion and decreased instances of scapular notching can be attained by inferiorly positioning the glenosphere on the scapula. But, if a situation arises where the glenosphere is unable to be placed in an inferior position, a humeral neck-shaft angle of 130° or 150°, or a more lateral center of rotation offset can be used to attain the same increase in motion and avoidance of scapular notching.

The study also included implant constructs which are currently not commercially available (e.g., 170° humeral neck-shaft angle) to examine possible improvement beyond current RSA. The results suggested the 170° angle was less desirable when compared to the current 130° to 150° humeral neck-shaft angle, showing increases in adduction deficit. Similarly, less desirable placements of the glenosphere on the glenoid superiorly and glenosphere tilting superiorly were also tested. Although a few combinations involving superior tilting of the component showed abduction ROM of greater than 90°, it has been shown biomechanically that this tilting increases the shear stresses at the baseplate-

glenoid interface[42] and as a consequence, we do not advocate placing the glenosphere in a superiorly tilted position. Clinically, however, there are instances where the surgeon may not have a choice. In these instances, the information given here can be of value.

The virtual computer simulation developed in this study also provided a powerful approach for simultaneous analysis of multiple factors in RSA. In a previous study,[75] the effect of four factors on abduction ROM and adduction deficit was quantified experimentally using a Sawbones© shoulder model: glenosphere location, glenosphere size, center of rotation offset, and humeral neck-shaft angle. The current computational method accurately duplicated the experimental measures with significant increase of analysis power (a total of 243 factor combinations examined vs. 81 combinations from the experimental study) and reduction of testing time. The addition of the fifth factor, the glenosphere tilt, into the study further demonstrated the importance of this factor in ROM and, particularly, in adduction deficit.

The limitations of this study need to be addressed. This study took a mechanical approach to examine ROM and adduction deficit under 5 primary surgical factor variations. In practice, there are many factors involved in the decision of what components to use in reverse shoulder arthroplasty. The amount of good bone available for fixation, stress concentration at the glenosphere-bone interface, soft-tissue impingement, the available space in the shoulder, the soft tissue

balance, and the strength of the remaining muscles all play roles in the decision of prosthetic attributes. Since this study did not take into account the soft tissue envelope and the bone available for component fixation, these considerations must be utilized when selecting appropriate components for any given patient.

The ROM determined in this study was passive, which should be considered as the maximum improvements that can be expected in active ROM after surgery. Our results identified 18 combinations with greater than 90° abduction ROM and no adduction deficit, which may be used clinically. The data also indicated that a number of other combinations had poor passive ROM outcomes and should be avoided. Determination of this passive ROM will help us to further improve active ROM which is affected by other factors such as soft tissue balance at the time of surgery and muscle power alteration. Furthermore, we limited the ROM to abduction/adduction in the scapular plane because of their primary importance in RSA. A more generalized three-dimensional simulation model may be developed in the future as other motion components, such as internal/external rotation, have also been shown to have clinical relevance.[86]

Another limitation with this model was the omission of anatomic variation among patients. The scapula and humerus modeled had typical geometric parameters that matched a subset of patients undergoing RSA. The intention was to provide an initial point of reference to understand how variations of humeral neck-shaft angle, glenosphere location, glenosphere tilt, center of rotation offset and implant

size were interrelated. Quantifying the role of anatomic variation in abduction ROM and adduction deficit would add a degree of complexity which should warrant a future study.

In conclusion, this study determined the maximum abduction impingement-free ROM and adduction deficit in association with 5 independent factors. Overall, glenospheres having a greater distance from the glenoid to the center of rotation and an inferior placement on the glenoid provide for greater ROM. Adduction deficit can best be improved by selecting a prosthesis with a varus humeral neck-shaft angle, and inferior placement on the glenoid. A number of combinations of independent factors were identified which could offer greater ROM without inferior impingement. This information will assist in the decision making of implant selection and surgical procedures, and future implant designs.

CHAPTER 7 - ARTICLE VI: ARC OF MOTION AND SOCKET DEPTH IN REVERSE SHOULDER IMPLANTS

Introduction

Reverse shoulder arthroplasty (RSA) has been increasingly used in the treatment of pseudoparalysis which is developed from severe rotator cuff deficiency. By utilizing a congruent glenosphere-humerosocket articulation, RSA provides a stable fulcrum for the remaining musculature which helps to restore this loss.

One of the major concerns in RSA is the variation of functional outcomes after implanting this non-anatomic prosthesis. Range of motion after RSA has been shown to vary from 30° to 180° in active elevation and from 10° to 65° in external rotation.[22] This variation in outcomes may be a result of changes in primary arcs of motion and the inherent impingement points attributable to differences in prosthetic design or modification of surgical technique. The most common impingement point is between the medial edge of the humerosocket and the lateral edge of the scapula. This impingement of the implant on the inferior scapular neck has been noted as the mechanism for the development of scapular notching.[21] Typically, the impingement, referred to as an adduction deficit, occurs when the arm is in a resting position. Progressive scapular

notching has been demonstrated to a variable degree radiographically correlating with poorer clinical outcomes.[21,22] It has even been implicated as the cause of failure in several patients.[76]

Impingement may also result in the introduction of prosthetic wear particles, creating additional concerns for the surgeon. Retrieval studies from total hip arthroplasty have offered evidence linking impingement to accelerated wear and dislocation from levering-out.[78,79] Recent work involving RSA shoulders has shown a dramatic decrease in patients pain relief between years 5 and 7.[80] Thus, for long-term clinical success of RSA, it is not only necessary, but critical to have a better understanding of the underlying mechanism associated with maximizing the impingement-free arc of motion.

Extensive research in total hip arthroplasty has revealed a decrease in the impingement-free range of motion as articular constraint increases.[78,79] This suggests that maximizing the impingement-free arc of motion occurs at the expense of ball/socket joint constraint. However, direct translation of the results from hip arthroplasty to RSA may not be straightforward because of the intrinsic differences in their anatomic structures and the non-anatomic reversed nature of RSA. In addition, understanding the relationship between the impingement-free arc of motion and articular constraint poses some unique challenges in RSA. Recent studies have demonstrated a number of concurrent design and surgical factors, including glenosphere placement on the glenoid, prosthetic size and

prosthetic shape, which can affect the impingent-free arc of motion.[75,85] Without simultaneously analyzing these factors, it is impossible to formulate a rationale regarding how articular constraint contributes to the impingement-free arc of motion in RSA.

In this study, we investigated how articular constraint would affect the abduction impingement-free arc of motion with a computer-simulated virtual shoulder model. Articular constraint was defined by the normalized humerosocket depth (socket depth/radius). The simulation also included the concurrent factors of glenosphere diameter, lateral center of rotation (COR) offset of the glenosphere from the glenoid, humeral neck-shaft angles and position of the glenosphere on the glenoid surface. We hypothesized that the impingement-free range of motion would decrease as articular constraint increased.

Materials and Methods

Computer Model

A computer aided design program, SolidWorks© (SolidWorks Corporation, Concord, MA), was used to simulate humeral abduction/adduction in relation to the glenoid in the scapular plane of the RSA. The simulation was based on algorithms similar to those reported in the literature.[75,87] The model included a scapula, a mounting block for the scapula, a glenosphere, a humerosocket, and

a humeral shaft fixed in a humerus. The scapula and humerus were imported from CT scan images of a left large Sawbones© shoulder model (Pacific Research Laboratories, Vashon, WA). The images were converted into a stereolithography file by the program Mimics (Materialize, Leuven; Belgium), and then imported into SolidWorks©.

Abduction impingement-free arc of motion was measured by total degrees of abduction from inferior impingement on the scapula to superior impingement on the acromion or the glenoid. Inferior impingement was defined by an adduction angle that kept the humerus from resting in a vertical position, i.e. the arm coming to rest at the side of the body. Any adduction past this point, or less than zero degrees, was noted as no adduction deficit since it was not anatomically possible.

Anatomical Validation

The model was anatomically validated prior to the virtual simulation by comparing the geometry of the scapula and humerus with 11 randomly selected patients who had CT scans performed preoperatively (8 rotator cuff deficiency with glenohumeral arthritis and 3 rotator cuff deficiency with glenohumeral arthritis after previous rotator cuff surgeries. Average age = 79.9; Min: 56, Max: 85). Seven parameters previously defined in the literature were used: glenoid height,

glenoid width, glenoid depth, glenoid retroversion, glenoid inclination, distance from coracoid base to articular surface, and humeral head radius.[82,83]

Mechanical Validation

The model was mechanically validated by comparing the abduction impingement-free arc of motion in the virtual simulations to an identically constructed experimental model previously reported in the literature[75] for 27 combinations including 3 COR lateral offsets (0, +5 and +10 mm), 3 ball/socket diameters (30, 36 and 42 mm), and 3 humeral neck-shaft angles (130°, 150° and 170°). The glenosphere was placed on the center of the glenoid without tilting following a definition of the glenoid center line for central screw fixation.[88]

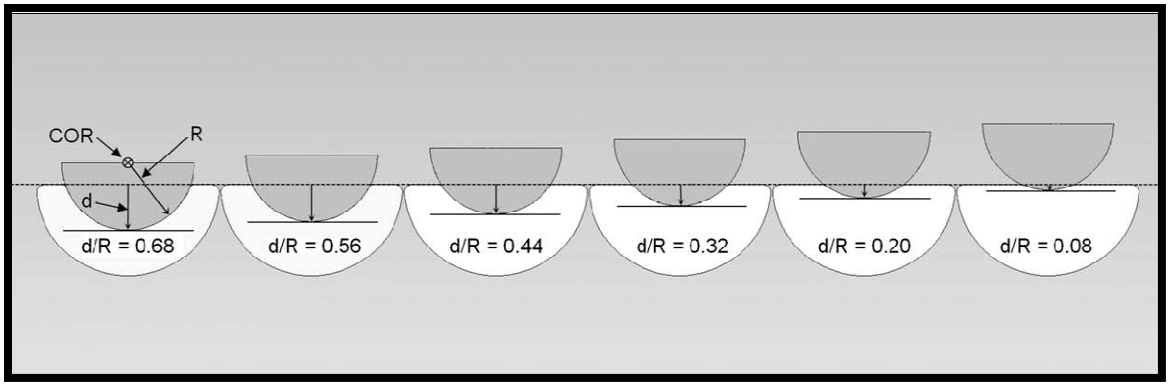

Figure 23. Illustration of the 6 different depth of sockets selected in this study.

Virtual Simulation

The impingement-free arc of motion was examined under 6 articular constraints defined by the humerosocket depth "d" normalized by its radius "R" (d/R): 0.08, 0.22, 0.32, 0.44, 0.56 and 0.68 (Figure 23). The use of the normalized depth rather than the absolute depth directly associated this parameter with the translational stability. It was previously demonstrated that translational stability ratio r_s of a ball-socket joint tested under a normal compressive force F_N and a shearing dislocation force F_s was given by:[55,56]

$$r_S = \frac{F_S}{F_N} = \frac{TAN(\theta)+\mu}{1-\mu \times TAN(\theta)} \quad (5)$$

Where μ is the coefficient of friction between the ball and socket, and θ is the incident angle between the ball and socket edge. For RSA, θ is determined as:[89]

$$TAN(\theta) = \frac{\sqrt{2\frac{d}{R}-\left(\frac{d}{R}\right)^2}}{1-\frac{d}{R}} \quad (6)$$

For each d/R, four concurrent factors were considered (Figure 24): 3 glenosphere/inner humerosocket diameters (2R) (30, 36, and 42 mm), 3 humeral neck-shaft angles (θ) (130°, 150°, and 170°), 3 lateral COR offsets (L) (0, +5, +10 mm), and 3 glenosphere positions on the glenoid (P) (superior: +13 mm, neutral:

0 mm and inferior: -13 mm). These tested factors covered all of the currently available RSA implants. The outer diameter of the humerosocket was held constant at 50 mm for all sizes tested.

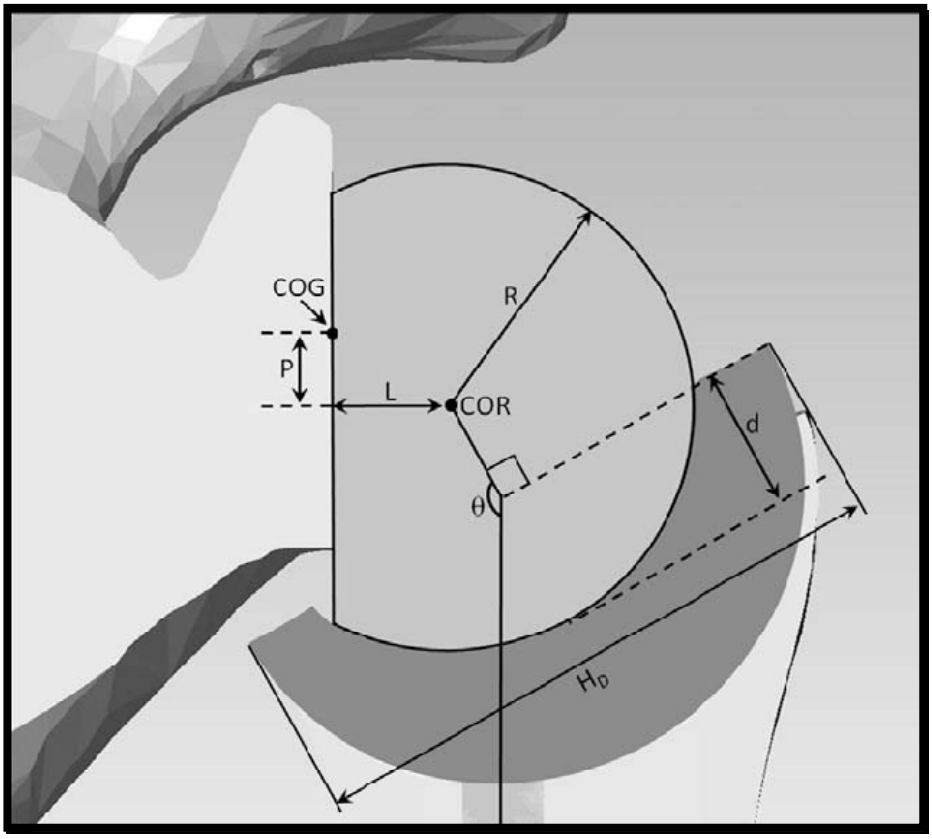

Figure 24. Illustration of parameters tested in study. (1) depth (d) to radius (R) ratio (d/R), (2) glenosphere diameter (2×R), (3) humeral neck-shaft angle (θ), (4) COR offset (L), (5) position of glenosphere on glenoid (P) from the center of the glenoid (COG) and (6) outer diameter of the humerosocket ($H_{D)}$.

Data Analysis

In the anatomical validation, the patient CT measurement was represented by a 95% confidence interval. The sample size of 11 was used according to a power analysis, which detected any difference greater than 0.75 standard deviation for

a two-sided test with 80% power (β=0.2) if α=0.05. In the mechanical validation, the abduction impingement-free ROM was compared between the virtual model prediction and experimental measurement for each of the 27 combinations. Linear regression was used to determine their correlation. Tests were performed with the use of JMP statistical software (SAS Institute, Cary, NC). In the virtual simulation, a total of 486 (6×3×3×3×3) conditions were tested. The impingement-free arc of motion was determined as a function of joint constraint at 6 discrete d/R's with 81 (3×3×3×3) concurrent factor combinations.

Results

Anatomical Validation

The glenoid model was 37.8 mm in height, 25.0 mm in width, 2.8 mm in depth, 7.6° in retroversion, 11.3° in inclination, and 4.0 mm from coracoid base to articular surface. The humeral head radius was 24.2 mm. Each value had no significant difference from its counterpart in the RSA patient data determined by 95% confidence intervals (33.0–38.2 mm, 24.2–29.4 mm, 2.4–4.4 mm, 6.1°–13.3°, 2.5°–11.5°, 2.6–4.8 mm and 20.9–24.7 mm, respectively; $p<0.05$).

Mechanical Validation

The virtual simulation of abduction impingement-free arc of motion duplicated what was found in the mechanical experiment. A very strong positive correlation existed between measurement and simulation with R^2=0.994 and p<0.0001.

Abduction Impingement-Free Arc of Motion

The 81 combinations which defined the impingement-free arc of motion in relation to the articular constraint (d/R) could be categorized into 3 classes (Table 9): class I arc of motion decreased with increased articular constraint. Class II arc of motion with a complex relationship to articular constraint. Class III arc of motion increased with increased articular constraint.

Class I consisted of 46 (57%) combinations. This included all the 27 combinations involving the inferior position. The largest decrease in arc of motion was 66° (from 102° to 36°) with 42 mm diameter, neutral glenosphere position, 0 mm COR offset, and 170° humeral neck-shaft angles. The impingement-free arc of motion averaged over these 46 combinations had a decrease of 38° (from 102° to 64°). There were 13 combinations without adduction deficit. All but one were at the inferior position, 10 had 130° humeral neck-shaft angles, and 7 were 10 mm COR lateral offset (Table 9). The largest decline in arc of motion was 26° (from 112° to 86°) with 30 mm diameter, inferior

glenosphere position, 10 mm COR offset, and 150° humeral neck-shaft angles. The averaged impingement-free arc of motion decreased 21° (from 94° to 73°).

30 combinations (37%) belonged to class II. The significant factors in this case were the superior glenosphere position (in 22 combinations) and the 150° humeral neck-shaft angle (in 12 combinations) (Table 9). The averaged impingement-free arc of motion had a maximum of 67° and a minimum of 63°. Among the 30 combinations, 3 showed no adduction deficit. All of them had 10 mm COR lateral offset and the 150° humeral neck-shaft angle. The averaged impingement-free arc of motion had a maximum of 83° and a minimum of 78°.

Class III had 5 combinations (6%) (Table 9). These combinations were all at the superior glenosphere position with 130° humeral neck-shaft angle. The largest increase was 24° (from 55° to 79°) with 30 mm diameter, superior glenosphere position, 10 mm lateral COR offset, and 130° humeral neck-shaft angle. The averaged increase was 15° (from 52° to 67°). There were 2 combinations in class III which had no adduction deficit. The largest increase was also 24°. The averaged increase was 22° (from 55° to 77°).

Table 9. Abduction impingement-free arc of motion of 486 individual tested conditions and its relation to 6 discrete articular constraints (d/Rs) in 81 concurrent factor combinations which can be divided into 3 classes.

d/R Ratio	0 mm Center of Rotation Offset					5 mm Center of Rotation Offset					10 mm Center of Rotation Offset				
	Glenosphere Diameter	Glenoid Placement	Humeral Angle	Impingement-Free Arc of Motion	Adduction Deficit	Glenosphere Diameter	Glenoid Placement	Humeral Angle	Impingement-Free Arc of Motion	Adduction Deficit	Glenosphere Diameter	Glenoid Placement	Humeral Angle	Impingement-Free Arc of Motion	Adduction Deficit
0.08	30 mm	Superior	130°	44	7	30 mm	Superior	130°	54	0	30 mm	Superior	130°	55	0
		Superior	150°	45	26		Superior	170°	55	37		Superior	150°	74	0
		Superior	170°	45	46		Superior	150°	56	17		Superior	170°	75	18
		Inferior	130°	71	0		Inferior	130°	82	0		Neutral	130°	86	0
		Neutral	150°	78	17		Neutral	130°	90	0		Inferior	130°	100	0
		Neutral	130°	79	0		Inferior	150°	101	0		Neutral	150°	106	0
		Neutral	170°	79	36		Neutral	150°	101	6		Inferior	150°	119	0
		Inferior	150°	87	0		Neutral	170°	102	25		Neutral	170°	123	1
		Inferior	170°	87	14		Inferior	170°	112	7		Inferior	170°	136	1
	36 mm	Superior	130°	47	2	36 mm	Superior	130°	52	0	36 mm	Superior	130°	54	0
		Superior	150°	48	21		Superior	150°	58	12		Superior	150°	70	3
		Superior	170°	48	40		Superior	170°	58	31		Superior	170°	70	22
		Inferior	130°	76	0		Inferior	130°	86	0		Neutral	130°	94	0
		Neutral	130°	85	0		Neutral	130°	90	0		Inferior	130°	96	0
		Neutral	150°	95	7		Inferior	150°	106	0		Neutral	150°	114	0
		Neutral	170°	96	26		Neutral	150°	109	0		Inferior	150°	116	0
		Inferior	150°	97	0		Neutral	170°	111	15		Neutral	170°	124	8
		Inferior	170°	104	9		Inferior	170°	121	2		Inferior	170°	135	0
	42 mm	Superior	130°	50	0	42 mm	Superior	130°	52	0	42 mm	Superior	130°	55	0
		Superior	150°	51	16		Superior	150°	61	8		Superior	170°	66	26
		Superior	170°	51	36		Superior	170°	61	27		Superior	150°	67	6
		Neutral	130°	80	0		Neutral	130°	84	0		Inferior	130°	92	0
		Inferior	130°	81	0		Inferior	130°	90	0		Neutral	130°	98	0
		Neutral	150°	100	0		Neutral	150°	104	0		Inferior	150°	112	0
		Inferior	150°	101	0		Inferior	150°	111	0		Neutral	150°	118	0
		Neutral	170°	102	15		Neutral	170°	113	8		Neutral	170°	119	17
		Inferior	170°	114	4		Inferior	170°	127	1		Inferior	170°	130	2
0.22	30 mm	Superior	130°	44	10	30 mm	Superior	130°	54	1	30 mm	Superior	130°	57	0
		Superior	150°	44	29		Superior	150°	54	21		Superior	150°	65	9
		Superior	170°	44	49		Superior	170°	54	40		Superior	170°	66	28
		Neutral	150°	66	23		Inferior	130°	79	0		Inferior	130°	89	0
		Inferior	130°	67	0		Neutral	130°	84	0		Neutral	130°	94	0
		Neutral	130°	67	3		Neutral	150°	90	11		Inferior	150°	109	0
		Neutral	170°	67	42		Neutral	170°	90	31		Neutral	170°	100	22
		Inferior	150°	85	0		Inferior	150°	98	0		Neutral	150°	110	2
		Inferior	170°	86	18		Inferior	170°	105	11		Inferior	170°	125	5
	36 mm	Superior	130°	46	5	36 mm	Superior	130°	54	0	36 mm	Superior	130°	55	0
		Superior	150°	46	25		Superior	150°	56	15		Superior	150°	67	6
		Superior	170°	46	44		Superior	170°	56	34		Superior	170°	67	25
		Inferior	130°	72	0		Inferior	130°	83	0		Inferior	130°	92	0
		Neutral	130°	80	0		Neutral	130°	92	0		Neutral	130°	99	0
		Neutral	150°	82	15		Inferior	150°	102	0		Inferior	150°	113	0
		Neutral	170°	82	34		Neutral	150°	105	4		Neutral	150°	120	0
		Inferior	150°	92	0		Neutral	170°	105	23		Neutral	170°	122	15
		Inferior	170°	96	13		Inferior	170°	119	6		Inferior	170°	131	0
	42 mm	Superior	130°	48	1	42 mm	Superior	130°	52	0	42 mm	Superior	130°	54	0
		Superior	150°	48	21		Superior	150°	58	11		Superior	170°	70	22
		Superior	170°	48	40		Superior	170°	58	31		Superior	150°	71	2
		Inferior	130°	76	0		Inferior	130°	87	0		Neutral	130°	93	0
		Neutral	130°	86	0		Neutral	130°	89	0		Inferior	130°	96	0
		Neutral	150°	96	6		Inferior	150°	106	0		Neutral	150°	114	0
		Neutral	170°	96	25		Neutral	150°	109	0		Inferior	150°	115	0
		Inferior	150°	97	0		Neutral	170°	112	14		Neutral	170°	123	8
		Inferior	170°	105	8		Inferior	170°	122	2		Inferior	170°	133	1
0.32	30 mm	Superior	170°	43	53	30 mm	Superior	130°	54	4	30 mm	Superior	130°	59	0
		Superior	130°	44	13		Superior	150°	54	24		Superior	150°	65	12
		Superior	150°	44	33		Superior	170°	54	43		Superior	170°	65	31
		Neutral	130°	55	9		Inferior	130°	75	0		Inferior	130°	87	0
		Neutral	150°	56	28		Neutral	130°	79	0		Neutral	130°	90	0
		Neutral	170°	56	48		Neutral	150°	79	17		Neutral	170°	100	27
		Inferior	130°	64	0		Neutral	170°	80	36		Neutral	150°	101	7
		Inferior	170°	77	23		Inferior	150°	96	0		Inferior	150°	107	0
		Inferior	150°	78	3		Inferior	170°	97	15		Inferior	170°	118	9
	36 mm	Superior	150°	44	29	36 mm	Superior	130°	55	0	36 mm	Superior	130°	57	0
		Superior	130°	45	9		Superior	150°	55	10		Superior	150°	66	9
		Superior	170°	45	48		Superior	170°	55	38		Superior	170°	66	28
		Inferior	130°	68	0		Inferior	130°	79	0		Inferior	130°	89	0
		Neutral	130°	68	2		Neutral	130°	85	0		Neutral	130°	95	0
		Neutral	150°	68	22		Neutral	150°	92	10		Inferior	150°	110	0
		Neutral	170°	68	41		Neutral	170°	92	30		Neutral	150°	110	2
		Inferior	150°	87	0		Inferior	150°	98	0		Neutral	170°	111	21
		Inferior	170°	87	18		Inferior	170°	106	10		Inferior	170°	125	2
	42 mm	Superior	130°	45	6	42 mm	Superior	130°	54	0	42 mm	Superior	130°	56	0
		Superior	170°	45	45		Superior	150°	55	16		Superior	150°	67	6
		Superior	150°	46	25		Superior	170°	56	35		Superior	170°	66	25
		Inferior	130°	72	0		Inferior	130°	82	0		Inferior	130°	92	0
		Neutral	130°	79	0		Neutral	130°	91	0		Neutral	130°	99	0
		Neutral	170°	81	35		Inferior	150°	102	0		Inferior	150°	113	0
		Neutral	150°	82	15		Neutral	170°	104	24		Neutral	150°	119	0
		Inferior	150°	92	0		Neutral	150°	105	4		Neutral	170°	121	16
		Inferior	170°	96	13		Inferior	170°	113	6		Inferior	170°	131	0

Class I - Decreased impingement-free arc of motion with increased humerosocket depth
Class II - No trend between impingement-free arc of motion and increased humerosocket depth
Class III - Increased impingement-free arc of motion with increased humerosocket depth

Table 9. (Continued)

d/R Ratio	0 mm Center of Rotation Offset					5 mm Center of Rotation Offset					10 mm Center of Rotation Offset				
	Glenosphere Diameter	Glenoid Placement	Humeral Angle	Impingement-Free Arc of Motion	Adduction Deficit	Glenosphere Diameter	Glenoid Placement	Humeral Angle	Impingement-Free Arc of Motion	Adduction Deficit	Glenosphere Diameter	Glenoid Placement	Humeral Angle	Impingement-Free Arc of Motion	Adduction Deficit
0.44	30 mm	Superior	150º	44	37	30 mm	Inferior	130º	7*	0*	30 mm	Superior	130º	63*	0*
		Neutral	130º	45	14		Superior	150º	55	27		Superior	150º	66	15
		Neutral	150º	45	34		Superior	170º	55	47		Superior	170º	67	34
		Superior	170º	45	56		Superior	130º	56*	7*		Inferior	130º	84*	0*
		Superior	130º	45	17		Neutral	130º	70*	2*		Neutral	130º	86*	0*
		Neutral	170º	46	53		Neutral	150º	70	22		Neutral	170º	92	31
		Inferior	130º	60	0		Neutral	170º	70	41		Neutral	150º	93	11
		Inferior	150º	69	8		Inferior	150º	90	0		Inferior	150º	103	0
		Inferior	170º	70	27		Inferior	170º	90	19		Inferior	170º	111	13
	36 mm	Superior	130º	44*	14*	36 mm	Superior	150º	54	23	36 mm	Superior	130º	60	0
		Superior	150º	44‡	33‡		Superior	170º	54	42		Superior	150º	66	12
		Superior	170º	44	53		Superior	130º	55*	3*		Superior	170º	66	31
		Neutral	130º	55*	9*		Inferior	130º	75*	0*		Inferior	130º	87	0
		Neutral	150º	55‡	29‡		Neutral	130º	78*	0*		Neutral	130º	90	0
		Neutral	170º	55	48		Neutral	150º	79	17		Neutral	170º	100	27
		Inferior	130º	64*	0*		Neutral	170º	79	36		Neutral	150º	100	7
		Inferior	170º	77	23		Inferior	150º	96	0		Inferior	150º	106	0
		Inferior	150º	78‡	3‡		Inferior	170º	97	15		Inferior	170º	117	7
	42 mm	Superior	150º	44‡	30‡	42 mm	Superior	150º	54	20	42 mm	Superior	130º	58	0
		Superior	170º	44	50		Superior	130º	55*	0*		Superior	150º	66	9
		Superior	130º	45*	10*		Superior	170º	55	39		Superior	170º	66	29
		Neutral	150º	65‡	24‡		Inferior	130º	78*	0*		Inferior	130º	88	0
		Neutral	170º	65	43		Neutral	130º	83*	0*		Neutral	130º	94	0
		Neutral	130º	65*	4*		Neutral	170º	88	32		Neutral	170º	108	23
		Inferior	130º	68*	0*		Neutral	150º	89	12		Neutral	150º	108	3
		Inferior	150º	84‡	0‡		Inferior	150º	98	0		Inferior	150º	109	0
		Inferior	170º	85	19		Inferior	170º	103	12		Inferior	170º	123	4
0.56	30 mm	Neutral	150º	35	39	30 mm	Superior	130º	60*	11*	30 mm	Superior	130º	70*	0*
		Neutral	130º	36	19		Neutral	150º	60	27		Superior	150º	70	18
		Neutral	170º	36	58		Superior	170º	60	50		Superior	170º	70	37
		Superior	130º	48	21		Neutral	130º	61*	7*		Inferior	130º	80*	0*
		Superior	170º	49	60		Neutral	170º	61	46		Neutral	130º	82*	0*
		Superior	150º	50	40		Superior	150º	61	29		Neutral	150º	84	16
		Inferior	130º	51	0		Inferior	130º	69*	0*		Neutral	170º	84	35
		Inferior	150º	60	13		Inferior	150º	82	3		Inferior	150º	100	0
		Inferior	170º	60	33		Inferior	170º	82	23		Inferior	170º	103	15
	36 mm	Neutral	130º	43*	15*	36 mm	Superior	130º	57*	7*	36 mm	Superior	130º	67	0
		Neutral	150º	43	35		Superior	170º	57	46		Superior	170º	68	35
		Neutral	170º	44	54		Superior	150º	59	26		Superior	150º	70	15
		Superior	130º	46*	18*		Neutral	150º	68	23		Inferior	130º	83	0
		Superior	170º	46	57		Neutral	170º	68	42		Neutral	130º	85	0
		Superior	150º	48	37		Neutral	130º	68*	3*		Neutral	170º	90	32
		Inferior	130º	60*	0*		Inferior	130º	71*	0*		Neutral	150º	91	12
		Inferior	150º	67	9		Inferior	150º	89	0		Inferior	150º	103	0
		Inferior	170º	68	28		Inferior	170º	89	19		Inferior	170º	109	11
	42 mm	Superior	150º	43	35	42 mm	Superior	170º	55	44	42 mm	Superior	130º	62	0
		Superior	170º	43	55		Superior	150º	56	24		Superior	170º	66	33
		Neutral	150º	50	31		Superior	130º	63*	0*		Superior	150º	67	13
		Neutral	170º	50	51		Inferior	130º	73*	0*		Inferior	130º	85	0
		Neutral	130º	51*	11*		Neutral	130º	74*	0*		Neutral	130º	88	0
		Inferior	130º	61*	0*		Neutral	170º	75	39		Neutral	170º	96	29
		Superior	130º	62*	15*		Neutral	150º	75	19		Neutral	150º	97	9
		Inferior	150º	73	6		Inferior	150º	94	0		Inferior	150º	105	0
		Inferior	170º	74	25		Inferior	170º	94	17		Inferior	170º	114	9
0.68	30 mm	Neutral	130º	26	24	30 mm	Neutral	130º	52	11	30 mm	Neutral	130º	75	0
		Neutral	150º	27	43		Neutral	150º	52	31		Neutral	150º	75	20
		Neutral	170º	27	63		Neutral	170º	52	51		Neutral	170º	75	40
		Inferior	130º	47	0		Inferior	130º	64	0		Inferior	130º	76	0
		Inferior	150º	48	21		Superior	150º	67	34		Superior	130º	79	0
		Inferior	170º	49	40		Superior	170º	67	54		Superior	150º	80	21
		Superior	150º	50	45		Superior	130º	68	14		Superior	170º	80	41
		Superior	130º	50	25		Inferior	150º	73	8		Inferior	150º	86	0
		Superior	170º	51	64		Inferior	170º	73	28		Inferior	170º	100	15
	36 mm	Neutral	130º	31	21	36 mm	Neutral	150º	54	29	36 mm	Superior	130º	75	0
		Neutral	150º	31‡	41‡		Neutral	130º	56	9		Superior	170º	75	39
		Neutral	170º	32	60		Neutral	170º	57	48		Superior	150º	76	19
		Superior	130º	52	23		Superior	170º	64	51		Inferior	130º	78	0
		Inferior	130º	53	0		Superior	130º	65	11		Neutral	170º	80	37
		Superior	170º	53	62		Inferior	130º	66	0		Neutral	130º	80	0
		Inferior	170º	57	34		Superior	150º	66	31		Neutral	150º	80	18
		Inferior	150º	58‡	13‡		Inferior	170º	78	25		Inferior	150º	99	0
		Superior	150º	74‡	43‡		Inferior	150º	79	5		Inferior	170º	99	17
	42 mm	Neutral	170º	36	58	42 mm	Superior	170º	60	49	42 mm	Superior	150º	70	18
		Neutral	150º	37‡	38‡		Neutral	170º	61	46		Superior	130º	71	0
		Neutral	130º	37	18		Superior	130º	61	9		Superior	170º	71	37
		Superior	170º	48	60		Superior	150º	61	29		Inferior	130º	80	0
		Superior	130º	49	20		Neutral	130º	62	6		Neutral	130º	82	0
		Superior	150º	49‡	40‡		Inferior	130º	68	0		Neutral	150º	85	15
		Inferior	130º	56	0		Neutral	150º	69	19		Neutral	170º	88	32
		Inferior	150º	61	12		Inferior	170º	82	23		Inferior	150º	100	0
		Inferior	170º	61	32		Inferior	150º	83	3		Inferior	170º	105	13

Class I - Decreased impingement-free arc of motion with increased humerosocket depth
Class II - No trend between impingement-free arc of motion and increased humerosocket depth
Class III - Increased impingement-free arc of motion with increased humerosocket depth

Discussion

The results revealed a paradox to our hypothesis, which initially seemed to be intuitive. The relationship between the impingement-free arc of motion and articular constraint could be grouped into 3 classes based on specific trends (Table 9). The majority of the combinations (57%) had decreased impingement-free arc of motion as articular constraint increased (class I), a result which was in favor of our hypothesis and could be anticipated from previous hip arthroplasty studies. However, the rest of the combinations did not follow this pattern: 37% had no such trend (class II) and 6% even demonstrated an increase in the impingement-free arc of motion with an increase in constraint (class III).

Certain concurrent factors play an important role in determination of the trends. The combinations which provide a consistent decrease in impingement-free arc of motion with increasing constraint (class I) are those in which the glenosphere is placed in the inferior position on the glenoid. A smaller humeral neck-shaft angle (130° – 150°) further results in reduction of adduction deficit (Table 9). On the other hand, when these three conditions are not met, the relationship between socket constraint and impingement-free arc of motion becomes much more unpredictable as seen in class II.

Class II and class III are unique to RSA and merit further discussion. One interpretation of these results was that this counter-intuitive behavior was

attributable to superior impingement on the acromion due to an increase in distance between the COR and the outer surface of the humerosocket as the articular constraint decreased (Figure 25). When the humerosocket had a stable constraint (e.g., d/R=0.56), the impingement-free arc of motion was 67°, measured from the inferior position (Figure 25-A) to the superior position (Figure 25-B). When the articular constraint was reduced, the distance between the COR and the outer surface of the humerosocket increased, which in turn resulted in humerosocket impingement on the acromion at a lower abduction angle. In our example (d/R=0.08), the impingement-free arc of motion when moving from the inferior position (Figure 25-C) to the superior position (Figure 25-D) decreased to 53°. This example further implies that depending on where impingement occurs, a trend of reduction in impingement-free abduction motion will appear as long as the decrease in constraint increases the critical distance between the COR and the outer surface of the humerosocket (or the residual humeral head). We, therefore, anticipate the existence of new combinations in class II and class III beyond the subset of 81 combinations identified here.

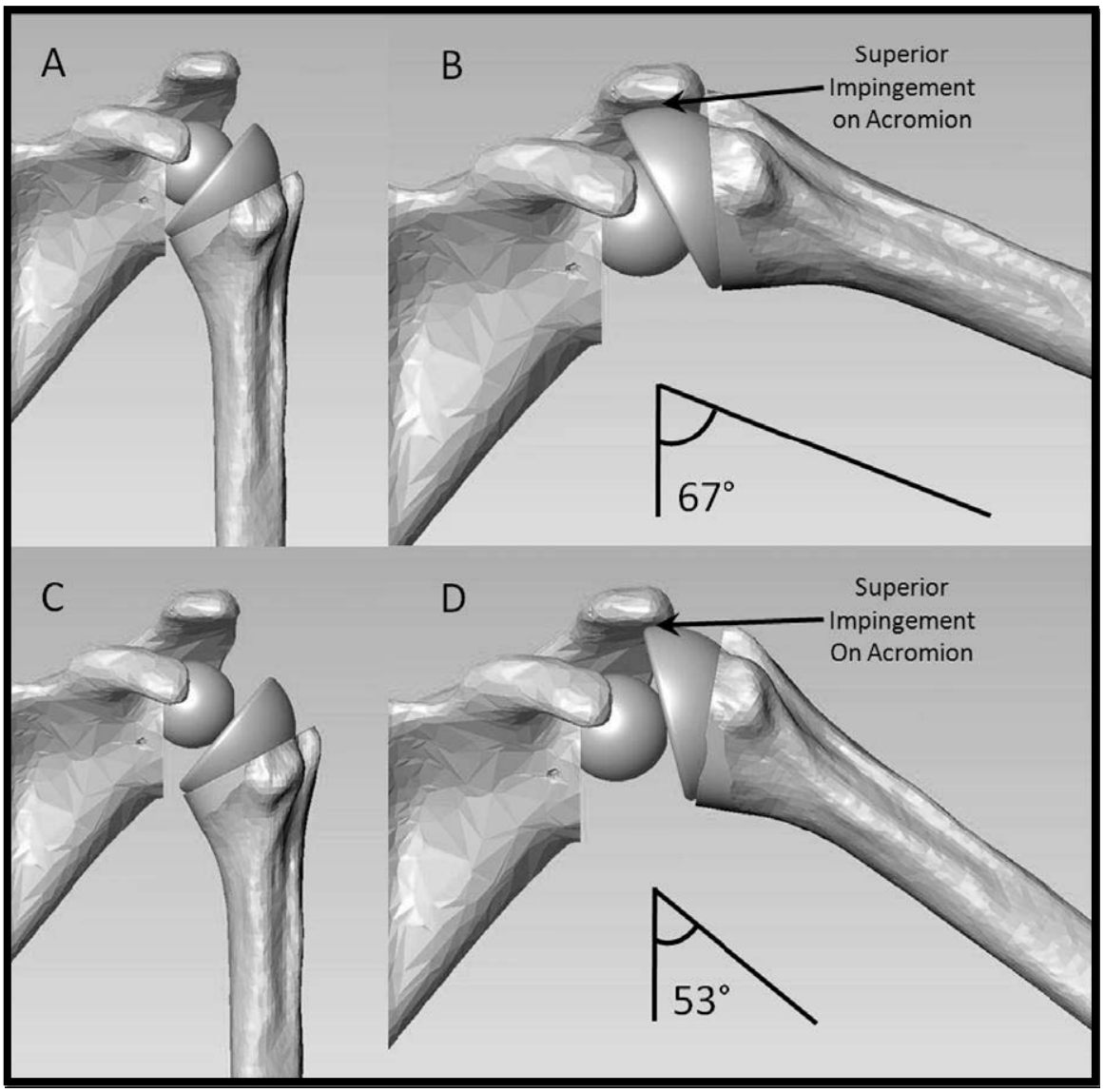

Figure 25. Illustration of decrease in ROM from a more constrained construct (A to B, d/R=0.56) to a less constrained construct (C to D, d/R=0.08). Decrease in the arc of motion due to earlier impingement of the humerosocket with the inferior surface of the acromion.

Most of the combinations in class III are associated with placement of the glenosphere superiorly. Such placement might be controversial as the superior position has not been recommended by manufacturers for implementation.

However, this does not necessarily mean the position is not relevant. Clinically, the situation may arise when a massive bony defect occurs on the glenoid and the superior position becomes the only option available for stable glenosphere placement. The positive relationship between the impingement-free arc of motion and joint constraint of class III was found uniquely in this position, suggesting the critical role it can play in RSA outcomes.

The results summarized in Table 9 not only highlighted the three classes but also listed every individual condition, including those of all the current commercial designs, with their range of motion. The table could be configured much more simply if only the three classes or the averaged information were illustrated. However, such an arrangement would lose the individual details which could be more important in surgeon's decision-making of implant selection and in engineer's gain for future design improvement.

The limitations of this study need to be addressed. First, the study took a mechanical approach to examine the effect of joint constraints on the arc of motion along with four concurrent factors. In practice, more factors are involved in the decision of what components to use. The amount of good bone available for fixation, stress concentration at the glenosphere-bone interface or the available space in the shoulder all play roles in the decision of prosthetic selection and are critical in preventing the implant from loosening. The strength of the remaining muscles is also important in providing additional stability to the

joint. Second, the arc of motion was passive which should be considered as the maximum improvements that can be expected in active motion after surgery. Also, the motion was limited to two-dimensional abduction/adduction in the scapular plane because this parameter is the primary concern for restoration of function in RSA. Other components, including internal/external rotation and flexion/extension, are also critical and should be considered in future studies. Finally, anatomic variation among patients was omitted. The model had typical geometric parameters that matched a subset of patients undergoing RSA. The intent was to provide an initial point of reference to understand how variations of concurrent factors were interrelated. Quantifying the role of anatomic variation in the arc of motion would add a degree of complexity which should warrant a future study.

In conclusion, this study revealed 3 distinct classes in RSA defining the relationship between the abduction impingement-free arc of motion and articular constraint. The impingement-free arc of motion, in most cases, decreased with the increase of the articular constraint (class I). However, there existed a number of combinations in which the impingement-free arc of motion had a complex relationship to articular constraint (class II) or increased with the increase of constraint (class III), suggesting the complexity of this relationship and its dependence on other concurrent factors. Surgeons may need to be aware of this unusual situation when the glenoid component has to be placed superiorly. For design engineers, in order to achieve the greatest range of

motion, a reduction in constraint is critical. Since this is at the cost of joint stability, utilizing other factors such as soft tissue compression on the joint may be important in designing new implants.

CHAPTER 8 - CONCLUSIONS, CURRENT WORK AND RECOMMENDATIONS FOR FUTURE WORK

Conclusions

Reverse shoulder arthroplasty remains one of the few procedures available to help patients suffering from irreparable cuff tear arthropathy. In the hands of a skilled surgeon, the reverse functions as designed and returns the patient to a relatively normal level of function. Although many surgeons continue to have successful outcomes with the reverse, the procedure remains difficult and is relegated to being a salvage procedure (i.e. performed when everything else fails). Even with its benefits, there remain complications related to instability, non-optimal range of motion, inferior scapular notching and deltoid tensioning. It was our attempt to shed some light on these problems, but there remains a great deal more to learn. The main points found during our research include:

(1) Mechanical failure of the baseplate can be reduced by tilting it inferiorly. This helps to more evenly distribute the forces underneath it.

(2) There is a linear correlation between center of rotation offset and range of motion. As the center of rotation offset is increased, range of motion increases. The main concern with this finding is the increased moment arm at the interface as the offset is increased. The largest offset currently available in reverse shoulder arthroplasty is 10 mm, thus anything larger than this has not been studied. Another factor regarding increasing offset is the quality of fixation of the baseplate. Larger glenosphere offsets can be used as long as stable baseplate fixation can be achieved. This maximum offset has yet to be tested and should be considered for future studies.

(3) In both an experimental study and a computer simulation, it was shown that center of rotation offset had the largest effect on range of motion followed closely by inferior placement of the glenosphere on the glenoid. In addition, it was found that using a more varus humeral neck-shaft angle reduced the chances of inferior scapular notching. These findings mirror our previous results and laid the groundwork for future uses of computer simulations.

(4) Instability can be reduced in reverse shoulder arthroplasty by increasing the joint compressive force and, to a lesser extent, by increasing the

humerosocket depth. Caution should be taken if the humerosocket depth is increased since this has a detrimental effect on range of motion.

(5) Three different classes of motion were found when looking at varying humerosocket depths: class I - motion decreased with increased depth, class II - complex relationship between motion and depth, and class III – motion increased with increased depth.

Current Work

The previous studies have helped solve some perplexing problems in reverse shoulder arthroplasty, but they also helped to guide us in our future endeavors. Our current studies include:

(1) The use of a reverse humerosocket in the setting of proximal humeral bone loss. Current solutions for proximal humeral bone loss in a setting of cuff tear arthropathy are poorly understood. We are working to find solutions to this problem by studying modular and non-modular humerosocket geometry in a Sawbones© proximal bone loss model.

(2) The effects of varying component geometry on joint volume and humeral displacement in a computer simulation. There is a poor understanding of

the effects of component geometry on soft tissues in reverse shoulder arthroplasty. One of the main tenets in reverse arthroplasty is correct tensioning of the deltoid to improve its efficiency. This tensioning can be achieved in various ways including: lengthening the arm by putting a more valgus humeral component, by increasing the glenosphere lateral offset or by implanting larger geometry components. We want to find answers to these soft tissue questions and we hope this study does that.

(3) The effects of eccentric glenospheres on the forces at the baseplate-bone interface. There is a drive to solve the problem of inferior scapular notching by placing the baseplate in an inferior position on the glenoid and by implanting an inferiorly eccentric glenosphere. The effects of an eccentric glenosphere have not been studied and may have detrimental effects on the survivability of the baseplate. We are in the process of running finite element studies to test different eccentric geometries and their effects on stress at the baseplate-bone interface.

Recommendations for Future Work

Although we are successfully studying basic biomechanical principles with current and previous work, there remain issues that have yet to be addressed due to their inherent complexity. One of the most important factors that has been

lacking in all previous and current work are the effects of soft tissues on reverse shoulder function. Although there exists six degree of freedom rigs that can approximate shoulder motion, they still do not correctly replicate the complex nature of individual muscle fibers firing to keep a joint in static equilibrium or to dynamically move it in a controlled fashion. In addition to general muscle characteristics, the complexity of muscle wrapping has yet to be efficiently implemented and will be a highly desirable addition to any future computer simulation. Future work should involve either the use of more actuators to improve the current rigs or more complex computer simulations that can accurately replicate muscle physiology and biomechanics.

REFERENCES

(1) Franklin JL, Barrett WP, Jackins SE, and Matsen FA, 3rd. Glenoid loosening in total shoulder arthroplasty. Association with rotator cuff deficiency. J Arthroplasty. 1988;3:39-46.

(2) Coughlin MJ, Morris JM, and West WF. The semiconstrained total shoulder arthroplasty. J Bone Joint Surg Am. 1979;61:574-81.

(3) Nwakama AC, Cofield RH, Kavanagh BF, and Loehr JF. Semiconstrained total shoulder arthroplasty for glenohumeral arthritis and massive rotator cuff tearing. J Shoulder Elbow Surg. 2000;9:302-7.

(4) Pugh DM, and McKee MD. Advances in the management of humeral nonunion. J Am Acad Orthop Surg. 2003;11:48-59.

(5) Brostrom LA, Wallensten R, Olsson E, and Anderson D. The Kessel prosthesis in total shoulder arthroplasty. A five-year experience. Clin Orthop. 1992;155-60.

(6) Post M, and Jablon M. Constrained total shoulder arthroplasty. Long-term follow-up observations. Clin Orthop. 1983;109-16.

(7) Cofield RH. Shoulder arthrodesis and resection arthroplasty. Instr Course Lect. 1985;34:268-77.

(8) Naranja RJ, Jr., and Iannotti JP. Surgical options in the treatment of arthritis of the shoulder: alternatives to prosthetic arthroplasty. Semin Arthroplasty. 1995;6:204-13.

(9) Souter WA. The surgical treatment of the rheumatoid shoulder. Ann Acad Med Singapore. 1983;12:243-55.

(10) Zeman CA, Arcand MA, Cantrell JS, Skedros JG, and Burkhead WZ, Jr. The rotator cuff-deficient arthritic shoulder: diagnosis and surgical management. J Am Acad Orthop Surg. 1998;6:337-48.

(11) Arman F. [Total shoulder arthroplasty vs. hemiarthroplasty]. Zentralbl Chir. 2003;128:17-21.

(12) Goutallier D, Postel JM, Zilber S, and Van Driessche S. Shoulder surgery: from cuff repair to joint replacement. An update. Joint Bone Spine. 2003;70:422-32.

(13) Orfaly RM, Rockwood CA, Jr., Esenyel CZ, and Wirth MA. A prospective functional outcome study of shoulder arthroplasty for osteoarthritis with an intact rotator cuff. J Shoulder Elbow Surg. 2003;12:214-21.

(14) Trail IA, and Nuttall D. The results of shoulder arthroplasty in patients with rheumatoid arthritis. J Bone Joint Surg Br. 2002;84:1121-5.

(15) Neer CS, 2nd, Watson KC, and Stanton FJ. Recent experience in total shoulder replacement. J Bone Joint Surg Am. 1982;64:319-37.

(16) Arntz CT, Jackins S, and Matsen FA, 3rd. Prosthetic replacement of the shoulder for the treatment of defects in the rotator cuff and the surface of the glenohumeral joint. J Bone Joint Surg Am. 1993;75:485-91.

(17) Field LD, Dines DM, Zabinski SJ, and Warren RF. Hemiarthroplasty of the shoulder for rotator cuff arthropathy. J Shoulder Elbow Surg. 1997;6:18-23.

(18) Baulot E, Chabernaud D, and Grammont PM. [Results of Grammont's inverted prosthesis in omarthritis associated with major cuff destruction. Apropos of 16 cases]. Acta Orthop Belg. 1995;61 Suppl 1:112-9.

(19) Grammont PM, and Baulot E. Delta shoulder prosthesis for rotator cuff rupture. Orthopedics. 1993;16:65-8.

(20) Rittmeister M, and Kerschbaumer F. Grammont reverse total shoulder arthroplasty in patients with rheumatoid arthritis and nonreconstructible rotator cuff lesions. Journal of Shoulder & Elbow Surgery. 2001;10:17-22.

(21) Sirveaux F, Favard L, Oudet D, Huquet D, Walch G, and Mole D. Grammont inverted total shoulder arthroplasty in the treatment of glenohumeral osteoarthritis with massive rupture of the cuff. Results of a multicentre study of 80 shoulders. J Bone Joint Surg Br. 2004;86:388-95.

(22) Valenti PH BD, Nerot C. Delta 3 reversed prosthesis for osteoarthritis with massive rotator cuff tear: long term results (>5 years). Shoulder Prosthesis. 2000. 2000;253-259.

(23) Harman M, Frankle M, Vasey M, and Banks S. Initial glenoid component fixation in "reverse" total shoulder arthroplasty: a biomechanical evaluation. J Shoulder Elbow Surg. 2005;14:162S-167S.

(24) Einhorn TA, Simon SR, and American Academy of Orthopaedic Surgeons.: Orthopaedic basic science : biology and biomechanics of the musculoskeletal system. Edited, xix, 873 p., Rosemont, Ill., American Academy of Orthopaedic Surgeons, 2000.

(25) Cameron HU, Pilliar RM, and MacNab I. The effect of movement on the bonding of porous metal to bone. J Biomed Mater Res. 1973;7:301-11.

(26) Ducheyne P, De Meester P, and Aernoudt E. Influence of a functional dynamic loading on bone ingrowth into surface pores of orthopedic implants. J Biomed Mater Res. 1977;11:811-38.

(27) Pilliar RM, Cameron HU, Welsh RP, and Binnington AG. Radiographic and morphologic studies of load-bearing porous-surfaced structured implants. Clin Orthop. 1981;249-57.

(28) Jasty M, Bragdon C, Burke D, O'Connor D, Lowenstein J, and Harris WH. In vivo skeletal responses to porous-surfaced implants subjected to small induced motions. J Bone Joint Surg Am. 1997;79:707-14.

(29) Jasty M, Bragdon CR, Zalenski E, O'Connor D, Page A, and Harris WH. Enhanced stability of uncemented canine femoral components by bone ingrowth into the porous coatings. J Arthroplasty. 1997;12:106-13.

(30) Lee TQ, Barnett SL, and Kim WC. Effects of screw types in cementless fixation of tibial tray implants: stability and strength assessment. Clin Biomech (Bristol, Avon). 1999;14:258-64.

(31) Whiteside LA. Four screws for fixation of the tibial component in cementless total knee arthroplasty. Clin Orthop. 1994;72-6.

(32) Qin YX, McLeod KJ, Guilak F, Chiang FP, and Rubin CT. Correlation of bony ingrowth to the distribution of stress and strain parameters surrounding a porous-coated implant. J Orthop Res. 1996;14:862-70.

(33) De Wilde L, Mombert M, Van Petegem P, and Verdonk R. Revision of shoulder replacement with a reversed shoulder prosthesis (Delta III): report of five cases. Acta Orthop Belg. 2001;67:348-53.

(34) Habermeyer P, and Ebert T. [Current status and perspectives of shoulder replacement]. Unfallchirurg. 1999;102:668-83.

(35) Boileau P, Watkinson DJ, Hatzidakis AM, and Balg F. Grammont reverse prosthesis: design, rationale, and biomechanics. J Shoulder Elbow Surg. 2005;14:147S-161S.

(36) Frankle M, Siegal S, Pupello D, Saleem A, Mighell M, and Vasey M. The Reverse Shoulder Prosthesis for glenohumeral arthritis associated with severe rotator cuff deficiency. A minimum two-year follow-up study of sixty patients. J Bone Joint Surg Am. 2005;87:1697-705.

(37) Werner CM, Steinmann PA, Gilbart M, and Gerber C. Treatment of painful pseudoparesis due to irreparable rotator cuff dysfunction with the Delta III reverse-ball-and-socket total shoulder prosthesis. J Bone Joint Surg Am. 2005;87:1476-86.

(38) Seebauer L. Reverse prosthesis through a superior approach for cuff tear arthropathy. Tech Shoulder Elbow Surg. 2006;7:13-26.

(39) Seebauer L, Walter W, and Keyl W. Reverse total shoulder arthroplasty for the treatment of defect arthropathy. Oper Orthop Traumatol. 2005;17:1-24.

(40) Nyffeler RW, Werner CM, and Gerber C. Biomechanical relevance of glenoid component positioning in the reverse Delta III total shoulder prosthesis. J Shoulder Elbow Surg. 2005;14:524-8.

(41) de Leest O, Rozing PM, Rozendaal LA, and van der Helm FC. Influence of glenohumeral prosthesis geometry and placement on shoulder muscle forces. Clin Orthop. 1996;222-33.

(42) Valenti PH, Boutens D, and Nerot C. Delta 3 reversed prosthesis for osteoarthritis with massive rotator cuff tear: long term results. In: Walch G, Boileau P, Molé D, editors. 2000 Prothéses d'épaule…recul de 2 à 10 ans. Paris, France: Sauramps Medical. 2001;253-259.

(43) Boulahia A, Edwards TB, Walch G, and Baratta RV. Early results of a reverse design prosthesis in the treatment of arthritis of the shoulder in elderly patients with a large rotator cuff tear. Orthopedics. 2002;25:129-33.

(44) Vanhove B, and Beugnies A. Grammont's reverse shoulder prosthesis for rotator cuff arthropathy. A retrospective study of 32 cases. Acta Orthop Belg. 2004;70:219-25.

(45) Lucas B, Asher M, McIff T, Lark R, and Burton D. Estimation of transverse plane pelvic rotation using a posterior-anterior radiograph. Spine. 2005;30:E20-7.

(46) Schep NW, van Walsum T, De Graaf JS, Broeders IA, and van der Werken C. Validation of fluoroscopy-based navigation in the hip region: what you see is what you get? Comput Aided Surg. 2002;7:279-83.

(47) Hasan SS, Leith JM, Campbell B, Kapil R, Smith KL, and Matsen FA, 3rd. Characteristics of unsatisfactory shoulder arthroplasties. J Shoulder Elbow Surg. 2002;11:431-41.

(48) Favard L, Lautmann S, Sirveaux F, Oudet D, Kerjean Y, and Huguet D. Hemi-arthroplasty *versus* reverse arthroplasty in treatment of osteoarthritis with massive rotator cuff tear. In: Walch G, Boileau P, Molé D, editors. 2000 Shoulder Prosthesis…Two to Ten Year Follow-up. Paris, France: Sauramps Medical. 2001;261-268.

(49) Rittmeister M, and Kerschbaumer F. Grammont reverse total shoulder arthroplasty in patients with rheumatoid arthritis and nonreconstructible rotator cuff lesions. J Shoulder Elbow Surg. 2001;10:17-22.

(50) Bufquin T, Hersan A, Hubert L, and Massin P. Reverse shoulder arthroplasty for the treatment of three- and four-part fractures of the proximal humerus in the elderly: a prospective review of 43 cases with a short-term follow-up. J Bone Joint Surg Br. 2007;89:516-20.

(51) Cazeneuve JF, and Cristofari DJ. [Grammont reversed prosthesis for acute complex fracture of the proximal humerus in an elderly population with 5 to 12 years follow-up]. Rev Chir Orthop Reparatrice Appar Mot. 2006;92:543-8.

(52) De Wilde L, Sys G, Julien Y, Van Ovost E, Poffyn B, and Trouilloud P. The reversed Delta shoulder prosthesis in reconstruction of the proximal humerus after tumour resection. Acta Orthop Belg. 2003;69:495-500.

(53) Van Seymortier P, Stoffelen D, Fortems Y, and Reynders P. The reverse shoulder prosthesis (Delta III) in acute shoulder fractures: technical considerations with respect to stability. Acta Orthop Belg. 2006;72:474-7.

(54) Wall B, Nove-Josserand L, O'Connor DP, Edwards TB, and Walch G. Reverse total shoulder arthroplasty: a review of results according to etiology. J Bone Joint Surg Am. 2007;89:1476-85.

(55) Anglin C, Wyss UP, and Pichora DR. Shoulder prosthesis subluxation: theory and experiment. J Shoulder Elbow Surg. 2000;9:104-14.

(56) Tammachote N, Sperling JW, Berglund LJ, Steinmann SP, Cofield RH, and An KN. The effect of glenoid component size on the stability of total shoulder arthroplasty. J Shoulder Elbow Surg. 2007;16:S102-6.

(57) Labriola JE, Lee TQ, Debski RE, and McMahon PJ. Stability and instability of the glenohumeral joint: the role of shoulder muscles. J Shoulder Elbow Surg. 2005;14:32S-38S.

(58) Parsons IM, Apreleva M, Fu FH, and Woo SL. The effect of rotator cuff tears on reaction forces at the glenohumeral joint. J Orthop Res. 2002;20:439-46.

(59) American Society for Testing and Materials (ASTM). Standard specification for ultra-high-molecular-weight polyethylene powder and fabricated for surgical implants. Designation F648-96.

(60) Friction Center Coefficient Database. Southern Illinois University. 2005.

(61) Linn FC. Lubrication of animal joints. I. The arthrotripsometer. J Bone Joint Surg Am. 1967;49:1079-98.

(62) Roberts BJ, Unsworth A, and Mian N. Modes of lubrication in human hip joints. Ann Rheum Dis. 1982;41:217-24.

(63) Scholes SC, and Unsworth A. Comparison of friction and lubrication of different hip prostheses. Proc Inst Mech Eng [H]. 2000;214:49-57.

(64) Oosterom R, Herder JL, van der Helm FC, Swieszkowski W, and Bersee HE. Translational stiffness of the replaced shoulder joint. J Biomech. 2003;36:1897-907.

(65) Brockett C, Williams S, Jin Z, Isaac G, and Fisher J. Friction of total hip replacements with different bearings and loading conditions. J Biomed Mater Res B Appl Biomater. 2006;81B:508-515.

(66) Kirk RE: Experimental design : procedures for the behavioral sciences. Edited, xiv, 921 p., Pacific Grove, Calif., Brooks/Cole, 1995.

(67) Matsen FA, 3rd, Chebli C, and Lippitt S. Principles for the evaluation and management of shoulder instability. J Bone Joint Surg Am. 2006;88:648-59.

(68) Endo K, Ikata T, Katoh S, and Takeda Y. Radiographic assessment of scapular rotational tilt in chronic shoulder impingement syndrome. J Orthop Sci. 2001;6:3-10.

(69) Lin JJ, Lim HK, and Yang JL. Effect of shoulder tightness on glenohumeral translation, scapular kinematics, and scapulohumeral rhythm in subjects with stiff shoulders. J Orthop Res. 2006;24:1044-51.

(70) Halder AM, Kuhl SG, Zobitz ME, Larson D, and An KN. Effects of the glenoid labrum and glenohumeral abduction on stability of the shoulder joint through concavity-compression: an in vitro study. J Bone Joint Surg Am. 2001;83-A:1062-9.

(71) Karduna AR, Williams GR, Williams JL, and Iannotti JP. Joint stability after total shoulder arthroplasty in a cadaver model. J Shoulder Elbow Surg. 1997;6:506-11.

(72) Halder AM, Zhao KD, Odriscoll SW, Morrey BF, and An KN. Dynamic contributions to superior shoulder stability. J Orthop Res. 2001;19:206-12.

(73) Lee SB, Kim KJ, O'Driscoll SW, Morrey BF, and An KN. Dynamic glenohumeral stability provided by the rotator cuff muscles in the mid-range and end-range of motion. A study in cadavera. J Bone Joint Surg Am. 2000;82:849-57.

(74) van der Helm FCT. Analysis of the kinematic and dynamic behavior of the shoulder mechanism. J Biomech. 1994;27:527-50.

(75) Gutiérrez S, Levy JC, Lee WE, 3rd, Keller TS, and Maitland ME. Center of rotation affects abduction range of motion of reverse shoulder arthroplasty. Clin Orthop Relat Res. 2007;458:78-82.

(76) Simovitch RW, Zumstein MA, Lohri E, Helmy N, and Gerber C. Predictors of scapular notching in patients managed with the Delta III reverse total shoulder replacement. J Bone Joint Surg Am. 2007;89:588-600.

(77) Nyffeler RW, Werner CM, Simmen BR, and Gerber C. Analysis of a retrieved delta III total shoulder prosthesis. J Bone Joint Surg Br. 2004;86:1187-91.

(78) Burroughs BR, Golladay GJ, Hallstrom B, and Harris WH. A novel constrained acetabular liner design with increased range of motion. J Arthroplasty. 2001;16:31-6.

(79) Malik A, Maheshwari A, and Dorr LD. Impingement with total hip replacement. J Bone Joint Surg Am. 2007;89:1832-42.

(80) Guery J, Favard L, Sirveaux F, Oudet D, Mole D, and Walch G. Reverse total shoulder arthroplasty. Survivorship analysis of eighty replacements followed for five to ten years. J Bone Joint Surg Am. 2006;88:1742-7.

(81) Gutiérrez S, Greiwe RM, Frankle MA, Siegal S, and Lee WE, 3rd. Biomechanical comparison of component position and hardware failure in the reverse shoulder prosthesis. J Shoulder Elbow Surg. 2007;16:S9-S12.

(82) Iannotti JP, Gabriel JP, Schneck SL, Evans BG, and Misra S. The normal glenohumeral relationships. An anatomical study of one hundred and forty shoulders. J Bone Joint Surg Am. 1992;74:491-500.

(83) Karelse A, Kegels L, and De Wilde L. The pillars of the scapula. Clin Anat. 2007;20:392-9.

(84) Kwon YW, Powell KA, Yum JK, Brems JJ, and Iannotti JP. Use of three-dimensional computed tomography for the analysis of the glenoid anatomy. J Shoulder Elbow Surg. 2005;14:85-90.

(85) Gutiérrez S, Levy JC, Frankle MA, Cuff D, Keller TS, Pupello DR, and Lee WE, 3rd. Evaluation of abduction range of motion and avoidance of inferior scapular impingement in a reverse shoulder model. J Shoulder Elbow Surg. 2008;17:608-15.

(86) Gerber C, Pennington SD, Lingenfelter EJ, and Sukthankar A. Reverse Delta-III total shoulder replacement combined with latissimus dorsi transfer. A preliminary report. J Bone Joint Surg Am. 2007;89:940-7.

(87) Gutiérrez S, Comiskey CAt, Luo ZP, Pupello DR, and Frankle MA. Range of impingement-free abduction and adduction deficit after reverse shoulder arthroplasty. Hierarchy of surgical and implant-design-related factors. J Bone Joint Surg Am. 2008;90:2606-15.

(88) Bicos J, Mazzocca A, and Romeo AA. The glenoid center line. Orthopedics. 2005;28:581-5.

(89) Gutiérrez S, Keller TS, Levy JC, Lee WE, 3rd, and Luo ZP. Hierarchy of stability factors in reverse shoulder arthroplasty. Clin Orthop Relat Res. 2008;466:670-6.

APPENDICES

Appendix A - Journal Publications

(1) Gutiérrez S, Levy JC, Lee WE 3rd, Keller TS, Maitland ME.
Center of rotation affects abduction range of motion of reverse shoulder arthroplasty. Clin Orthop Relat Res. 2007 May;458:78-82.

(2) Gutiérrez S, Greiwe RM, Frankle MA, Siegal S, Lee WE 3rd.
Biomechanical comparison of component position and hardware failure in the reverse shoulder prosthesis. J Shoulder Elbow Surg. 2007 May-Jun;16(3 Suppl):S9-S12. Epub 2006 Sep 20.

(3) Gutiérrez S, Frankle MA, Keller TS, Levy JC, Lee WE 3rd, Luo ZP.
Hierarchy of Stability Factors in Reverse Shoulder Arthroplasty. Clin Orthop Relat Res. 2008 Mar;466(3):670-6. Epub 2008 Feb 10.

(4) Gutiérrez S, Levy JC, Frankle MA, Cuff D, Keller TS, Pupello, DR, Lee WE 3rd.
Evaluation of abduction range of motion and avoidance of inferior scapular impingement in a reverse shoulder model. J Shoulder Elbow Surg. 2008 Jul-Aug;17(4):608-15. Epub 2008 Mar 6.

Appendix A (Continued)

(5) Gutiérrez S, Comiskey CA 4th, Luo ZP, Pupello DR, Frankle MA. Range of impingement-free abduction and adduction deficit after reverse shoulder arthroplasty. Hierarchy of surgical and implant-design-related factors. J Bone Joint Surg Am. 2008 Dec;90(12):2606-15.

(6) Gutiérrez S, Luo ZP, Levy JC and Frankle MA. Arc of motion and socket depth in reverse shoulder implants. Clin Biomech. 2009, In Press.

Appendix B - Book Chapters

(1) Frankle MA, Virani N, Pupello D and Gutiérrez S.

Rotator cuff deficiency of the shoulder. Chapter 8; Rationale and biomechanics of the Reverse Shoulder Prosthesis: the american experience. Thieme. 2008:76-104.

Appendix C - Poster/Podium Presentations

(1) European Society for Surgery of the Shoulder and the Elbow, Budapest, Hungary, 2002.

a) Poster presentation: The effect of proximal prosthetic humeral geometry on the stability of tuberosity reconstruction for four-part proximal humerus fractures.

(2) American Shoulder and Elbow Society (ASES) focused meeting, Las Vegas, NV, 2003.

a) Poster presentation: A comparison of micromotion for two different semi-constrained shoulder replacements used in rotator cuff deficient patients.

b) Poster presentation: Achieving adequate glenoid fixation during semi-constrained total shoulder arthroplasty used in rotator cuff-deficient patients.

c) Poster presentation: The effects of proximal prosthetic humeral geometry on the stability of tuberosity reconstruction for four-part proximal humerus fractures.

Appendix C (Continued)

d) Poster presentation: Influence of prosthesis design on moment arms of the deltoid in rotator cuff deficient shoulders.

(3) 9th International Congress on Surgery of the Shoulder, Washington D.C., 2004.

a) Podium presentation: Differences in deltoid forces between four humeral joint configurations.

b) Poster presentation: Influence of prosthesis design on moment arms of the deltoid in rotator cuff deficient shoulders.

c) Poster presentation: In-vitro comparison of glenoid component fixation for two different semi-constrained shoulder replacements.

(4) 1st International Symposium Treatment of Complex Shoulder Problems, January 15-17, Tampa, Florida, 2004.

a) Podium presentation: The effects of different reverse baseplate angles on interface forces and component micro-motion.

Appendix C (Continued)

b) Podium presentation: Differences in deltoid forces between four humeral joint configurations.

(5) 2nd International Symposium - Treatment of Complex Shoulder Problems, January 13-15, Tampa, Florida, 2005.

a) Podium presentation: Deltoid forces in reverse shoulder implants.

b) Podium presentation: SEM analysis of failed reverse shoulder baseplates.

(6) European Society for Surgery of the Shoulder and the Elbow, Rome-Italy, 2005.

a) Poster presentation: Deltoid force comparison between lateralized and medialized reverse shoulder prostheses.

b) Poster presentation: Screw failure in a reverse shoulder prosthesis.

c) Poster presentation: Component positioning and hardware failure in the reverse shoulder prosthesis.

Appendix C (Continued)

(7) European Society for Surgery of the Shoulder and the Elbow, Athens-Greece, 2006.

a) Poster presentation: Outcomes of reverse shoulder prostheses using a lateral center of rotation and inferiorly tilted glenoid component.

(8) American Academy of Orthopaedic Surgeons, Chicago, 2006.

a) Poster presentation: Component positioning and hardware failure in the reverse shoulder prosthesis.

(9) 10th International Congress of Shoulder and Elbow Surgery, Costa do Sauipe, Bahia, Brazil, 2007.

a) Podium presentation: Biomechanical evaluation of range of motion and avoidance of scapular notching in reverse shoulder implants.

b) Podium presentation: Stability in reverse shoulder implants: an experimental and analytical.

Appendix C (Continued)

(10) 6th Combined Meeting of Orthopaedic Research Societies, Honolulu, Hawaii, October 20-24, 2007.

a) Podium presentation: Stability and range of motion in reverse shoulder implants.

b) Poster presentation: Evaluation of abduction range of motion and avoidance of inferior scapular impingement associated with reverse shoulder implants.

(11) 54th Annual Meeting of the Orthopaedic Research Society, March 2-5, 2008 in San Francisco, California.

a) Poster presentation: Stability in reverse shoulder arthroplasty.

b) Poster presentation: Humerosocket depth in reverse shoulder arthroplasty regulates the priority of surgical factors in abduction range of motion.

c) Poster presentation: Hierarchy of surgical factors in abduction range of motion and inferior impingement of reverse shoulder arthroplasty.

Appendix C (Continued)

(12) Biennial AAOS/ASES Shoulder and Elbow Meeting, Orlando, 2008.

a) Podium presentation: Computer simulation to determine how to avoid inferior scapular impingement of the humerosocket associated with reverse shoulder implants.

ABOUT THE AUTHOR

Sergio Gutiérrez received a Bachelor's in both Chemical Engineering and Biology in 2002 from the University of South Florida (USF). He obtained his Master's in Biomedical Engineering at USF in 2004. Currently, he is Director of Operations for the Biomechanics and Surgical Skills Laboratories at the Foundation for Orthopaedic Research and Education (FORE). He developed his research skills under the mentorship of Dr. William Lee and Dr. Mark Frankle. Both were instrumental in his ability to become a published researcher.

Sergio is a founding partner in a medical device incubator called Healthcare Creations, LLC where he developed his skills in writing provisional patents, designing implants, prototyping them and eventually testing these new medical devices. In addition to his interest in the biomedical field, he is a founding partner in an iPhone software development company called Serrick Software, LLC where he is helping develop unique software ideas for the iPhone.